ANALYSIS OF FLOW SEPARATION IN ANNULAR DIFFUSER

A MAJOR PROJECT -II REPORT

SUBMITTED IN PARTIAL FULFILMENT OF THE REQUIREMENT
FOR THE AWARD OF THE DEGREE OF

MASTER OF TECHNOLOGY
IN
THERMAL ENGINEERING

By

PAWAN KUMAR YADAV
(2K13/THE/16)

UNDER THE SUPERVISION OF

Dr. B. B. ARORA

MECHANICAL ENGINEERING DEPARTMENT

DELHI TECHNOLOGICAL UNIVERSITY

SHAHABAD DAULATPUR
BAWANA ROAD, DELHI-110042,
INDIA

SESSION 2013-2015

DECLARATION

I, hereby declare that the work embodied in the dissertation entitled "**ANALYSIS OF FLOW SEPARATION IN ANNULAR DIFFUSER"** in partial fulfilment for the award of degree of MASTER OF TECHNOLOGY with specialization in "THERMAL ENGINEERING", submitted to Delhi Technological University, is an original piece of work carried out by me under the supervision of Dr. B. B. ARORA, Mechanical Engineering Department, Delhi Technological University. The matter of this work either full or in part have not been submitted to any other institution or University for the award of any other Diploma or Degree or any other purpose what so ever.

PAWAN KUMAR YADAV

Roll No. 2K13/THE/16

CERTIFICATE

Date: _____

This is to certify that the work embodied in the dissertation entitled **"ANALYSIS OF FLOW SEPARATION IN ANNULAR DIFFUSER"** by **PAWAN KUMAR YADAV, (**Roll No.-**2K13/THE/16)** in partial fulfilment of requirements for the award of Degree of **Master of Technology** in **Thermal Engineering** of **Delhi Technological University, Delhi** is an authentic record of student's own work carried by him under my supervision.

This is also certified that this dissertation has not been submitted to any other Institute or University for the award of any other diploma or degree.

Dr. B. B. ARORA

Mechanical Engineering Department

Delhi Technological University

Delhi- 110042

ACKNOWLEDGEMENT

It is a great pleasure to acknowledge our gratitude to all the people involved, directly or indirectly in the completion of this project.

It is distinct pleasure to express my deep sense of gratitude and indebtedness to my learned supervisor **Dr. B. B. ARORA** who devoted valuable hours for this assignment and providing the motivational guidance during the entire preparation of this project, answering the number of technical queries despite his busy schedule. His valuable suggestions, constructive criticism and timely help proved extremely fruitful.

I am also grateful to **Prof. (Dr.) R. S. Mishra**, Head, Department of Mechanical Engineering, Delhi Technological University for providing the experimental facilities. His constant support, co-operation and encouragement for successful completion of this work is indebt-able.

I would also like to take this opportunity to present my sincere regards to my teachers for their kind support and encouragement.

I am thankful to **Mr. Deepak and Rahul**, staff of computational fluid dynamics lab, for all assistance during execution of this project work.

This research work would not have become possible without strong cooperation, immense support and keen involvement of my friends and colleagues specially **Mr. Shailesh, Ashish, Rashid, and Ashwani**.

All my academic pursuits become a perceptible reality just because of my parents, brother **Ashok & Shiv** and special thanks to my Wife **Anita** who played a pivotal role at each step providing encouragement and support in every possible way. My sincere

thanks to entire dear and near ones who contributed directly or indirectly for accomplishing this arduous task.

PAWAN KUMAR YADAV

Roll No. 2K13/THE/16

ABSTRACT

A diffuser is a equipment which is used for converting the kinetic energy of received fluid into pressure. When fluid passes through the diffuser there is incessant retardation of the fluid flow due to which kinetic energy changes into pressure energy. This process is called diffusion. Diffuser is a important element in flow machinery .

The present work involves the CFD analysis of flow separation in annular diffuser. The annular diffuser considered in the present case has both the hub and casings are diverging with unequal angles and hub half angle keeping constant as 5°. The geometries of all the diffusers are calculated for constant area ratio 2 and 3 and equivalent cone angle of 20^0. Swirl angle of 0^0, 7.5^0, 12.5^0, 17.5^0 & 25^0 are introduced at the inlet. The characteristic quantities such as static pressure distribution at hub and casing walls, velocity profiles at various sections and flow patterns have been presented for studying the flow separation.

Results are analyzed and it reveals that at lower swirl angle the separation is near to the casing whereas at higher swirl the point of separation shifts towards hub side. Introduction of swirl is found to substantially increase the rate of rise of static pressure at casing wall. The difference in static pressure between hub and casing wall increases with increase in swirl angle. The point of flow separation tends to shift away from the casing wall and can be completely vanished with high degree of inlet swirl however it may appear at the hub.

CONTENTS

Title			Page No.
Declaration			ii
Certificate			iii
Acknowledgment			iv-v
Abstract			vi
Contents			vii-ix
List of Figures			x-xii
List of Tables			xii
Nomenclature			xiii-xiv
CHAPTER 1		**INTRODUCTION**	**1-9**
1.1		Axial diffuser	2
1.2		Radial diffuser	2
1.3		Curved wall diffuser	3
1.4		Annular diffuser	4
1.5		Principal for diffuser design	5
1.6		Performance parameters	5-7
	1.6.1	Static Pressure Recovery Coefficient	6
	1.6.2	Diffuser Effectiveness	6
	1.6.3	Total Pressure Loss Coefficient	6
1.7		Swirling flows	7-9
	1.7.1	Physics of Swirling and Rotating Flows	7
	1.7.2	Method of swirl generation	8
1.8		Motivations	9
CHAPTER 2		**LITERATURE REVIEW**	**10-22**
2.1		Geometric Parameters	12-15
	2.1.1	Effect of Geometric Parameters	13
	2.1.2	Passage Divergence and Length	13
	2.1.3	Wall Contouring	15
2.2		Effects of flow Parameters	16-21
	2.2.1	Aerodynamic Blockage	16
	2.2.2	Inlet Swirl	17

	2.2.3	Inlet Turbulence	20
	2.2.4	Mach number Influence	20
	2.2.5	Reynolds Number Influence	21
2.3		Boundary Layer Parameter	21-22
	2.3.1	Boundary Layer Suction	22
	2.3.2	Blowing and Injection	22
CHAPTER 3		**MATHEMATICAL MODELLING**	**23-33**
3.1		Conservation Principals	23-25
	3.1.1	Mass Conservation Equation (Continuity Equation)	24
	3.1.2	Momentum Conservation Equations	24
3.2		Turbulence Modelling	25-27
	3.2.1	Choosing a Turbulence Model	26
3.3		The STANDARD, RNG, and REALIZABLE k-ε models	27-29
	3.3.1	The RNG k-ε Model	27
	3.3.2	Transport Equations for the RNG k-ε Model	28
	3.3.3	Modelling the Effective Viscosity	29
3.4		Turbulence Modelling in swirling flows	29-33
	3.4.1	Modelling Axisymmetric Flows with Swirl or Rotation	30
	3.4.2	Solution Strategies for Axisymmetric Swirling Flows	30
	3.4.3	Step-By-Step Solution Procedures for Axisymmetric Swirling Flows	31
CHAPTER 4		**CFD ANALYSIS**	**34-41**
4.1		Program Capabilities	34-35
4.2		Planning CFD Analysis	35-36
	4.2.1	Definition of the Modelling Goals	35
	4.2.2	Grid Generation and its Independence	36
	4.2.3	Choice of the Computational Model	36
	4.2.4	Choice of Physical Models	36
	4.2.5	Determination of the Solution Procedure	36
4.3		Discretization	36-38
4.4		Convergence criteria	38
4.5		Implementation of boundary conditions	38-39
	4.5.1	Inlet boundary condition	39

4.5.2	Outlet boundary condition	39
4.5.3	Wall boundary condition	39-40
4.6	Simulation Procedure	40-41
CHAPTER 5	**VALIDATION**	**42-47**
5.1	Grid Independence	42
5.1.1	Validation with Experimental results	42
5.2	Turbulence model validation	43-47
5.2.1	Validation with Experimental results	43-47
CHAPTER 6	**RESULT AND DISCUSSION**	**48-50**
6.1	Velocity Profile	48-49
6.2	Pressure Recovery Coefficient	49-50
6.3	Conclusion	50
CHAPTER 7	**FUTURE SCOPE OF WORK**	**51**
REFERENCES		**52-59**
APPENDIX		**84-85**

LIST OF FIGURES

S. No.	Title	Page No.
Figure 1.1	Basic diffuser geometries	3
Figure 1.2	Annular Diffuser Geometrical Parameters	4
Figure 1.3	Typical Radial Distribution of ω in a Free Vortex	8
Figure 5.1	Experimental Longitudinal Velocity (0°), AR 2	44
Figure 5.2	Longitudinal Velocity (0°) by CFD, AR 2	45
Figure 5.3	Experimental Longitudinal Velocity (12.5°), AR 2	46
Figure 5.4	Experimental Swirl Velocity (12.5°), AR 2	47

List of Contours of Static Pressure and Velocity Magnitude

Fig No-1	AR= 2, Swirl Angle = 0^0	60
Fig No-2	AR= 2, Swirl Angle = 7.5^0	61
Fig No-3	AR= 2, Swirl Angle = 12.5^0	62
Fig No-4	AR= 2, Swirl Angle = 17.5^0	63
Fig No-5	AR= 2, Swirl Angle = 25^0	64
Fig No-6	AR= 3, Swirl Angle = 0^0	65
Fig No-7	AR= 3, Swirl Angle = 7.5^0	66
Fig No-8	AR= 3, Swirl Angle = 12.5^0	67
Fig No-9	AR= 3, Swirl Angle = 17.5^0	68
Fig No-10	AR= 3, Swirl Angle = 25^0	69

List of pressure coefficient graphs

Fig No-11	AR 2, Pressure coefficient for 0^0 swirl	70
Fig No-12	AR 2, Pressure coefficient for 7.5^0 swirl	70
Fig No-13	AR 2, Pressure coefficient for 12.5^0 swirl	71
Fig No-14	AR 2, Pressure coefficient for 17.5^0 swirl	71
Fig No-15	AR 2, Pressure coefficient for 25^0 swirl	72
Fig No-16	AR 3, Pressure coefficient for 0^0 swirl	72
Fig No-17	AR 3, Pressure coefficient for 7.5^0 swirl	73
Fig No-18	AR 3, Pressure coefficient for 12.5^0 swirl	73
Fig No-19	AR 3, Pressure coefficient for 17.5^0 swirl	74
Fig No-20	AR 3, Pressure coefficient for 25^0 swirl	74

List of longitudinal and swirl velocity graphs

Fig No-21	AR 2, Longitudinal Velocity for 0° swirl	75
Fig No-22	AR 2, Longitudinal Velocity for 7.5° swirl	75
Fig No-23	AR 2, Longitudinal Velocity for 12.5° swirl	76
Fig No-24	AR 2, Longitudinal Velocity for 17.5° swirl	76
Fig No-25	AR 2, Longitudinal Velocity for 25° swirl	77
Fig No-26	AR 2, Swirl Velocity for 7.5° swirl	77
Fig No-27	AR 2, Swirl Velocity for 12.5° swirl	78

Fig No-28	AR 2, Swirl Velocity for 17.5° swirl	78
Fig No-29	AR 2, Swirl Velocity for 25° swirl	79
Fig No-30	AR 3, Longitudinal Velocity for 0° swirl	79
Fig No-31	AR 3, Longitudinal Velocity for 7.5° swirl	80
Fig No-32	AR 3, Longitudinal Velocity for 12.5° swirl	80
Fig No-33	AR 3, Longitudinal Velocity for 17.5° swirl	81
Fig No-34	AR 3, Longitudinal Velocity for 25° swirl	81
Fig No-35	AR 3, Swirl Velocity for 7.5° swirl	82
Fig No-36	AR 3, Swirl Velocity for 12.5° swirl	82
Fig No-37	AR 3, Swirl Velocity for 17.5° swirl	83
Fig No-38	AR 3, Swirl Velocity for 25° swirl	83

LIST OF TABLES

S. No.	**Title**	**Page No.**
Table 1	Geometric Parameters of Annular Diffuser	85

NOMENCLATURE

A	Area
AR	Area ratio
B	blockage factor
C	Constants
C_P	Pressure recovery co-efficient
C_{PI}	Ideal pressure recovery co-efficient
D	Diameter
G	generation of turbulence kinetic energy
g	acceleration due to gravity
K	Total pressure loss co-efficient
k	Turbulent kinetic energy
P	Static pressure
P_t	Total pressure
Re	Reynolds number
S	Swirl Number of flow
S_m	Mass added
U	Velocity
w	Swirl velocity
x, y, z	Cartesian coordinate system
Y_M	fluctuating dilatation in compressible turbulence.

Symbols

$\bar{\bar{\tau}}$	Stress tensor
μ	laminar viscosity
μ_t	turbulent viscosity
2θ	Equivalent cone angle
Γ	Circulation
ε	Turbulent kinetic energy dissipation rate
η	Diffuser effectiveness
θ	Wall angle
ν	Kinematics viscosity
ξ	Total pressure loss co-efficient
ρ	Density
Σ	Turbulent Prandtl no.

CHAPTER 1 INTRODUCTION

The function of a diffuser is to retard the fluid flow and to recover total pressure. It is hard to arrange for an proficient deceleration of fluid flow than to obtain an efficient acceleration.

Diffusers play a very important role in many fluid equipment to change kinetic energy into pressure energy. The effectiveness of this conversion procedure is vital as it affects the overall performance of the mechanism. The pressure recovery, which is use to calculate of performance of diffusers, depends on a number of dynamical and geometrical constraint. Some geometrical constraint that control the performance of a diffuser are length of inlet and duct size, diffuser's area ratio, angle of expansion, diffuser length, profile of the outlet duct with several discharge conditions, etc. The dynamical constraints are inlet velocity profile, boundary layer parameters, Reynolds number, Mach number etc. In the present work, two parameters namely inlet velocity and the geometry of the diffuser were selected in order to study their effects on the flow structure and performance of annular diffusers. Flow separation mainly depends on swirling flow in the diffuser and consequently the performance of the diffuser depends on it. Therefore, to optimize design of diffuser more attention is paid to the prevision of the swirling flow characteristics. It is found that flows in the annular diffusers are strongly dependent on the shapes of the inlet and outlet parameters.

Diffusers are widely used in compressors like centrifugal and axial flow, ram jets, inlet segment of jet engines etc. Exchange of kinetic energy takes place in these rotating machineries to achieve the desired purpose. Therefore, huge amount, approximately 50% of the total energy transferred, of residual kinetic energy go together with the work input and work withdrawal processes. Therefore minute

change in pressure recovery can improve the efficiency appreciably. So diffusers are extremely essential for high performance of turbo machinery.

1.1 AXIAL DIFFUSER :– In these diffusers, fluid flows alongside the axis of diffusers and there is incessant retardation of the flow.

Axial diffuser is divided in to the following categories-

• Conical diffuser

• Channel diffuser

• Annular diffuser

The basic geometric parameters for these type of diffusers are as follows:

For **conical diffuser:**-

Non dimensional length, L/W_1

Aspect ratio, $AS = b/W_1$

Area ratio, $AR = A_2/A_1$

$AR=1+2(L/W_1)\tan\theta$

For **channel diffuser:**-

Non dimensional length, L/D_1

Area ratio, $AR = A_2/A_1$

$AR=[1+2(L/D_1)\tan\theta]^2$

For **annular diffuser:**-

Non-dimensional length, $L/\Delta r$ or L/h

Area ratio, $AR = A_2/A_1$

$AR=1+2(L/h_1)\sin\theta$ (For equiangular case)

1.2 RADIAL DIFFUSER :– In this diffusers fluid flows in radially outward direction in restricted space between the two boundaries. Diffuser used in radial turbo

machinery comes under this group. They may be vane less and vane types. This type of diffuser may change kinetic energy into static pressure rise by one or two methods –1) a reduction in the average velocity by increase in flow passage area, 2) to recover in angular velocity according to the conservation of angular momentum by changing the mean flow path radius.

1.3 CURVED WALL DIFFUSER :– In modern time most of the aircrafts use curved wall diffuser. In aircraft engines a number of modifications may bring in non uniformities and higher level of turbulence in flow field incoming the diffuser. In addition, mechanical and structural condition place limits on the length of the passage. Curved wall diffuser is helpful in this case and well-suited with downstream condition of flow.

Curved diffusers are broadly classified as –

- Half diffuser or part turn diffuser.
- U- diffuser.
- S- Diffuser.
- Y-Diffuser.

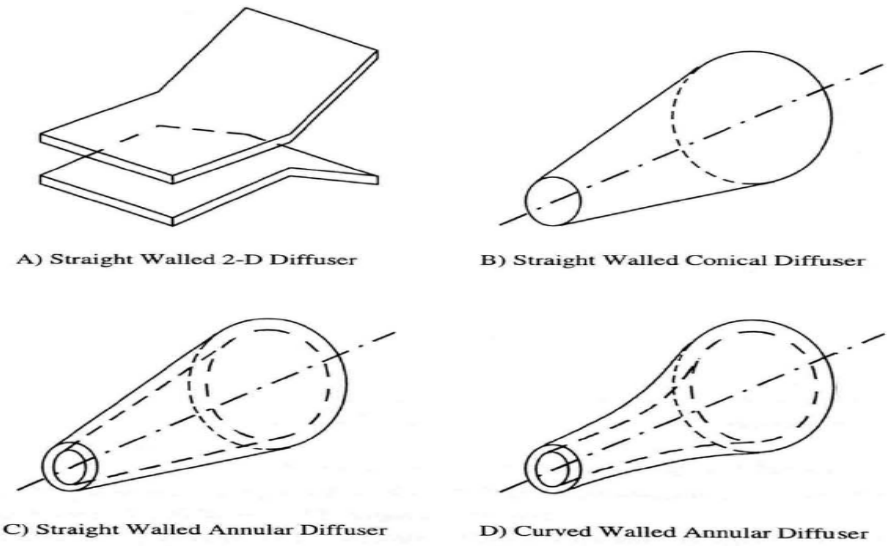

Fig.1.1 Basic diffuser geometries [Glyn Norris ,1997]

1.4 ANNULAR DIFFUSER

A review of diffuser research has discovered that more investigations have been carried out on 2D and conical diffusers. A lot of work covering annular diffusers was done in the experimental laboratory. Annular diffuser are enormously used in aircraft applications. Annular diffuser can achieve the maximum pressure recovery in the shortest possible length. In annular diffuser, an inner surface is present to direct the flow radially outward so excellent performance is achievable with large wall angles. Since there is an inner surface that can be changed independently of the outer surface, the annular diffuser yields the possibility of inserting many different geometric combinations. Since the numbers of free variables are large, it is unmanageable to define the crucial geometric parameters for annular diffusers ***Goebel and Japikse [1981]***. The important variables to describe the geometry of annular diffuser are two wall angles, area ratio, non-dimensional length and inlet radius ratio. Geometry becomes more complex when the number of variables increases. This has not been economically feasible by experiments and hence the development of computational fluid dynamic method takes place to explore the performance characteristics of annular diffuser ***Arora, and Pathak [2005]***. The present study investigates the unequal angle type of annular diffuser. In these types of annular diffusers both hub and casing are diverging outward with different angle of divergence. Hub angle is kept constant at 5°.

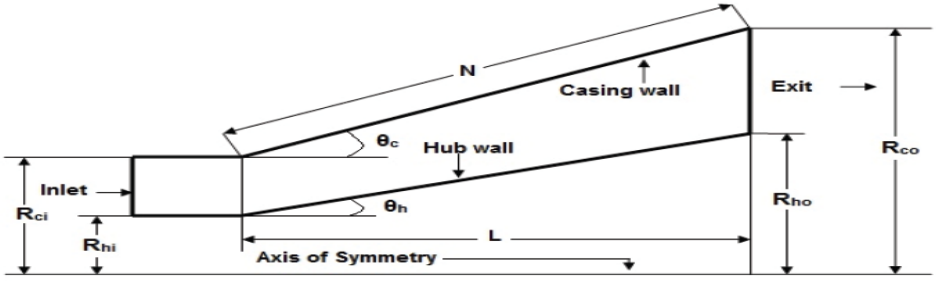

Fig.1.2 Annular Diffuser Geometrical Parameters [Arora B.B., 2014]

1.5 PRINCIPLE FOR DIFFUSER DESIGN

Since flow in diffusers are subjected to an adverse pressure gradient there is potential danger for flow separation to occur which leads to loss in performance and damage of downstream equipment. The aim of design is to keep the adverse pressure gradient as high as possible, but below a critical limit, by controlling the length versus area-ratio of the diffuser.

The design requirements for a good diffuser are as following:-

Convey the flow efficiently by transferring a portion of the kinetic energy into a static pressure rise.

1. It must accept a variety of inlet conditions including extreme swirl, blockage and Mach number.
2. Deliver the fluid with reasonable velocity and angle profiles without separated regions.
3. Wall curvature must not have a deleterious effect upon passage performance.
4. Pressure recovery achieved over a short axial length.

While obtaining the best possible design, some limitations are imposed on a diffuser.

1. Limited length
2. Specified area ratio
3. Specified cross- sectional shape
4. Maximum static pressure recovery
5. Minimum stagnation pressure loss

1.6 PERFORMANCE PARAMETERS

Performance parameters are extremely assistive in designing and forecasting the performance of diffusers. These parameters expose that diffuser geometry will give the desire output or not. The following parameters are important to find out diffuser performance.

1.6.1 Static Pressure Recovery Coefficient :–

A diffuser is normally used either to recover static pressure or to minimize total pressure loss in a pipe or in a duct. The pressure recovery coefficient of a diffuser is most commonly defined as the static pressure rise through the diffuser divided by the inlet dynamic head.

$$C_p = \frac{p_2 - p_1}{\frac{1}{2}\rho v^2_{av1}} \tag{1}$$

Where subscripts 1 and 2 refers to diffuser inlet and outlet conditions respectively. v_{av1} represents the average velocity at the inlet. An ideal pressure recovery can be defined if the flow is assumed to be isentropic. Then, by employing the conservation of mass, this relation can be converted to an area ratio for incompressible flow.

$$C_{pi} = 1 - \frac{1}{AR^2} \tag{2}$$

1.6.2 Diffuser Effectiveness :–

The diffuser effectiveness is simply the relation between the actual recovery and the ideal pressure recovery.

$$\eta = \frac{C_p}{C_{pi}} \tag{3}$$

This is an excellent parameter for judging the probable level of performance when it is necessary to estimate the expected performance under unknown conditions, relative to available data.

1.6.3 Total Pressure Loss Coefficient :–

The total pressure loss coefficient reflects the efficiency of diffusion and drag of the system. The most common definition of loss coefficient is as the ratio of total pressure rise to the diffuser inlet dynamic head.

$$K = \frac{\overline{p}_{01} - \overline{p}_{02}}{\frac{1}{2}\rho v^2_{av1}} \tag{4}$$

$$K = \frac{\left(\overline{u}_1^2 - \overline{u}_2^2\right)}{U_i^2} - C_p \quad = \quad \left(\alpha_1 - \alpha_2 \middle/ AR^2\right) - C_p \tag{5}$$

Where p_{02} is the total pressure in the core region at the exit, the over bar indicate the mass averaged quantity, and α_1 and α_2 are the kinetic energy parameters at the inlet and exit of the diffuser. For the case where the velocity profile at the inlet of diffuser is flat with a thin wall boundary layer, $\alpha_1=1$. However, due to the thickening of boundary layer through the diffuser, α_2 is generally greater than unity. Nonetheless, it is often assumed that kinetic energy coefficient are equal to unity, than

$$K = C_{pi} - C_p \tag{6}$$

Since flow in diffusers are subjected to an adverse pressure gradient there is a potential danger for flow separation to occur which could lead to loss in performance as well as damage downstream equipment. The aim of design is to keep the adverse pressure gradient as high as possible, but below a critical limit, by controlling the length versus area-ratio of the diffuser.

The overall efficiency of the turbo machine is strongly influenced by the performance of the diffuser. Thus if excellent turbo machinery performance is to be obtained, the detailed processes which happens in diffusing elements must be carefully understood and thoroughly optimized.

1.7 SWIRLING FLOWS

1.7.1 Physics of Swirling and Rotating Flows :-

In swirling flows, conservation of angular momentum ($r\omega$ or $r^2\Omega$ = constant) tends to create a free vortex flow, in which the circumferential velocity, ω, increases sharply as the radius, r, decreases (with ω finally decaying to zero near r = 0 as

viscous forces begin to dominate). A tornado is one example of a free vortex. Figure depicts the radial distribution of ω in a typical free vortex.

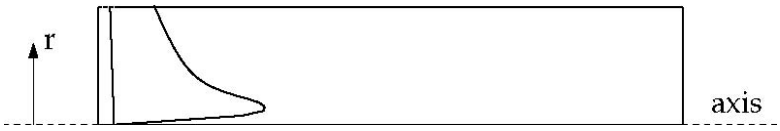

Fig.1.3 Typical Radial Distribution of ω in a Free Vortex

It can be shown that for an ideal free vortex flow, the centrifugal forces created by the circumferential motion are in equilibrium with the radial pressure gradient:

$$\frac{\partial p}{\partial r} = \frac{\rho \omega^2}{r} \tag{7}$$

As the distribution of angular momentum in a non-ideal vortex evolves, the form of this radial pressure gradient also changes, driving radial and axial flows in response to the highly non-uniform pressures that result. Thus, as you compute the distribution of swirl in your FLUENT model, you will also notice changes in the static pressure distribution and corresponding changes in the axial and radial flow velocities. It is this high degree of coupling between the swirl and the pressure field that makes the modeling of swirling flows complex.

In flows that are driven by wall rotation, the motion of the wall tends to impart a forced vortex motion to the fluid, wherein w/r or Ω is constant. An important characteristic of such flows is the tendency of fluid with high angular momentum (e.g., the flow near the wall) to be flung radially outward. This is often referred to as "radial pumping", since the rotating wall is pumping the fluid radially outward.

1.7.2 Method of swirl generation :-

Methods of including rotation in a stream of fluid can be divided into three principle category:

- Tangential entry of the fluid stream, or a part of it, into the cylindrical duct.
- The use of guide vanes in axial tube flow.

- Rotation of mechanical devices which impart swirling motion to the fluid passing through them. This includes rotating vanes or grids and rotating tubes.

1.8 MOTIVATIONS

The purpose of this study is to investigate the level of knowledge and in certain important areas the lack thereof, concerning the performance of annular diffusers. For decades investigators have conducted individual studies without a careful consideration of how all the studies may be interwoven. A pattern of consistent behaviour among the database elements for annular diffusers is established in this investigation. However, it may be of even greater significance that the investigation reveals areas where critical design knowledge is missing. It will be observed that conducting individual investigations of annular diffuser performance has blinded most investigators from seeing the larger picture and the critical interactions between the different variables which have been discussed in the literature. This study begins by looking at historical data, then proceeds to investigate the parametric dependence, resulting in the development of a preliminary design set of equations and then finally by careful examination of further investigations which are needed before the annular diffuser design problem will be well understood.

CHAPTER-2 LITERATURE REVIEW

When fluid flow takes through a diffuser there is reduction of mean kinetic energy and a consequently increase in pressure. There is a normal trend in a diffusing process for the flow to split away from the walls of the diverging path, reverse its direction, and flow back in direction of the pressure gradient. If the deviation is too rapid, this can cause the formation of eddies with transfer of some kinetic energy into internal energy and thus reduction in useful pressure rise. When the angle of divergence will be small, diffuser will be long and therefore a high value of skin friction loss will occur. Due to the added pressure loss, flow separation in a diffuser is to be avoided. Excluding many strongly separated flows, for example the flow over a backward facing step, the point of flow separation, is not defined by the geometry but entirely by the pressure gradient in diffuser. Therefore, flow in diffusers are very susceptible and are hard to predict with numerical means. Diffusers have been studied widely in the past, since this is a very common flow configuration. Apart from the characterization of diffusers, these flows are used to study elementary physics of pressure-driven flow separations.

Starting 1950s through the 1980s considerable amount of research was done in the experimental laboratory to discover some of the unusual performance characteristics of annular diffusers. Conversely By the late 1980s, the experimental research had reduced considerably due to a lack of government funding in a number of countries where the work had previously been extensive. It is, therefore, convenient to review the data which has been existing and to look for patterns within this data. It is also necessary to find out how this data may best be used in future design studies and where it desires to be further enhanced. Much of the inventive data was taken in order

to sustain studies of axial compressor discharge diffusion as flow leaves a compressor and enters a combustion chamber. Other work was done for exhaust diffusers of hydroelectric turbines, small gas turbines, and turbochargers. While these topics are still significant today and there are important unanswered questions, the level of activity has reduced. Now important research topics must be cautiously selected for the more narrow studies possible in future years.

A lot of tests were carried out by many persons on geometric parameter of diffuser. ***Sovran et. al. [1967]*** who tested more than hundred different geometries, almost which had conically diverging centre bodies with an inlet radius ratio [Ri/Ro] of 0.55 to 0.70. The tests were carried out with a thin inlet boundary layer and the diffusers have free discharge. The tests were present as contours of pressure recovery plotted against area ratio and non-dimensional length. ***Howard et. al. [1967]*** also examined symmetrical annular diffusers with centre bodies of unvarying diameter, using fully developed flow at inlet. The limits of the different flow regimes and the best possible performance lines were established. Some other researchers also bestowed in the field of annular diffuser and resolved various important results. Much of the extent data covering the annular diffusers was done in the experimental laboratory to find out some of the strange performance characteristics of annular diffusers. But there are still some vital unanswered questions because of the numbers of independent variables are large for annular diffusers. In the annular diffuser the flow happen between two boundary surfaces which can varies independently.

This chapter involves a organized study of different flow and geometric parameters which control the overall and internal performance of annular diffusers. In this regard the available literature has been studied with a view to make remarks on the state of the art and to know the scope of further research on the subject.

2.1 GEOMETRIC PARAMETERS

Any diffuser geometry with growing area in the flow path constitutes subsonic diffuser geometry, therefore, the number of different diffusers geometries can be obtained in infinite ways, though in practice sufficient design data are available for limited numbers of geometries.

1. Rectangular cross section plan diffusers
2. Conical diffuser
3. Annular diffuser

Some of the non dimensional parameters that are found to be significant in terms of diffuser performance is area ratio, AR, the area ratio of diffuser exit to inlet areas .The area ratio determine the theoretical diffusion of pressure recovery expected.

The second important parameter is the ratio of the length of the diffuser to the inlet throat half-width *(l/d)*, may be used as the key parameters for the design of the diffuser.

The third geometric parameter usually used in displaying diffuser performance is the wall divergence angle, 2θ, for planar and conical diffusers.

Area ratio and non dimensional length narrates the overall diffusion and pressure gradient correspondingly, which is the main feature in boundary layer development. ***Markland et. al. [1986]*** discovered that a variation in the AR from 2.5 to 8.0 has a small consequence on the loss coefficients of the 2-D diffuser. ***Sharan[1972]*** found that for a constant AR the performance of diffuser drops with the increase in diffusion angle. ***Reneau et. al. [1967]*** accomplished that for 2D straight diffusers, the maximum pressure recovery at a constant AR occurs in the range of diffuser angle equal to 6-8degree.

2.1.1 Effect Of Geometric Parameters

In an annular diffuser, variation of pressure recovery and inlet condition of flow is influenced by a number of different geometric constraint. The fundamental equations of motion disclose the importance of both geometric and aerodynamic parameters on the decisive performance of annular diffuser. The specification of a wide range of geometric parameters is essential before the performance of diffuser is given. The different geometric parameters and their influence on diffuser performance is reviewed in this section. ***Arora B.B et. al. [2005]*** established effect of geometry on the performance of annular diffuser. ***Krystyna prync-skotniczny [2006]*** carried numerical investigation of the impact of conical diffuser geometry change on velocity distribution in its outlet cross-section. ***Japikse Dr. David [2000]*** give relationship of annular diffuser performance with geometry, swirl and blockage.

2.1.2 Passage Divergence And Length

Area ratio, AR, and non-dimensional length dictates the overall diffusion and pressure–gradient correspondingly, which is the major factor in boundary layer development. ***Henry et. al. [1958]*** conducted the experiment on subsonic annular diffuser. They have taken two diffusers with area ratio 2.1 and divergence of 5º and 10º and tested at various Mach number. They found that most of data clusters around a line of constant Effectiveness. It is also noticed that the inner wall is being starved of fluid. If elevated divergence had been used, then one might foresee stall on the inner surface. An experimental study is carried out by ***Kmonicek et. al. [1974]*** in which, the pressure loss coefficient is caught out on the basis of the work of compression required to cope with the static pressure rise, the results are very fascinating but difficult to understand due to use of unconventional terminology. ***Sovran et. al. [1967]*** and ***Howard et. al. [1967]*** produced the first broadly used

annular diffuser maps for channel diffusers. ***Sovran et. al. [1967]*** conducted a lot of performance measurements which spanned a broad collection of geometric types of diffusers. The map is only a broad illustration of the bulk of configurations tested in the vicinity of their best performance areas. The inferior diffusers are not well defined by the map. These maps also show best possible diffuser geometrics under diverse conditions and two optimum lines are established. The same results were found out by ***Howard et. al. [1967].*** The important difference between this and the ***Sovran et. al. [1967]*** map was that the second was made for very low inlet aerodynamic blockage whereas the former study was carried out for fully developed inlet profiles, implying high aerodynamic blockage. Along the line of peak recovery there is quite good agreement between the two maps but in the section of heavy transitory stall the maps disagree substantially.

Johnston [1953] and ***Johnston [1959]*** conducted the study of four different annular diffusers. Three of them agree adequately well with the basics ***Sovran et. al. [1967]*** map, one of them disagree significantly; the strong disagreement in other diffuser is probably due to stall. ***Srinath [1968]*** considered four equiangular annular diffuser with 2θ equals to 7º, 10º, 15º and 20º correspondingly. Tests were described with a array of L/Δr values. An broad study of annular diffusers with a circular cross section was studied by ***Ishikawa et. al. [1989]***. The author establish that the performance of the diffuser differed notably depending on whether it is parallel or diverging for L/r1 greater than about 2. When both types have the same non dimensional length and area ratio, the parallel diffuser has the higher C_P. The lines of optimum performance are also depicted. ***Ishikawa et. al. [1989]*** also attempted to compare their results with those of ***Sovran et. al. [1967]*** for a conventional annular diffuser for the same wall length and area ratio, their diffuser was superior, but since the inlet conditions were

different in the two studies, this conclusion is only tentative. It was also found that the addition of a conical centre body improves the performance of simple conical diffusers with appreciable or large stall. The experiment carried out by ***Moller [1965]*** who designed an axial to radial band with the purpose of eliminating diffusion in the inlet region; found that the peak pressure recovery for the whole band and radial diffuser sections was 0.88 and 0.82 for the low blockage and high blockage cases, respectively. ***Cockrell et. al. [1963]*** found that a variation in the area ratio from 2.5 to 8.0 has a little effect on the loss coefficients of conical diffusers. ***Kumar Manoj et. al.[2012]*** carried out investigation to study distribution of mean velocity, static pressure and total pressure on parallel hub diverging casing type annular diffuser on area ratio 2.01 and casing divergence angle of 10.09°. Pressure recovery coefficient decreases with the enlargement in passage length and increases with the growing area ratio keeping other factors constant.

2.1.3 Wall Contouring

Numerous annular diffuser studies have been published in which contoured walls were an essential part of the design problem. ***Thayer [1971]*** found that curved wall diffusers had pressure recovery as high as 0.61 to 0.65 for an area ratio of 2.15. An extensive study by ***Stevens et. al. [1980]*** reported that for curved wall diffuser, good pressure recovery was achieved for a loss significantly below the level which would be expected from pressure recovery loss correlation , but pressure recovery values were lower than those which would be expected from the ***Sovran et. al. [1967]*** map. Upon careful assessment, it was determined that the boundary layers in this diffuser are different from those which would be expected in most diffuser studies. ***Takehira et. al. [1977]*** presented extensive data for a large set of both straight annular diffusers and curved wall diffusers, and decided that the use of strong curvature at the exit of

diffuser was not debilitating but did produce a penalty compared to no curved diffusers or diffusers with curvature at the inlet.

An additional study by ***Japikse [2000]*** shows that for pressure recovery wall contouring is an significant parameter. ***Adkins et. al. [1983]*** tried out an annular diffuser of constant outer radius and a conical centre body with cones of dissimilar angles. In general with decreasing cone angle the pressure recovery increases for various area ratios, but the 132º and sometimes the 45º-cone angle produced lower pressure recoveries than an equivalent sudden expansion. This was accredited to a large and rapid separation at the base of the cone where the diffuser starts. To improve the performance ,a radius to the base of the cone is added so that it smoothly blended into the upstream hub.

Kumar Manoj et. al.[2012] examined the annular diffuser with different equivalent cone angles of 10°,20°& 30° with no inlet swirl for flow separation and pressure recovery. Coefficient of performance diminishes with the increase in the equivalent angle of the diffuser at both hub and casing walls at the exit.

2.2 EFFECTS OF FLOW PARAMETERS

2.2.1 Aerodynamic Blockage

In comparison to channel and conical diffusers, aerodynamic blockage on annular diffuser is much less. The basic boundary layer equations disclose the consequence of the displacement thickness as a characteristic length scale of the inlet boundary layer flow. ***Stratford et. al. [1965]*** accepted the importance of the boundary layer displacement thickness to pressure recovery method .It is evident that thin inlet boundary layer should be helpful to high diffuser recovery and as the inlet boundary thickness increases, longer diffusers are necessary to achieve high level of recovery.

Thayer [1971] reported that pressure recovery as high as 0.61 to 0.65 is possible for curved wall diffusers for an area ratio of 2.15. An extensive study by ***Stevens et. al. [1980]*** found that for curved wall diffuser, fine pressure recovery was detected for a loss significantly below the level which would be expected from pressure recovery loss correlation , but pressure recovery values were lower than those which would be expected from the ***Sovran et. al. [1967]*** map. ***Klein [1995][31]*** compared ***Stevens et. al. [1980]*** data with the result of ***Sovern et. al. [1967]*** for an inlet blockage of .02 and with forecasting using the latter's method for diffuser performance for larger blockages. A inclusive study on the effect of aerodynamic blockage on annular diffuser performance carried out by ***Goebel et. al. [1981].*** Similar calculations were made at 20º and 40º of inlet swirl. In all cases the data pattern was in the course of reduced pressure recovery for increased aerodynamic blockage. Upon careful examination, it was found that the boundary layers in this diffuser are different. ***Mazumdar P.M. et. al.[2003]*** done aerodynamic design optimization. First, the influence of inlet situation on annular diffuser performance is more complex than for channel and conical diffuser. In this case, both the hub and casing surfaces can develop boundary layers with considerably different histories. As they pass through the diffuser the two differing boundary layers will experience different growth processes. Additionally, blockage on one wall has the effect of altering the effective flow area and hence the core flow velocity, thus influencing the growth of the boundary layer on the opposite wall. Because of this reason complex interactions can build up within the diffuser.

2.2.2 Inlet Swirl

The performance of an annular diffuser can itself influence the method of swirl generation and, therefore, concern must be given first to this problem. Most of the

experiment have done to generate swirl in a radial inflow plane with the intention of the advantage of simple cascade design geometry. Some investigators have preferred to use axial cascade design which have the advantage that they more narrowly simulate specific turbo machinery flow situation and allow control of the spacing between the diffuser and the vanes in form that may be more characteristic of an actual turbo machine. An efficient sealing is not possible in axial cascade due to tip and hub leakage because the axial cascades are of a variable geometry type. In addition to inlet swirl, there may be changes in inlet turbulence intensity, velocity or total pressure gradients, vorticity or wake shading, and inlet aerodynamic blockage may change indirectly as a function of the swirl angle as it is varied. The consequence of swirl variation must be traced from the performance data. ***Dovzhik et. al. [1975]*** also presented the same type of analysis that the best performance can be reached between the ranges of 10º to 20º of inlet swirl angle. A study is presented by ***Japikse et. al. [1978]*** of an exhaust diffuser and hood, found that considerable recovery has been achieved even up to swirl angle in excess of 40º.***Kochevsky A.N. [2004]*** studied numerical analysis of swirling flow in annular diffusers with a rotating hub placed at the exit of hydraulic machines. Another numerical investigation of swirl flow on conical diffuser was done by the ***Walter Gyllenram et. al. [2006] . Najafi A.F. [2004]*** have done analysis of turbulent swirling decay pipe flow. The flow behavior through a revolving honeycomb and consequential downstream swirling decay flow along a fixed pipe have been investigated in this research. For the prediction of the downstream flow, the rotating honeycomb have major importance. The flow field characteristics obtained by the honeycomb tubes have a significant effect on the downstream flow. ***Ogor Buntiæ et. al. [2006]*** gives the adaptive turbulence model for swirling flow.

Kumar Manoj et. al.[2011] carried out investigation to predict flow performance inside the parallel hub and diverging casing annular diffuser of area ratio 3. The outcome of various inlet swirl angles between 0° and 25° has been calculated to forecast the reversal of flow and separation of flow from the wall. The result of inlet swirl on the pressure recovery coefficient has also calculated. It is found that the longitudinal velocity decreases downstream continuously regardless of whether the inlet flow is swirling or non-swirling. With the application of swirl, the flow is shifted towards casing wall hence making the flow stronger towards casing than hub wall. Also the recovery is faster towards the casing wall. As the flow proceeds downstream, the effect of swirl decreases gradually and the recovery is negligible in the direction of the diffuser exit.

Arora B.B. et. al. [2010] carried out investigation using k-ε RNG turbulence mode to find out the point of flow separation and pressure recovery coefficient on Annular diffuser of a particular Area ratio 2. Analysis disclose that at lower swirl angle the separation is close to the casing while at higher swirl the point of separation shifts in the direction of hub side.

Arora B.B. et. al. [2009] carried out analysis for flow regime with different experimentally obtained inlet velocity profiles with or without swirl and found that pressure recovery coefficient increases through the diffuser passage. With the introduction of swirl the recovery is faster and the flow is forced in the direction of casing wall thus building the flow stronger towards casing than hub wall. Also the outcome of swirl appears to slowly perish as the flow continues downstream and the revival is small near the diffuser exit.

2.2.3 Inlet Turbulence

Cockrell et. al. [1963] found that diffuser performance rises as approach length increases. This is due to changes in turbulence which increases mixing transverse to flow directions, thus reducing the distortions. Definitely, the core turbulence intensity of increasing pipe flow rises considerably from La /D is equal to 20 to 45 and then remains nearly invariable. The statistics of ***Coladieiepro et. al. [1974]*** have integrated both low and high inlet turbulence intensity levels and this might be the reason for the strange measurements observed at different blockage. Study of ***Stevens et. al. [1969]*** and ***Stevens et. al. [1973]*** showed that significant betterments in radial momentum transport were attained by turbulence making grids and wall spoilers***. Hesterman et. al. [1995]*** and ***Klein [1995]*** also show that escalating the level of turbulence to 6 – 8.5 % is favorable in increasing the pressure recovery and removing the separation of stalled diffuser. ***Ubertini et. al. [2000]*** determined the flow development in terms of the mean and fluctuating components of the velocity and turbulence dissipating eddy length scales in annular exhaust diffuser. The K-ε and other turbulent models are assessed by ***Arora.B.B. et. al [2005]*** with respect to their applicability in swirling flows. In the majority of the past numerical simulations, swirling air is inserted perpendicular to the axis***. Leschziner M.A.[2004]*** had done modelling on turbulent separated flow in the perspective of aerodynamic applications. Experimental and computational studies of turbulent separating internal flows done by ***Tornblom Olle[2006].*** From the above study the conclusion is that the influence of increasing inlet turbulence intensity increases pressure recovery.

2.2.4 Mach number Influence

A number of reports have revealed measurement at different Mach number. Most annular diffuser study has been executed at low inlet mach numbers. The research by

Wood et. al. [1958], ***Thayer [1971]***, and ***Japikse et. al. [1978]*** reveal virtual independence of revival with Mach number up to some stage of around 0.80 to 1.1. The actual level depends on method of measurement and the type of inlet. ***Wood et. al. [1958]*** show that a shock structure must be presented before the performance begins to deteriorate, but the reference Mach number may have little to do with the actual shock location and shock structure. In most cases, the reduction of performance with Mach number is very slight but in a few cases there can be a degradation of five or ten point of performance recovery.

2.2.5 Reynolds Number Influence

Viscosity is an vital constraint in any fluid dynamic process and generally appears in the form of a Reynolds number. Typically, diffusers are characterized by a Reynolds number based on an inlet hydraulic diameter. All studies reveal that when the flow is in the fully turbulent regime, the Reynolds number is a reasonably weak parameter. ***Crockrell et. al. [1963]*** state that a variation of the inlet Reynolds number has no significant effect on the diffuser performance if this variation is uncoupled from its effects on the inlet boundary layer parameters. Whenever inlet boundary parameters remain constant, the variation of Reynolds number within the range of 2×10^4–7×10^5, the diffuser performance would be nearly independent of Reynolds number. ***Sharan [1972]*** found that when Reynolds number increases, there is no variation in pressure recovery for thick boundary layers.

2.3 BOUNDARY LAYER PARAMETER

The behavior of the boundary layers at the diffuser walls regulate the flow in diffuser. The pressure rise is produced by deceleration of the flow through the diffuser. The wall shear layers are thus subjected to a positive or adverse pressure gradient. Adverse

pressure gradients can cause the wall boundary layers to thicken and possibly separate from the diffuser walls, forming areas of backflow in the diffuser. The blockage of flow area is because of the net result of thickening of the wall boundary layers or the creation of regions of backflow, which brings down the effective area existing to the flow. Drop in effective area of flow results in reduced pressure rise through the diffuser.

2.3.1 Boundary Layer Suction

The outcome of suction consists in the exclusion of decelerated fluid particles from the boundary layer before the separation. ***Wilbur et. al. [1955]*** shown that suction control is not proficient when applied in an broad backflow region. ***Wilbur et. al. [1957]*** investigated the suction incident and found the decrease in the measured total pressure loss by 63% and a suction flow rate of 2.3% increased the static pressure rise by 25 – 60% . Experiments by ***Juhasz [1974]*** on short annular diffuser showed that the diffuser exit profiles could be shifted either towards the hub or towards the casing of annulus by bleeding off a small fraction of the flow through the inner and outer wall respectively. Boundary Layer Suction for both channel and conical diffuser with large divergence angle is also adopted by ***Ackert [1967]***.

2.3.2 Blowing and Injection

Wilbur et. al. [1955] show that , 33% increases in the calculated static pressure rise and 50% reduction in the measured total pressure loss can be achieved by an injection rate of 3.4%. ***Juhasz [1974]*** conducted experiments on the consequence of injecting secondary fluid into wide angle conical diffusers through annular slot at inlet and found the result in significant enhancement in the uniformity of exit flow and in the magnitude of pressure recovery.

CHAPTER 3 MATHEMATICAL MODELING

FLUENT allows complete modelling capacities for extensive range of incompressible laminar and turbulent fluid problems. In FLUENT, a wide range of mathematical models for transport phenomena (like heat transfer, swirl and chemical reactions) is combined with the facility to model complex geometries. The variety of problems that can be addressed is very broad. The turbulence models provided have wide range of applicability without the necessity for fine tuning to a specific application.

FLUENT uses four equations to simulate a 2-D flow problem in addition to the turbulence modeling equations. These four equations are

- Conservation Principle
  - Momentum equation
  - Continuity equation
- Velocity Equations
  - X- velocity equation
  - Y- velocity equation

3.1 CONSERVATION PRINCIPALS

Conservation laws can be deduced in view of a given quantity of matter or control mass and its extensive properties, such as mass, momentum and energy. This approach is used to analyse the dynamics of solid bodies. In fluid flows, however it is not easy to follow a parcel of matter. It is more suitable to deal with the flow within a certain spatial area we call a control volume, rather than a parcel of matter, which rapidly passes through the region of interest. For all fluid flows the two extensive properties mass and momentum are solved. Flows linking heat and mass transfer or

compressibility, a supplementary equation of energy conservation are solved. When the flow is turbulent, additional flow transport equations are solved

3.1.1 The Mass Conservation Equation (Continuity Equation)

The equation for mass conservation or continuity equation, can be written as follows:

$$\frac{\partial p}{\partial t} + \nabla.\left(\rho \vec{v}\right) = S_m \tag{8}$$

Equation is the common form of the mass conservation equation and is valid for incompressible as well as compressible flows. S_m is the mass added to the continuous phase from the dispersed second phase (e.g., due to vaporization of liquid droplets) and any user-defined sources.

The continuity equation for 2D axisymmetric geometries is given by

$$\frac{\partial p}{\partial t} + \frac{\partial}{\partial x}\left(\rho v_x\right) + \frac{\partial}{\partial r}\left(\rho v_r\right) = S_m \tag{9}$$

Where x is the axial coordinate, r is the radial coordinate, v_x is the axial velocity, and v_r is the radial velocity.

3.1.2 Momentum Conservation Equations

Conservation of momentum in an inertial (non-accelerating) reference frame is given by

$$\frac{\partial}{\partial t}\left(\rho \vec{v}\right) + \nabla.\left(\rho \vec{v}\vec{v}\right) = -\nabla p + \nabla.\left(\bar{\bar{\tau}}\right) + \rho \vec{g} + \vec{F} \tag{10}$$

where p is the static pressure, τ is the stress tensor (described below), and ρg and F are the gravitational body force and external body forces (e.g., that arise from interaction with the dispersed phase), respectively. F also contains other model-dependent source terms such as porous-media and user-defined sources.

The stress tensor τ is given by

$$\bar{\bar{\tau}} = \mu\left[\left(\nabla \vec{v} + \nabla \vec{v}^{T}\right) - \frac{2}{3}\nabla \cdot \vec{v} I\right] \tag{11}$$

Where μ is the molecular viscosity, I is the unit tensor, and the second term on the right hand side is the effect of volume dilation.

The axial and radial momentum conservation equations for 2D axisymmetric geometries are given by

$$\frac{\partial}{\partial t}(\rho v_x)+\frac{1}{r}\frac{\partial}{\partial x}(r\rho v_x v_x)+\frac{1}{r}\frac{\partial}{\partial r}(r\rho v_r v_x)=-\frac{\partial p}{\partial x}+\frac{1}{r}\frac{\partial}{\partial x}\left[r\mu\left(2\frac{\partial v_x}{\partial x}-\frac{2}{3}(\nabla\cdot\vec{v})\right)\right]+\frac{1}{r}\frac{\partial}{\partial r}\left[r\mu\left(\frac{\partial v_x}{\partial r}+\frac{\partial v_r}{\partial x}\right)\right]+F_x \quad (12)$$

and

$$\frac{\partial}{\partial t}(\rho v_r)+\frac{1}{r}\frac{\partial}{\partial x}(r\rho v_x v_r)+\frac{1}{r}\frac{\partial}{\partial r}(r\rho v_r v_r) = -\frac{\partial p}{\partial r}+\frac{1}{r}\frac{\partial}{\partial x}\left[r\mu\left(\frac{\partial v_r}{\partial x}+\frac{\partial v_x}{\partial r}\right)\right]+\frac{1}{r}\frac{\partial}{\partial r}\left[r\mu\left(2\frac{\partial v_r}{\partial r}-\frac{2}{3}(\nabla\cdot\vec{v})\right)\right]-2\mu\frac{v_r}{r^2}+\frac{2}{3}\frac{\mu}{r}\left(\nabla\cdot\vec{v}\right)+\rho\frac{v_z^2}{r}+F_r \quad (13)$$

Where

$$\nabla\cdot\vec{v}=\frac{\partial v_x}{\partial x}+\frac{\partial v_r}{\partial r}+\frac{v_z}{r} \quad (14)$$

And v_z is the swirl velocity

For 2D swirling flows, the tangential momentum equation may be written as

$$\frac{\partial}{\partial t}(\rho v_z)+\frac{1}{r}\frac{\partial}{\partial x}(r\rho v_x v_z)+\frac{1}{r}\frac{\partial}{\partial r}(r\rho v_r v_z)=\frac{1}{r}\frac{\partial}{\partial x}\left[r\mu\frac{\partial v_z}{\partial x}\right]-\rho\frac{v_r v_z}{r}+\frac{1}{r^2}\frac{\partial}{\partial r}\left[r^3\mu\frac{\partial}{\partial r}\left(\frac{v_z}{r}\right)\right] \quad (15)$$

3.2 TURBULENCE MODELLING

Turbulent flows are identified by changeable velocity fields. These variations mix with transmitted quantities such as energy, momentum, and species concentration, and

due to this reason the transported quantities fluctuate as well. Since these fluctuations can be of high frequency, they are computationally too expensive to simulate directly in practical engineering calculations. As an alternative, the instantaneous (exact) governing equations can be ensemble-averaged, time-averaged, or otherwise manipulated to eliminate the small scales, resulting in a modified set of equations that are computationally simple to solve. Although, the customized equations hold added unknown variables, turbulence models are desirable to decide these variables in terms of known quantities.

3.2.1 Choosing a Turbulence Model

It is the reality that no single turbulence model is generally accepted as better-quality for all categories of problems. The selection of turbulence model will depend on circumstances such as the stage of accuracy required, the physics covered in the flow, the existing computational resources, the conventional practice for a specific class of problem and the amount of time available for the simulation. Person needs to be aware of the capabilities and restrictions of the different options to make the most suitable choice of model for your problems. The intention of this segment is to give an outline of issues related to the turbulence models provided in FLUENT. The computational effort and cost in terms of CPU time and memory of the individual models is presented here. Though it is not possible to state categorically which model is greatest for a specific application, universal guidelines are presented here to choose the appropriate turbulence model for the flow.

FLUENT provides the following choices of turbulence models:

- Spalart-Allmaras model
- k- ε models

- Standard k- ε model
- Renormalization-group (RNG) k- ε model
- Realizable k- ε model

- k- ω models
  - Standard k- ω model
  - Shear-stress transport (SST) k- ω model
- Reynolds stress model (RSM)
- Large eddy simulation (LES) model

3.3 THE STANDARD, RNG, AND REALIZABLE k-ε MODELS

All these models have similar forms, with transport equations for k and ε. The major differences in the models are as follows:

- the technique of calculating turbulent viscosity
- the turbulent Prandtl numbers governing the turbulent diffusion of k and ε
- the generation and destruction terms in the ε equation

3.3.1 The RNG k-ε Model

The RNG-based k-ε turbulence model is derived from the instantaneous Navier-Stokes equations, using a mathematical technique called "renormalization group" (RNG) methods. It is similar in form to the standard k-ε model, but includes the following refinements:

- The RNG model has an supplementary term in its ε equation that appreciably improves the accurateness for rapidly strained flows.
- The consequence of swirl on turbulence is incorporated in the RNG model, enhancing precision for swirling flows.

- The RNG theory provides an logical formula for turbulent Prandtl numbers, whereas the standard k-ε model uses user-specified, constant values.
- While the standard k-ε model is a high-Reynolds-number model, the RNG theory provides an analytically-derived differential formula for effective viscosity that accounts for low-Reynolds-number effects. Efficient use of this feature does, however, depend on an suitable treatment of the near-wall region.

These characteristics make the RNG k-ε model more precise and reliable for a wider class of flows than the standard k-ε model.

3.3.2 Transport Equations for the RNG k-ε Model

The RNG k- ε model has a similar form to the standard k-ε model:

$$\frac{\partial}{\partial t}(\rho k)+\frac{\partial}{\partial x_i}(\rho k u_i)=\frac{\partial}{\partial x_j}\left[\alpha_k \mu_{eff}\frac{\partial k}{\partial x_j}\right]+G_k+G_b-\rho\varepsilon-Y_M+S_k \quad (16)$$

and

$$\frac{\partial}{\partial t}(\rho \varepsilon)+\frac{\partial}{\partial x_i}(\rho \varepsilon u_i)=\frac{\partial}{\partial x_j}\left[\alpha_k \mu_{eff}\frac{\partial \varepsilon}{\partial x_j}\right]+C_{1\varepsilon}\frac{\varepsilon}{k}(G_k+C_{3\varepsilon}G_b) - C_{2\varepsilon}\rho\frac{\varepsilon^2}{k}-R_\varepsilon+S_\varepsilon \quad (17)$$

In these equations, G_k represents the generation of turbulence kinetic energy due to the mean velocity gradients. G_b is the generation of turbulence kinetic energy due to buoyancy. Y_M represents the contribution of the fluctuating dilatation in compressible turbulence to the overall dissipation rate,. The quantities α_k and α_ε are the inverse effective Prandtl numbers for k and ε, respectively. S_k and S_ε are user-defined source terms.

3.3.3 Modeling the Effective Viscosity

The scale elimination procedure in RNG theory results in a differential equation for turbulent viscosity:

$$d\left(\frac{\rho^2 k}{\sqrt{\varepsilon\mu}}\right) = 1.72\frac{\hat{\nu}}{\sqrt{\hat{\nu}^3 - 1 + C_\nu}} \tag{18}$$

where $\hat{\nu} = \mu_{eff}/\mu$ $\qquad C_{\hat{\nu}} \approx 100$

Equation is integrated to attain an accurate explanation of how the effective turbulent transport varies with the effective Reynolds number (or eddy scale), allowing the model to better handle low-Reynolds-number and near-wall flows.

In the high-Reynolds-number limit, Equation gives

$$\mu_t = \rho C_\mu \frac{k^2}{\varepsilon} \tag{19}$$

with C_μ =0.0845, derived using RNG theory. It is interesting to note that this value of Cμ is very close to the empirically-determined value of 0.09 used in the standard k- ε model.

3.4 TURBULENCE MODELING IN SWIRLING FLOWS

In modeling turbulent flow with a considerable amount of swirl (e.g., cyclone flows, swirling jets), one should consider FLUENT's advanced turbulence models: the RNG k-ε model, realizable k- ε model, or Reynolds stress model. The suitable choice depends on the strength of the swirl, which can be estimated by the swirl number. The swirl number is defined as the ratio of the axial flux of angular momentum to the axial flux of axial momentum:

$$S = \frac{\int r\omega\vec{\upsilon}.d\vec{A}}{\vec{R}\int u\vec{\upsilon}.d\vec{A}} \tag{20}$$

where R is the hydraulic radius.

For swirling flows found in devices such as swirl combustors and cyclone separators, near-wall turbulence modeling is quite often a secondary concern at most. The reliability of the predictions in these cases is mainly checked by the accuracy of the turbulence model in the core section. However, in cases where walls actively contribute in the generation of swirl (i.e., where the secondary flows and vertical flows are generated by pressure gradients), non-equilibrium wall functions can repeatedly improve the predictions since they use a law of the wall for mean velocity sensitized to pressure gradients.

3.4.1 Modelling Axisymmetric Flows with Swirl or Rotation

A 2D axisymmetric problem that includes the prediction of the swirl or circumferential velocity can be solved. The assumption of axisymmetry implies that there are no circumferential gradients in the flow, but that there may be non-zero circumferential velocities.

3.4.2 Solution Strategies for Axisymmetric Swirling Flows

The difficulties connected with solving swirling and rotating flows are a consequence of the high degree of coupling between the momentum equations, which is introduced when the effect of the rotational terms is large. A high degree of rotation brings in a large radial pressure gradient which causes the flow in the axial and radial directions. This, in turn, decides the distribution of the swirl or rotation in the field. This coupling may bring about imbalances in the solution process, and may need special solution techniques in order to attain a converged solution. Solution techniques that may be helpful in swirling or rotating flow calculations include the following:

(Segregated solver only) Use the PRESTO! Scheme (enabled in the Pressure list for Discretization in the Solution Controls panel), which is well-suited for the sharp pressure gradients involved in swirling flows.

Make sure that the mesh is adequately refined to resolve large gradients in pressure and swirl velocity.

(Segregated solver only) Change the under-relaxation parameters on the velocities, perhaps to 0.8–1.0 for swirl and 0.3–0.5 for the radial and axial velocities.

(Segregated solver only) Use a sequential or step-by-step solution procedure, in which some equations are temporarily left inactive.

If necessary, start the calculations using a low inlet swirl velocity or rotational speed, increasing the swirl or rotation gradually in order to arrive at the final desired operating condition.

3.4.3 Step-By-Step Solution Procedures for Axisymmetric Swirling Flows

Flows with a high degree of swirl or rotation will be easier to solve if the following step-by-step solution procedure is used, in which only preferred equations are left active in each step. This approach allows to establish the field of angular momentum, then leave it fixed while update the velocity field, and then finally to couple the two fields by solving all equations simultaneously.

Since the coupled solvers solve all the flow equations simultaneously, the following procedure applies only to the segregated solver.

In this procedure, use the Equations list in the Solution Controls panel to turn individual transport equations on and off between calculations.

1. If problem involves inflow/outflow, begin by solving the flow with no rotation or swirl effects. That is, allow the axisymmetric option instead of the Axisymmetric Swirl option in the Solver panel, and do not put any rotating

boundary conditions. The resulting flow-field data can be used as a starting speculation for the full problem.

2. Enable the Axisymmetric Swirl option and set all rotating/swirling boundary conditions.
3. Begin the forecast of the rotating/swirling flow by solving only the momentum equation describing the circumferential velocity. This is the Swirl Velocity listed in the Equations list in the Solution Controls panel. Let the rotation "diffuse" throughout the flow field, based on the boundary condition inputs. In a turbulent flow simulation, leave the turbulence equations active during this step. This step will establish the field of rotation throughout the domain.
4. Turn off the momentum equations describing the circumferential motion (Swirl Velocity). Leaving the velocity in the circumferential direction fixed, solve the momentum and continuity (pressure) equations in the other coordinate directions. This step will establish the axial and radial flows that are a result of the rotation in the field. Again, if problem involves turbulent flow, leave the turbulence equations active during this calculation.
5. Turn on all of the equations simultaneously to obtain a fully coupled solution. Note the under-relaxation controls suggested above.

In addition to the steps above, to simplify calculation by solving isothermal flow before adding heat transfer or by solving laminar flow before adding a turbulence model. These two methods can be used for any of the solvers (i.e., segregated or coupled).

Gradual increase of the rotational or swirl speed to get better solution stability .Because the rotation or swirl defined by the boundary conditions can cause large complex forces in the flow, FLUENT calculations will be less stable as the speed of

rotation or degree of swirl increases. Hence, one of the most effective controls that can apply to the solution is to solve rotating flow problem starting with a low rotational speed or swirl velocity and then slowly increase the magnitude up to the desired level. The procedure for accomplishing this is as follows:

1. Set up the problem using a low rotational speed or swirl velocity in the inputs for boundary conditions. The rotation or swirl in this first attempt might be selected as 10% of the actual operating conditions.
2. Solve the problem at these conditions, perhaps using the step-by-step solution strategy outlined above.
3. Save this initial solution data.
4. Modify inputs (boundary conditions). Increase the speed of rotation, perhaps doubling it.
5. Restart the calculation using the solution data saved in step 3 as the initial solution for the new calculation. Save the new data.
6. Continue to increase the speed of rotation, following steps 4 and 5,until you reach the desired operating condition.

CHAPTER 4 CFD ANALYSIS

FLUENT is a modern computer program for modeling fluid flow and heat transfer in complex geometries. FLUENT allows complete mesh flexibility, solving flow problems with unstructured meshes that can be generated about complex geometries with relative simplicity. Supported mesh types include 2D triangular/quadrilateral, 3D tetrahedral/hexahedral/pyramid/wedge, and mixed (hybrid) meshes. Based on the flow solution FLUENT also refine or coarsen grid.

4.1 PROGRAM CAPABILITIES

The FLUENT solver has the following modeling capabilities:

- 2D planar, 2D axisymmetric, 2D axisymmetric with swirl (rotationally symmetric), and 3D flows.
- Quadrilateral, triangular, hexahedral (brick), tetrahedral, prism (wedge), pyramid, polyhedral, and mixed element meshes.
- Steady-state or transient flows.
- Inviscid, laminar, and turbulent flows.
- Incompressible or compressible flows, including all speed regimes (low subsonic, transonic, supersonic, and hypersonic flows).
- Chemical species mixing and reaction, including homogeneous and heterogeneous combustion models and surface deposition/reaction models.
- Newtonian or non-Newtonian flows.
- Heat transfer, including forced, natural, and mixed convection, conjugate (solid/fluid) heat transfer, and radiation.
- Cavitations model.

- Free surface and multiphase models for gas-liquid, gas-solid, and liquid-solid flows.
- Lagrangian trajectory calculation for dispersed phase (particles/droplets/bubbles), including coupling with continuous phase and spray modelling.
- Phase change model for melting/solidification applications.
- Lumped parameter models for fans, pumps, radiators, and heat exchangers.
- Porous media with non-isotropic permeability, inertial resistance, solid heat conduction, and porous-face pressure jump conditions.
- Acoustic models for predicting flow-induced noise.
- Multiple reference frame (MRF) and sliding mesh options for modeling multiple moving frames.
- Inertial (stationary) or non-inertial (rotating or accelerating) reference frames.
- Volumetric sources of mass, momentum, heat, and chemical species.
- Mixing-plane model for modeling rotor-stator interactions, torque converters, and similar turbo-machinery applications with options for mass conservation and swirl conservation.

FLUENT is ideally suited for incompressible and compressible fluid-flow simulations in complex geometries.

4.2 PLANNING CFD ANALYSIS

The following consideration should be taken while planning CFD analysis:

4.2.1 Definition of the Modeling Goals:

What specific results are required from the CFD model and how will they be used? What degree of accuracy is required from the model?

4.2.2 Grid Generation and its Independence:

What type of element will be used? What size of the mesh should be kept so as to optimize between accuracy and time and resources being consumed?

4.2.3 Choice of the Computational Model:

How to isolate a piece of the complete physical system to be modeled? Where will the computational domain begin and end? What boundary conditions will be used at the boundaries of the model? Can the problem be modeled in two dimensions or is a three-dimensional model required? What type of grid topology is best suited for this problem?

4.2.4 Choice of Physical Models:

Is the flow inviscid, laminar, or turbulent? Is the flow unsteady or steady? Is heat transfer important? Is the fluid incompressible or compressible? Are there other physical models that should be applied?

4.2.5 Determination of the Solution Procedure:

Can the problem be solved simply, using the default solver formulation and solution parameters? Can convergence be accelerated with a more judicious solution procedure? Will the problem fit within the memory constraints of the computer, including the use of multigrain? How long will the problem take to converge on the computer?

Careful consideration of these issues before beginning CFD analysis will contribute significantly to the success of modeling effort.

4.3 DISCRETIZATION

With the help of the finite volume technique the governing equations are transformed into algebraic equations that can be solved numerically. This control volume method

consists of integrating the governing equations concerning each control volume, yielding separate equations that keep each quantity on a control-volume basis.

Discretization of the governing equations can be represented most easily by considering the steady-state conservation equation for transport of a scalar quantity ϕ. This is established by the subsequent equation written in integral form for an random control volume V as follows:

$$\iint \rho\phi\vec{v}.d\vec{A} = \iint \Gamma_{\phi}\nabla\phi.d\vec{A} + \int_{V} S_{\phi}dV \tag{21}$$

where

ρ = density

v = velocity vector A = surface area vector

Γϕ = diffusion co-efficient for ϕ

ϕ = gradient of ϕ

Sϕ = source of ϕ per unit volume

Above equation is useful to each control volume, or cell, in the computational domain. Discretization of Equation on a given cell yields

$$\sum_{f}^{N_{faces}} \rho_f v_f \phi_f .\vec{A}_f = \sum_{f}^{N_{faces}} \Gamma_{\phi}\left(\nabla\phi\right)_n .\vec{A}_f + S_{\phi}V \tag{22}$$

Where

N_{faces} = number of faces enclosing cell

ϕf = value of ϕ convected through face f

$\rho_f v_f A_f$ = mass flux through the face

A_f = area of face f, A

$(\nabla\phi)_n$ = magnitude of ∇ϕ normal to face f

V = cell volume

The equations take the same general appearance as the one given above and apply without much difficulty to multi-dimensional, unstructured meshes composed of arbitrary polyhedral, the discrete values of the scalar ϕ at the cell centers. On the other hand, face values ϕf is necessary for the convection terms in equation and have to be interpolated from the cell center values. This is accomplished using an upwind scheme. Upwind means that the face value ϕf is resulting from quantities in the cell upstream, or "upwind," relative to the direction of the normal velocity v_n

4.4 CONVERGENCE CRITERIA

Finally there is necessities to set the convergence criteria for the iterative method. Usually, there are two degrees of iterations, within which the linear equations are solved and other iteration that cover the non-linearity and coupling of the equations. From both, the efficiency and accuracy point of view, the decision to stop the iterative process on each level is important. If the solution of the discretized equations be likely to correct the solution of the differential as the grid spacing tends to be zero then numerical is said to be convergent. For convergence criteria around 10^{-6} for X velocity variable, the results are stable in the present problem.

4.5 IMPLEMENTATION OF BOUNDARY CONDITIONS

Each control volume provides one algebraic equation. Volume integrals are estimated for every control volume, but flux through control volume faces coinciding with the domain boundary requires special action. These boundary fluxes must be identified, or be expressed as a combination of interior values and boundary data. Two types of boundary conditions need to be specified.

4.5.1 Inlet boundary condition

The present analysis involves the velocity with and without swirl. The integration of velocity without swirl can be specified by any one of the velocity specification methods described in FLUENT. Turbulence intensity is specified as

$I = 0.16(Re_{DH})^{-1/8}$ x100

The inlet based on the Reynolds number with respect to equivalent flow diameter.

Where, Re_{DH} is the Reynolds number based on the hydraulic diameter.

Tangential component of velocity will also have to be defined along with axial component for specifying the velocity in case of flow with swirl. Velocity components are calculated on the basis of inlet swirl angle. In the present case swirl angle of 0, 7.5, 12.5, 17.5, 25 degrees are considered. Inlet velocity of 60 m/s with flat profile is considered for both the cases.

4.5.2 Outlet boundary condition

Atmospheric pressure condition is implemented at the outlet boundary condition and set a “back flow” conditions is also assigned if the flow reverses direction at the pressure outlet boundary during the solution process. In the “back flow” condition turbulence intensity is specified based on the equivalent flow diameter.

4.5.3 Wall boundary condition

Wall boundary conditions are used to attach fluid and solid regions. In viscous flows the no slip boundary condition is imposed at the walls. Wall roughness affects the drag (resistance) and heat and mass transfer on the walls. Therefore roughness consequences were considered for the present analysis and a specified roughness based on law of wall modified for roughness is considered. Two inputs, physical roughness height and the roughness constant, to be specified and the default

roughness constant (0.5) is assigned which suggests the uniform sand grain roughness.

4.6 SIMULATION PROCEDURE

STEP 1: Modeling (In Gambit):

- Diffuser geometry is formed.
- Stabilizing length equal to D was attached at inlet.
- Boundary layer was attached to both the hub and casing wall with growth factor 1.1 and 10 rows.
- The model has been meshed with quadratic-mesh. Fine meshing with spacing 0.07 was done and mesh elements range from 12000 – 75000 elements.
- Boundary conditions taken were for velocity at inlet, pressure at outlet and wall type for both the hub and casing.
- Fluid was specified as air for the continuum type and the mesh was exported to Fluent for post processing.

STEP 2: Post Processing (In Fluent):

- Grid was checked and scaled.
- 2D axisymmetric solver and segregated solution method was chosen.
- Air was chosen as the fluid for flow, and its properties were selected.
- RNG k-ε models is selected.
- At air inlet section, the inlet velocity of 60 m/s with different swirl intensity was specified.
- Turbulence intensity of 3% based on inlet flow diameter was specified. At the exit section, the pressure was specified being equal to atmospheric pressure.

- Second order upwind scheme was selected to solve continuity and momentum equations.
- Convergence criteria of 10^{-6} were taken.
- Solution was initialized at inlet and made to iterate until it converges.

Once solution is converged, various data for pressure and velocity were obtained and graphs were plotted.

CHAPTER 5 VALIDATION

5.1 GRID INDEPENDENCE

For grid independence an experimental inlet profile[6] with hub and casing diverging at angle of 5° & 11° respectively with swirl of 12.5° separately at a velocity profile of 60m/s. The grid independence is studied for the RNG k-ε model employing four sizes of grids to examine the sensitivity of grid. As we decrease the mesh size we get a more fine mesh and better results, but due to more numbers of nodes the computation time increases. So we have to optimize the grid size with the accuracy required. We took the following mesh sizes:

	Element Type	Mesh Size	No. of Cells	No. of Face	No. of Nodes	Computation Time (hrs)
Coarse mesh	**Quad.**	**0.09**	**44924**	**89826**	**45012**	**3.1**
Fine mesh	**Quad.**	**0.08**	**56262**	**112520**	**56522**	**5.9**
Finer mesh	**Quad.**	**0.07**	**65640**	**131275**	**65850**	**11.3**
Finer mesh	**Quad.**	**0.06**	**81254**	**162485**	**82543**	**18.5**

5.1.1 Validation with experimental results [6]:-

Velocity Graph:

Figure 5.2 shows results of RNG k-ε model with the mesh size of 0.08 and 0.09 cm shows deviation in their values. The results of mesh size 0.06 and 0.07 remain almost same, thus mesh size of 0.07 cm is considered for present CFD modeling to reduce the computational time without compromising the accuracy.

5.2 TURBULENCE MODEL VALIDATION

FLUENT provide many models to model the turbulence in the flow like :

- k- ε models
  - Standard k- ε model
  - Renormalization-group (RNG) k- ε model
  - Realizable k- ε model
- Reynolds stress model (RSM)

RNG k-ε model were tested against an experimental profile [6] with hub and casing diverging at angle of 5° & 11° respectively with swirl of 12.5° separately at a velocity profile of 60m/s.

5.2.1 Validation with experimental results [6]:-

Velocity Graph with velocity of 60m/s and no swirl (0°):

Figure 5.1 shows that RNG k-ε model nearly closer to the experimental results [6].

- At x= 0.3L: RNG and Realizable are very close to the experimental results.
- At x= 0.5L: RNG and Realizable are very close to the experimental results, but Realizable start differing from experimental results
- At x= 0.7L: Only RNG model is in agreement to the experimental results
- At x= 0.9L: Only RNG model has least deviation from experimental results.

Velocity Graph with velocity of 60m/s and swirl of 12.5°:

Figure 5.3 & 5.4 shows that RNG k-ε model closer to the experimental results [6].

- At x= 0.3L: Approximately every model varies from experimental results.
- At x= 0.5L: RNG and Reynolds Stress model are close to the experimental results.

- At x= 0.7L: Only RNG model is in agreement to the experimental results.
- At x= 0.9L: Only RNG model results are closer to the experimental results

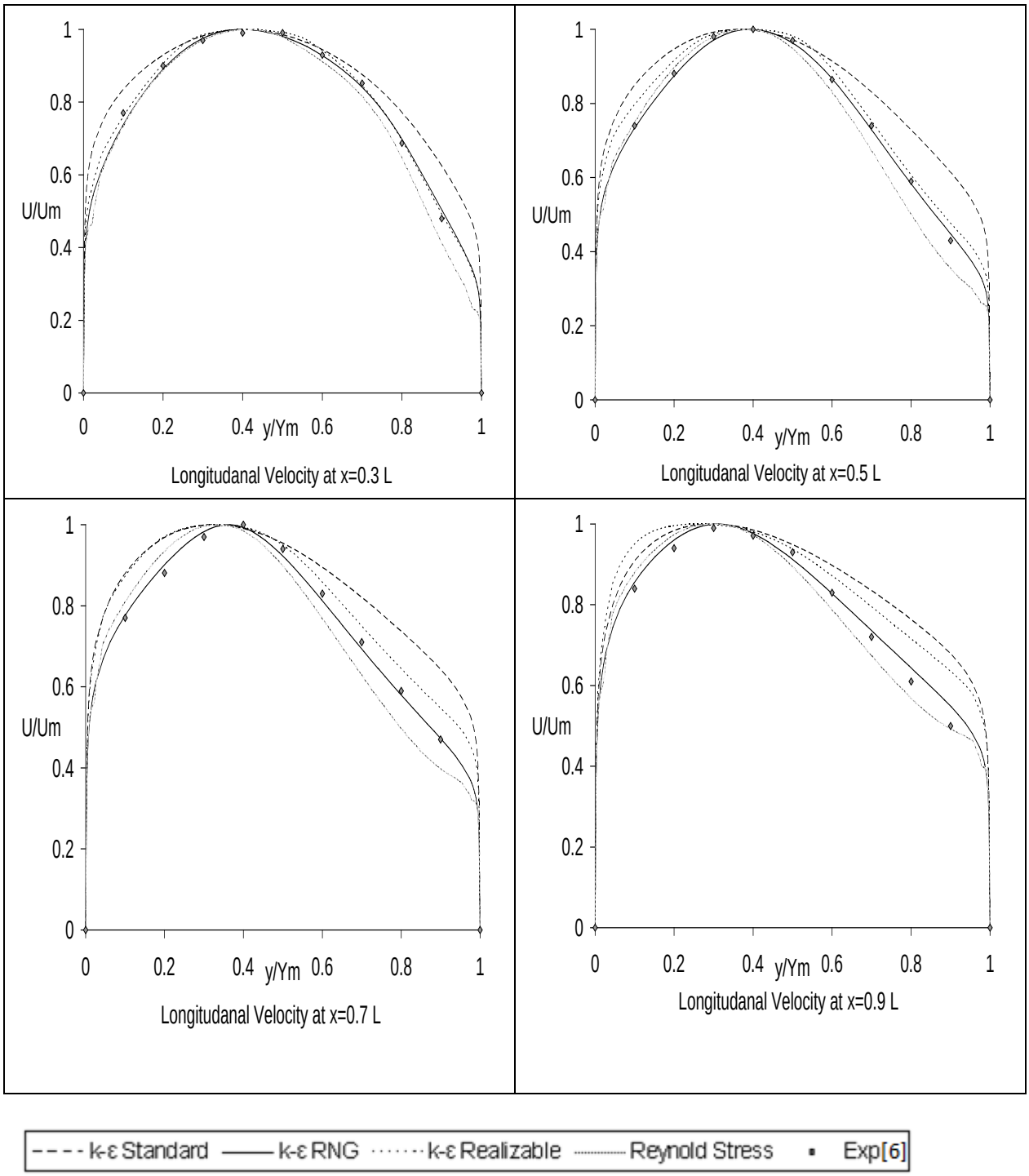

Figure 5.1: Experimental Longitudinal Velocity (0°), AR 2

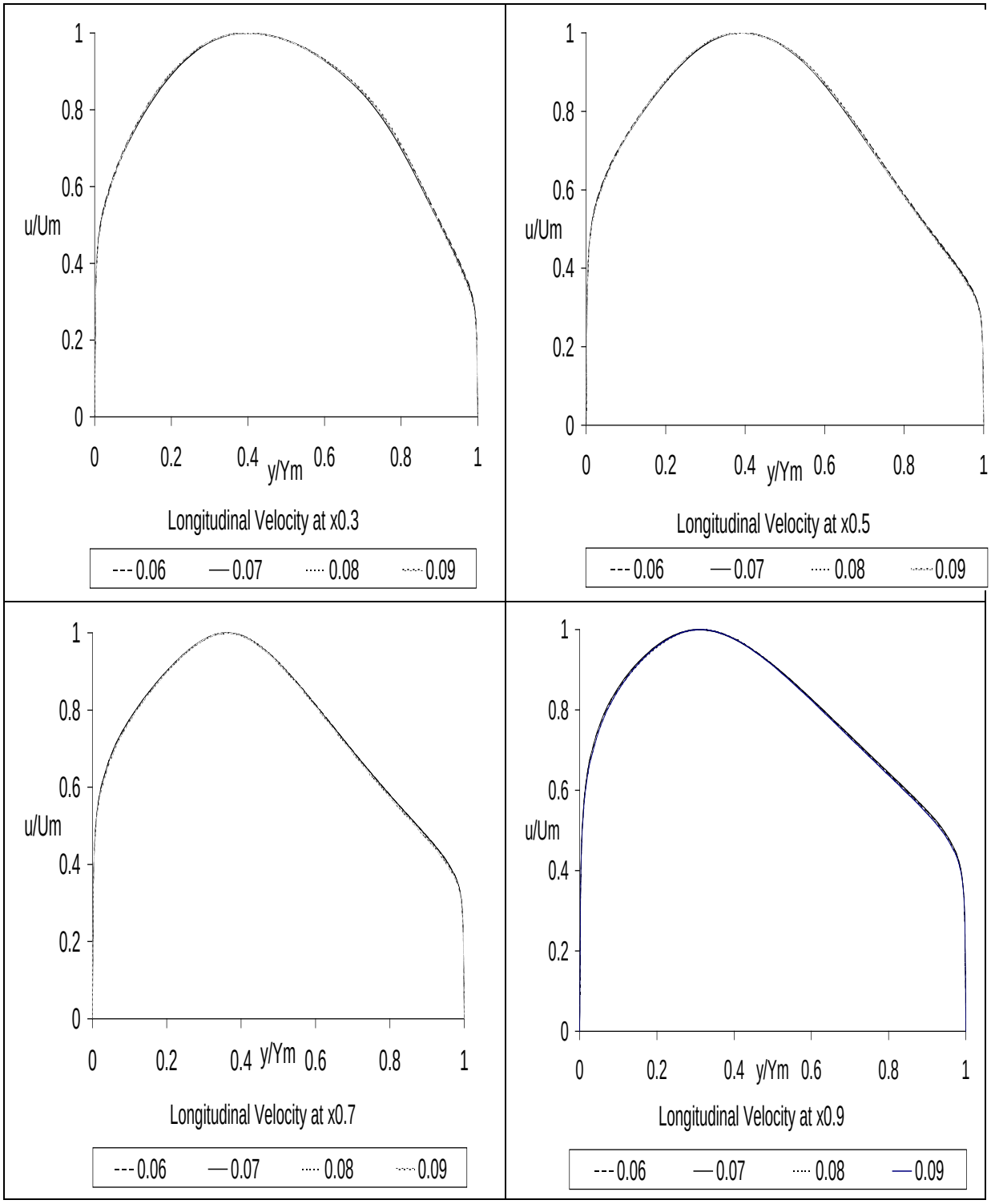

Figure 5.2: Longitudinal Velocity (0°) by CFD, AR 2

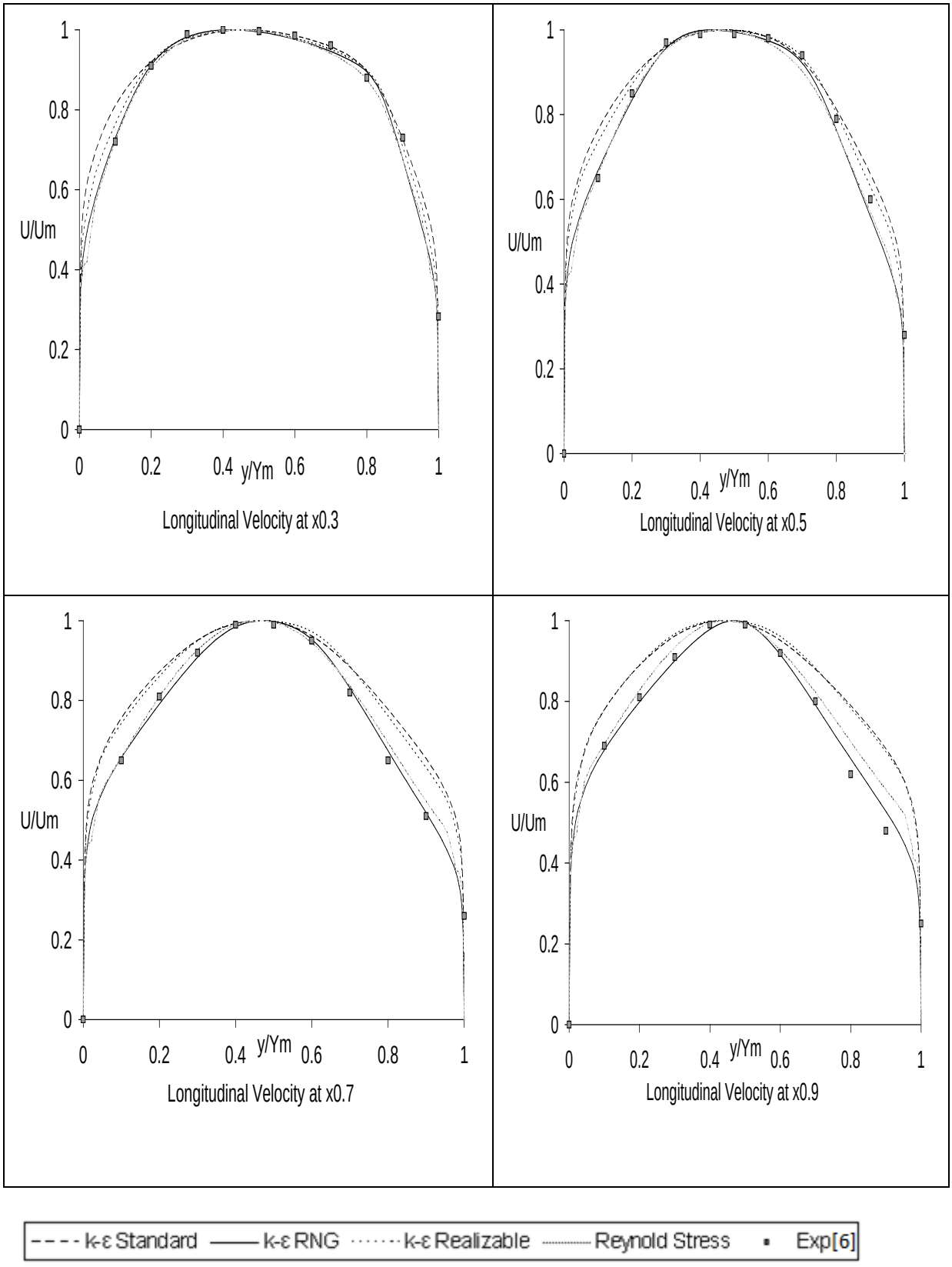

Figure 5.3: Experimental Longitudinal Velocity (12.5°), AR 2

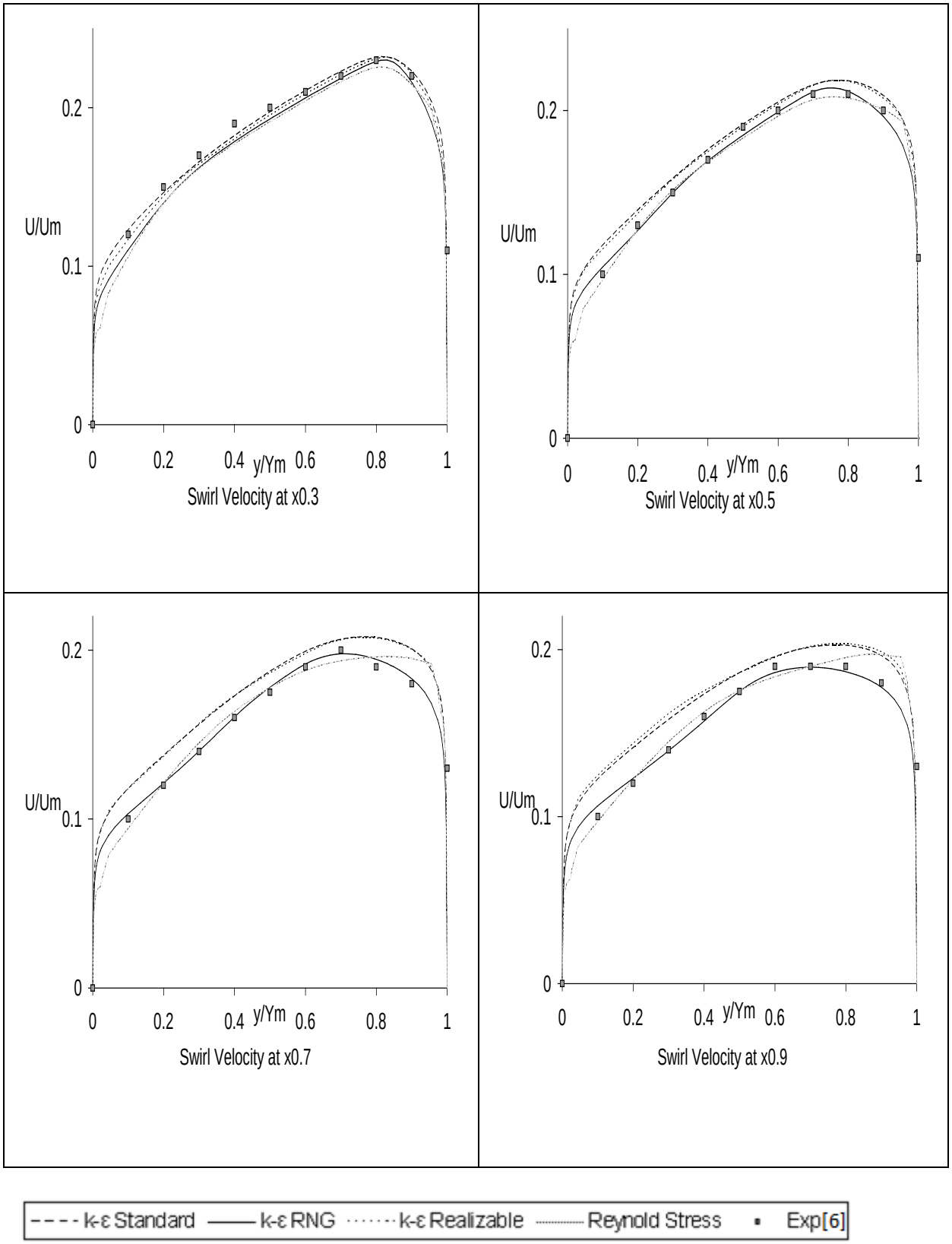

Figure 5.4: Experimental Swirl Velocity (12.5°), AR 2

CHAPTER 6 RESULT AND DISCUSSION

In the current thesis, analysis of flow in the annular diffusers is studied with the help of GAMBIT and FLUENT for area ratio 2 and 3. Analysis gives the consequence of geometry on the pressure recovery coefficient. The following decisions can be drained from the results.

Fig 1-20 shows the result rendered by FLUENT. In these figures fluid characteristics like static pressure, velocity magnitude, total pressure and swirl velocity are shown by different colors.

Flow inside the unequal casing and hub angle annular diffusers with and without the effects of inlet swirl have been forecasted using the FLUENT code. The following decisions can be drawn from the results:

6.1 Velocity Profile

Figure 21-25 and 30-34 shows the longitudinal velocity profiles for area ratio 2 & 3 respectively. Figure 26-29 and 35-38 shows the swirl velocity profiles for area ratio 2 & 3 respectively. These profiles are shown as non-dimensional velocity in a mathematical relation with diffuser section height y/Ym for the area ratio 2 and 3 respectively. The velocity profiles are represented for various inlet swirl angles 0°, 7.5°, 12.5°, 17.5° & 25°. All the velocity profiles have been demonstrated in terms of non-dimensional velocity as the proportion of local velocity to the local maximum velocity, wherever velocity is required. The casing position is represented by y/Ym =1 whereas hub position of the span is represented by y/Ym =0. The graphs are shown at various tracks of the diffuser span at x/L= 0.1, 0.3, 0.5,0.7 & 0.9 for the area ratio 2 & 3 and different inlet swirl angles.

Figure 21-38, exemplify that the flow is hub generated for no swirl circumstance and when the swirl is brought in then there is shift in the flow in the direction of casing from hub. The pinnacle of the velocity occurs at y/Ym= 0.44 for area ratio 2 at x/L =0.91, while it is at y/Ym =0.40 for area ratio 3. The flow is pushed in the direction of the casing with the application of swirl. Flow separation occurs at casing side up to 12.5° swirl angle and it shifts towards hub side for 17.5° and 25° swirl angle.

It is reasonably important as looked at the figure 21-25 and 30-34. As the inlet swirl enhances the peak velocity in all the cases shifts on the way to the casing side. With the growing swirl, the velocity on the hub surface decreases for same area ratio. With the addition in the area ratio, the shift enhances to larger amount for same inlet velocity profile. This is because of the fact that the stall grows at the casing wall with addition in the area ratio. As seen in the figure 21-25 and 30-34, with the application of swirl, the stall tends to shift to the hub side from casing.

6.2 Pressure Recovery Coefficient

Figure 11-20 shows pressure recovery coefficient (Cp) at casing wall and hub side for area ratio 2 & 3 in a mathematical relation with non-dimensional diffuser channel (x/L) for different inlet swirl angles 0°, 7.5°, 12.5°, 17.5° & 25°. In each case, with the diffuser length, Cp increases. In the start of the diffuser passage, the increase in Cp is quick and afterwards it decreases in the direction of diffuser channel.

Cp is more for growing swirl for area ratio 2. Beyond x/L = 0.98 and x/L = 0.54, Cp is smaller than the flow without swirl at 17.5º and 25º inlet swirl respectively. For 25º inlet swirl, Cp is maximum up to diffuser channel length of 0.37. Cp is maximum for 17.5º

inlet swirl from x/L= 0.37 to 0.70, then from 0.70 till the end Cp is highest for 12.5º inlet swirl.

For area ratio 3, Cp is lesser than the flow with no swirl ahead of x/L =0.65 and x/L =0.31 for 7.5º and 25º inlet swirl correspondingly. Cp is maximum for 25º inlet swirl up to 0.21 of diffuser channel length, it is maximum for 17.5º inlet swirl from 0.21 to 0.41 and ahead of 0.41, it is maximum for 12.5º inlet swirl.

6.3 CONCLUSION

RNG *k*- ε model was utilized to forecast the performance of the axial annular diffuser. Following conclusion is drawn back from the predicted computational results for area ratios 2 and 3:

1. The longitudinal velocity diminishes continuously as the flow goes on downstream, regardless of whether the inlet flow is swirling or non-swirling.
2. Due to the growth of boundary layer, velocity profiles take different shapes at different places of the flow channel.
3. For non swirling flow, the maxima of velocity at any diffuser cross-section is not at the middle, instead it is in the direction of the hub side and with the application of swirl it changes in the direction of the casing.
4. The flow is forced in the direction of casing wall with the application of swirl, as a result the flow becomes strong in the direction of casing.
5. Increase in Pressure recovery coefficient, Cp, with the diffuser length. With the application of swirl the revival is quicker on the way to the casing wall. Though the retrieval diminishes with the diffuser passage.

CHAPTER 7 FUTURE SCOPE OF WORK

1. Annular diffuser with hub and casing diverging at unequal angle is considered in the present study. Future work can be done on other diffusers like rectangular, conical, radial type diffusers etc.
2. Area ratio and angle of divergence are the important parameters which indicate the overall diffusion and hence further studies can be extended by varying these parameters.
3. This work was done for sub–sonic incompressible flow only. The additional range of work can be extended to sonic flow, hypersonic flow and compressible flow.
4. This investigation is done for a diverging section of diffuser. Because the geometry is an significant parameter and hence geometry variation can be done for further studies.
5. The analysis is performed with RNG k-ε model for swirling flows. Higher order discretization schemes and better turbulence models can be used for further studies.
6. In many realistic situations the flow is non uniform .In this study uniform inlet velocity profile is considered at the inlet of the diffuser. Hence the inlet velocity profiles represent the area of great interest for further studies.
7. The present analysis is done for stationary hub and casing. Further studies can be done on rotating hub and casing diffuser.
8. Suction, blowing and injection of boundary layer can decrease the flow separation at diffuser walls. These property can be incorporated for further studies.

REFERENCES

1. Ackert J., 1967, “Aspect of Internal Flow”, Fluid Mechanics of Internal Flow, Ed. Sovaran G., Elsevier Amsterdam, pp l.
2. Adkins R.C., Jacobsen O.H., Chevalier P., 1983, “A Premilary Study of Annular Diffuser With Constant Diameter Outer Wall” ASME paper no. 83-GT-218
3. Adkins R.C., 1983, “A simple Method for Design Optimum Annular Diffusers” ASME Paper No. 83-GT-42.
4. Anderson M.G, 2008 "FLUENT CFD versus Sovran & Klomp Diffuser Data Benchmark study" 46th AIAA Aerospace Sciences Meeting and Exhibit 7-10 January 2008, Reno, Nevada at American Institute of Aeronautics and Astronautics pp 1-26.
5. Arora B.B., 2014, “Performance analysis of parallel hub diverging casing axial annular diffuser with 20 degrees equivalent cone angle”,Australian Journal of Mechanical Engineering, Vol. 12, No. 2, 2014 pp.179-194.
6. Arora B.B., 2007, “Aerodynamic Analysis of Diffuser”, Ph.D Thesis, 2007, DU, Delhi.
7. Arora B.B. ,Pathak B.D.,2005,“Flow characteristics of parallel hub diverging casing axial annular diffusers”. ISME publication pp. 794-798.
8. Arora B. B., Pathak B. D., 2008, “Effect of Swirl on the intake of Turbocharger,” SAE International. Paper No. SAE Number 2008-28-00 69. DOI:10.4271/2008-28-0069. pp.476-482.

9. Arora B. B., Pathak B. D., 2009, “Effect of Geometry on the Performance of Annular Diffuser,” International Journal of Applied Engineering Research, Vol.5, No.20, pp. 2639-2652, ISSN 0973-4562.
10. Arora B.B., Kumar M., Maji S., 2010, “ Study of Inlet conditions on Diffuser Performance,” International Journal of Theoretical and applied Mechanics, Vol.5, No.2, pp. 201-221, ISSN 09736085.
11. Arora B.B., Kumar M., Maji S., 2010, “ Analysis of flow separation in wide angle annular diffusers,” International Journal of Applied Engineering Research, Vol.5, No.20, pp. 3419-3428, ISSN 0973-4562.
12. Arora B. B., Pathak B. D,2011, “CFD analysis of axial annular diffuser with both hub and casing diverging at unequal angles,” International Journal of dynamics of fluid Vol.7, No.1, pp. 109-121, ISSN 0973-1784.
13. Awai T., Nakagawa T., Sakai T., 1986, “Study of Axially Curved Mixed Flow Vane-less Diffuser”. Bull JSME 29, 1759-1764.
14. Cockrell D.J., Markland E., 1963, “A Review of Incompressible Diffuser Flow” Aircraft Engg. Volume 35, pp 286.
15. Coladipietro R., Schneider, J.M., Sridhar, K.1974, “Effects of Inlet Flow Conditions on the Performance of Equiangular Annular Diffusers,” Trans. CSME 3 (2), pp. 75-82.
16. Dovzhik S.A., Kartavenko, V.M., 1975, “Measurement of the Effect of Flow Swirl on the Efficiency of Annular Ducts and exhaust Nozzles of Axial Turbo-machines,” Fluid Mechanics/Soviet Research 4(4), 156-172.
17. Filipenco V. G. Deniz S. Johnston J. M. Greitzer E. M. Cumpsty N. A., 2000, “Effects of Inlet Flow Field Conditions on the Performance of Centrifugal Compressor Diffusers: Part 1- Discrete- Passage Diffuser”, Janaury 2000).

18. Glyn Norris ,1997, "Flows Through S-Shaped Annular, Inter-Turbine Diffusers" , Ph.D Thesis,1997, University of Durham.
19. Goebel J. H., Japikse D., 1981, “The Performance of an Annular Diffuser Subject to Various Inlet Blockage and Rotor Discharge Effects “. Consortium Final Report, Creare TN-325.
20. Gomez L. Mohan R. Shoham O., 2004, “Swirling Gas–Liquid Two-Phase Flow— Experiment and Modeling Part I: Swirling Flow Field”, June 8, 2004.
21. Hesterman R., Kim S., Ban Khalid A., Witting S., 1995. “Flow Field and Performances Characteristics of Combustor Diffusers : A Basic Study”. Trans. ASME Journal Engineering for Gas Turbine and Power 117, pp 686-694.
22. Hoadley D., 1970. “Three Dimensional Turbulent Boundary Layers in an Annular Diffuser” Ph.D. Thesis University of Cambridge.
23. Hoadley D., Hughes D .W, 1969. “Swirling Flow in an Annular Diffuser”. University of Cambridge, Department of Engineering, Report CUED/A-Turbo/TR5.
24. Howard J. H. G., Thornton-Trump A. B., Henseler H. J., 1967. “Performance and Flow Regime for Annular Diffusers ”. ASME Paper No. 67-WA/FE-21.
25. Ishkawa K, Nakamura I, 1989. “An Experimental Study on The Performance of Mixed Flow Type Conical Wall Annular Diffuser”, ASME FED-69.
26. Ivana B., Walter G., Eugene O., Håkan N., Albert R., 2006. “An Adaptive Turbulence Model for Swirling Flow” Conference on Turbulence and Interactions TI2006, May 29 – June 2.
27. Japikse D., 1986. “A New Diffuser Mapping Technique- Studies in Component Performance: Part 1”. ASME Paper No. 84-GT-237, Amsterdam, June 1984

28. Japikse D., and Pampreen, R.,1978. “Annular Diffuser Performance for an Automotive Gas Turbine,” ASME Publication 78-GT-147.
29. Japikse D., 1980. “The Influence of Inlet Turbulence on Diffuser Performance,” Concepts ETI, Inc., Design Data Sheet No. 1.
30. Japikse D., 2000. “Performance of Annular Diffusers Subject to Inlet Flow Field Variations and Exit Distortion,” Presented at the ISROMAC conference in Honolulu, Hawaii, March 26-30.
31. Johnston I.H., 1953. “Effect of Inlet Conditions on the Flow in Annular Diffusers” National Gas Turbine Establishment Memo No. 167,Cp No.178
32. Johnston J. P., 1959. “Summary of Results of Test on Short Conical Diffuser with Flow Control Inserts”: as of June 1, 1959.Ingersoll —Rand TN No. 71.
33. Juhasz A.J., 1974. “Performance Of An Asymmetric Annular Diffuser With Non Diverging Inner Wall Using Suction”, NASA TN -7575.
34. Kamonicek V., Hibs M., 1974. “Results of Experimental and Theoretical Investigation of Annular Diffuser.” CSIRO, Division of Mechanical Egg.
35. Klein A., 1995. “Characteristics of Combustor Diffusers.” Program Aerospace Science 31, 171-271.
36. Kochevsky A.N., 2000. “Numerical Investigation of Swirling Flow in Annular Diffusers with a Rotating Hub Installed at the Exit of Hydraulic Machines” J. Fluids Eng. 123(3), 484-489.
37. Kochevsky Alexey N, 2004, “Computation of internal fluid flows in channels using the CFD software tool Flow-Vision”.
38. Krystyna prync-skotniczny, 2006. “Numerical analysis of the impact of the conical diffuser geometry change on velocity distribution in its outlet cross section”. Mechanics Vol 25 no. 2.

39. Kumar M., Arora B.B., Maji S., Maji S., 2011, “Effect of inlet swirl on the flow behavior inside annular diffuser,” International Journal of dynamics of fluid Volume 7, Number 2, pp. 181-188. ISSN 0973-1784.
40. M.A. Leschziner, 2004. “Modelling turbulent separated flow in the context of aerodynamic applications” Fluid Dynamics Research 38 (2004) 174 – 210.
41. Kumar M., Arora B.B., Maji S., Maji S, 2012, “Effect of Equivalent Cone Angle on the Performance of Parallel Hub Diverging Casing Annular Diffuser,” International Journal of Fluids Engineering. ISSN 0974-3138 Volume 4, No.2., pp. 97-10.
42. Kumar M., Arora B.B., Maji S., Maji S, 2012, “Effect of Area Ratio and Inlet Swirl on the Performance of Annular Diffuser” International Journals of Applied Engineering Research, ISSN 0973-4562, Volume 7, Number 13, pp. 1493-1506.
43. Mahalakshmi N.V., Krithiga G., Sandhya S., Vikraman J., Ganesan V., 2007, “Experimental investigations of flow through conical diffusers with and without wake type velocity distortions at inlet” Experimental Thermal and Fluid Science (2007), doi: 10.1016/j.expthermflusci. 2007.
44. Markland, 1986. “A New Diffuser Mapping Technique — Studies in Component Performance: Part 1,” ASME Paper No. 84-GT-237, Amsterdam, June 1984.
45. Moller ES., 1965. “Radial Flow without Swirl between Parallel Disks Having both Supersonic and Subsonic Regions.” ASME Paper No. 65-FE-11.
46. Moller E.S, 1965. “Radial Diffuser Using Incompressible Flow between Disks.” ASME paper no. 65-FE-12.

47. Najafi, A. F., 2004. “Investigation of Internal Turbulent Swirling Flow, Single Phase and Two Phase Flow”, Ph. D. dissertation, Sharif University of Technology, 24–30.
48. Olle Tornblom, 2006 “Experimental and computational studies of turbulent separating internal flows”. ISBN 91-7178-416-0.
49. Peterson Victor L, 1984, “Impact of Computers on Aerodynamics Research and Development”.
50. Shaalan M. R. A., Shabaka, I. M. M., 1975. “An Experimental Investigation of the Swirling Flow Performance of an Annular Diffuser at Low Speed,” ASME Paper No. 75-WA/FE-17.
51. Sharan V K, 1972. “Diffuser Performance Co-Relations”. JASI, Volume 24, pp 415.
52. Sovran G., Klomp E.D., 1967. “Experimentally Determined Optimum Geometries for Rectilinear Diffusers with Rectangular, Conical or Annular Cross- Section,” Fluid Dynamics of Internal Flow, Elsevier Publishing Company.
53. Srinath T, 1968, “An Investigation of the Effects of Swirl on The Flow Regimes and Performance of Annular Diffuser With Equal Inner and Outer Cone Angles”. M.A. Science Thesis , University of Waterloo Canada.
54. Stafford, W. Wilbur, James T. Higginbotham, 1955. “Investigation of Two Short Annular Diffuser Configurations Utilizing Suction and Injection as Means of Boundary Layer Control”. NACA RM L54K18.
55. Stafford W. Wilbur, James T.H. 1957. “Investigation of Short Annular Diffuser Configuration Utilizing Suction as a Means of Boundary Layer Control”, NACA TN-3996.

56. Steenbergen, W., and Voskamp, J., 1998. “The rate of decay of swirl in turbulent pipe flow”. Flow Measurements and Instrumentations, 9, pp. 67–78.
57. Stefano U. and Uberto D., 2000. “Flow Development and Turbulence Length Scales within an Annular Gas Turbine Exhaust Diffuser”, Experimental Thermal and Fluid Science, Vol. 22, pp.55-70.
58. Stevens S. J., Fry P., 1973. “Measurements of the Boundary Layer Growth in Annular Diffusers”. Journal Aircraft Feb., pp 73-89.
59. Stevens S. J., Williams G. J., 1969. “Performance of Annular Diffusers” Gas Turbine Collaboration Committee Report No. 299.
60. Stevens S. J., Williams G. J., 1980. “The Influence of Inlet Conditions on the Performance of Annular Diffuser”. Trans. ASME Journal Fluids Egg. 102, 357-363.
61. Stratford B.S., Tubbs H., 1965,"The Maximum Pressure Rise Attainable in Subsonic Diffusers", Journal of the Royal Aeronautical Society, Technical Note, April.
62. Takehira A., et. al., 1977. “An Experimental Study of the Annular Diffusers in Axial-Flow Compressors and Turbines” Japan Society of Mechanical Engineers, Paper No.39, 1977.
63. Thayer E B, 1971 “Evaluation of Curved Wall Annular Diffuser” ASME paper no .71 -WA/FE-35.
64. Tom B. & Brane Š., Marko H. & Ferdinand T., 2006. “Heat Transfer Influenced by Turbulent Airflow inside an Axially Rotating Diffuser”. Flow Turbulence Combust (2006) 80:3–19.
65. Ubertini S. and Desideri U., 2000, “ Experimental performance analysis of an annular diffuser with and without struts,” Elsevier, J. Experimental Thermal and Fluid Science Vol. 22, Number 3, September 2000, pp.183-195.

66. Walter G., 2006 “Analytical and numerical investigation of steady and unsteady turbulent swirling flow in diffuser” thesis for licentiate of engineering no. 2006:05 ISSN 1652-8565.
67. Wilbur, S.W. and Higginbotham, J. T.,1955, “Investigation of two short annular diffuser configurations utilizing suction and injection as a means of boundary layer control” , NACA RML54K18.
68. Wood C.C., Henry J. R., 1958. “Effects of Shock Boundary Layer Interaction on the Long and Short Subsonic Annular Diffuser” .NACA RM L58A31.

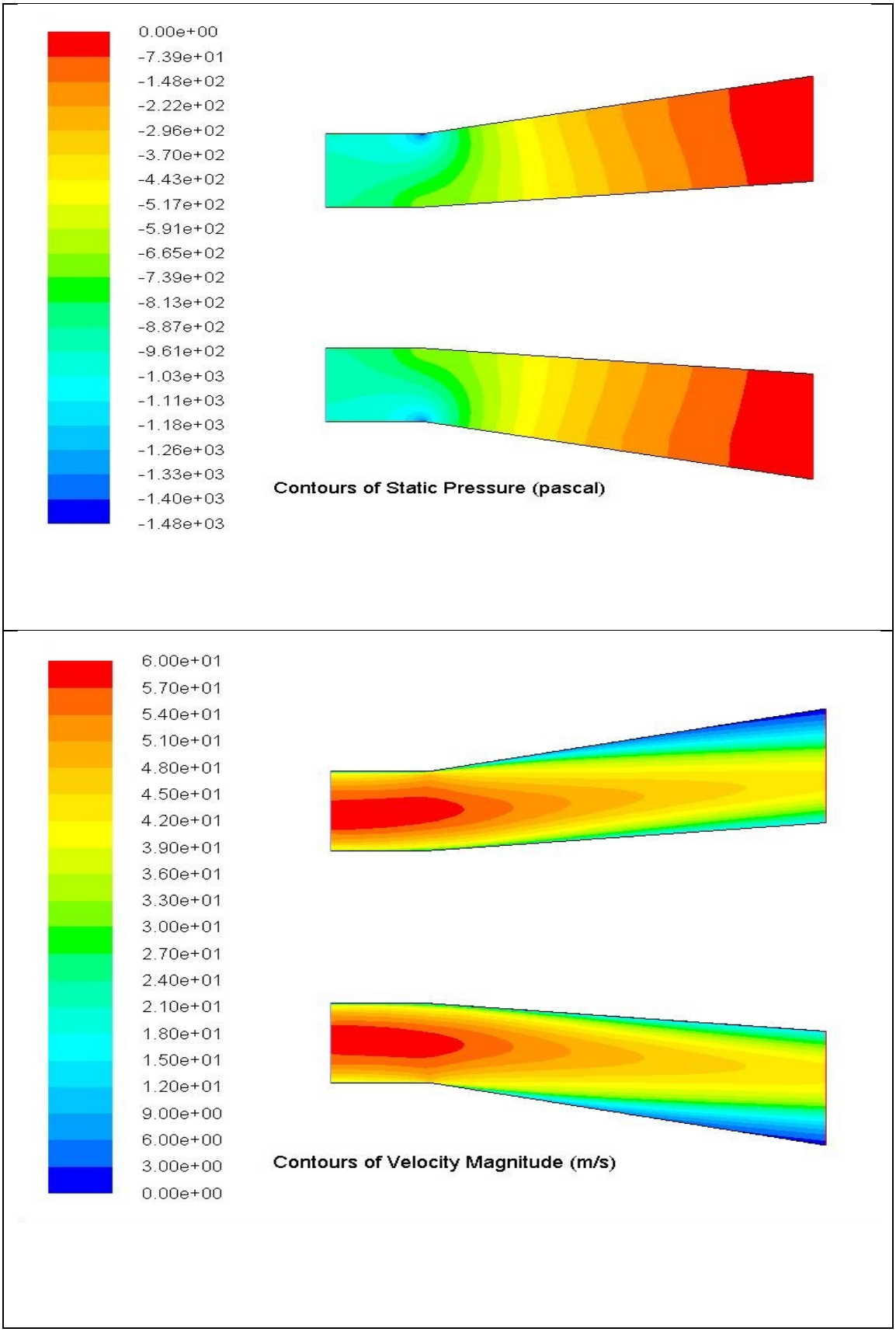

Fig No-1 AR= 2, Swirl Angle = 0^0 , Velocity = 60m/s

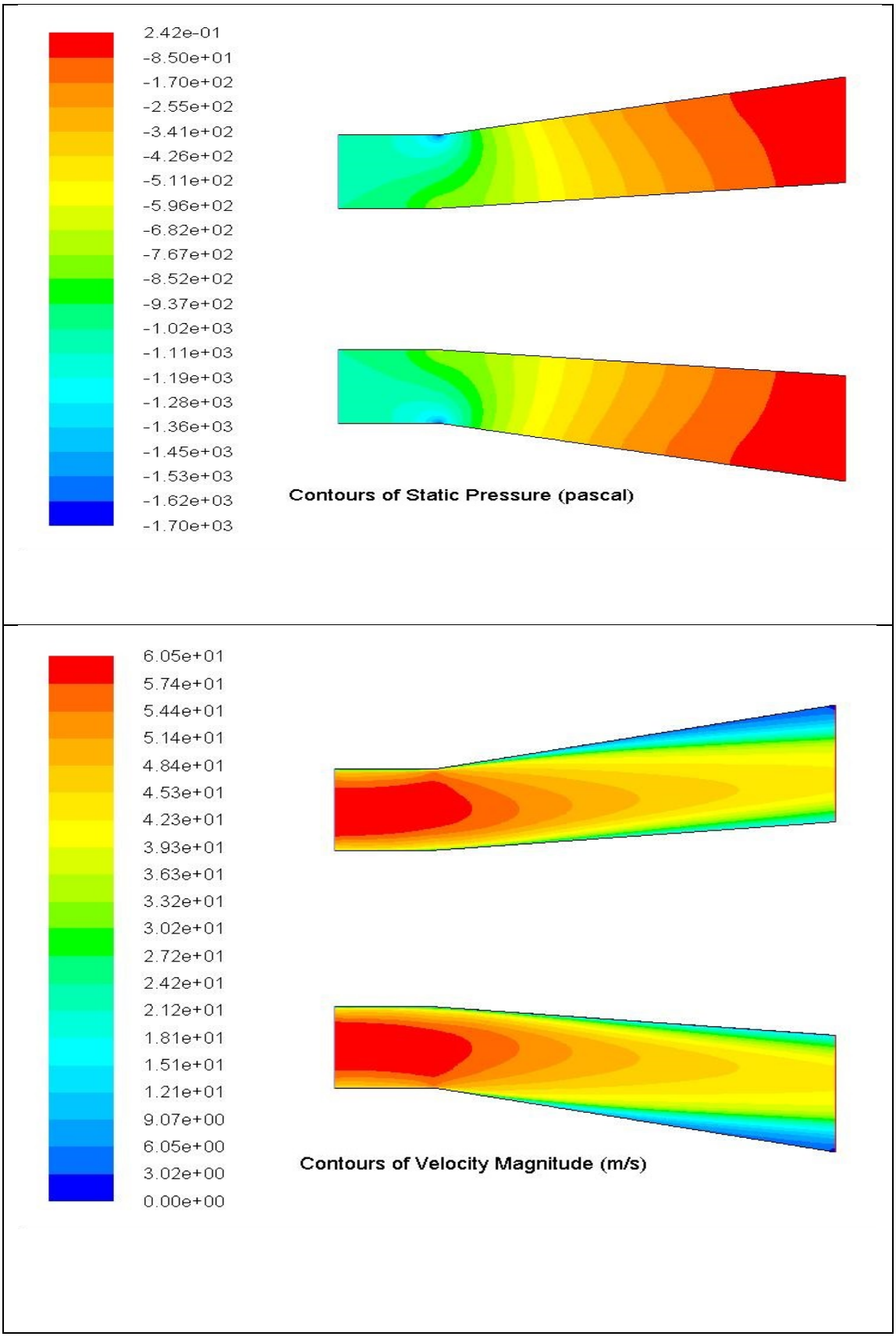

Fig No-2 AR= 2, Swirl Angle = 7.5^0 , Velocity = 60m/s

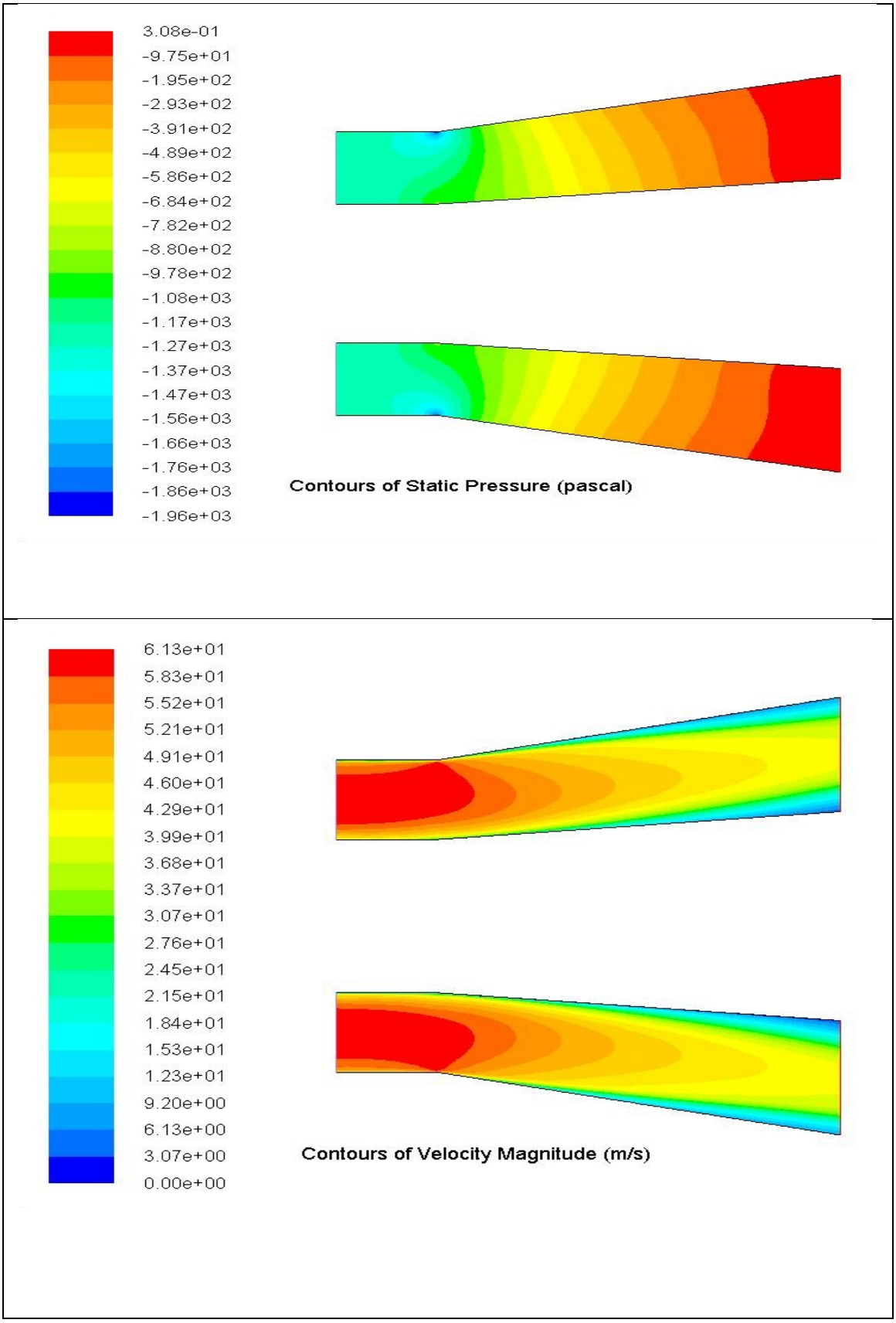

Fig No-3 AR= 2, Swirl Angle =12.5^0 , Velocity = 60m/s

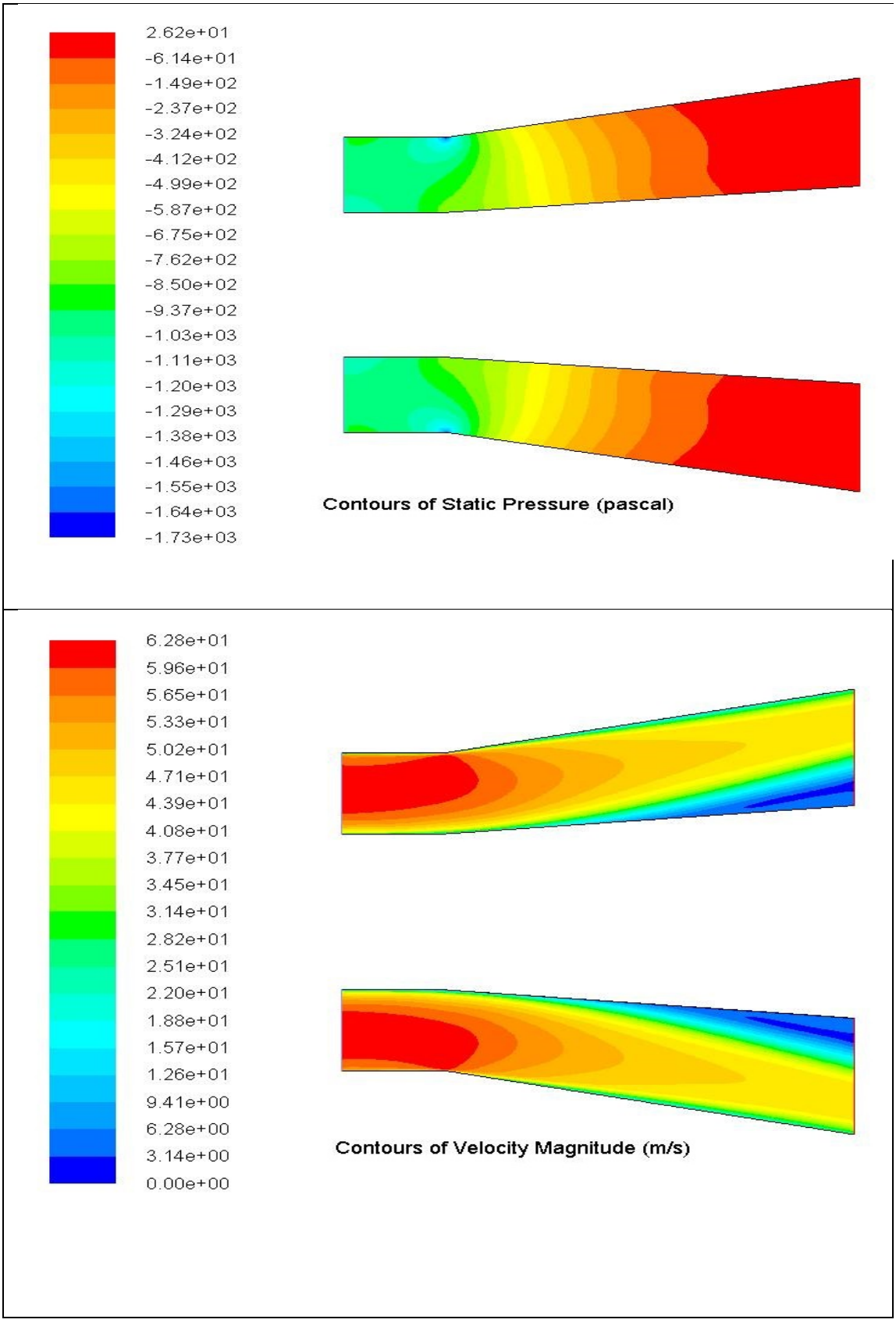

Fig No-4 AR= 2, Swirl Angle = 17.5^0 , Velocity = 60m/s

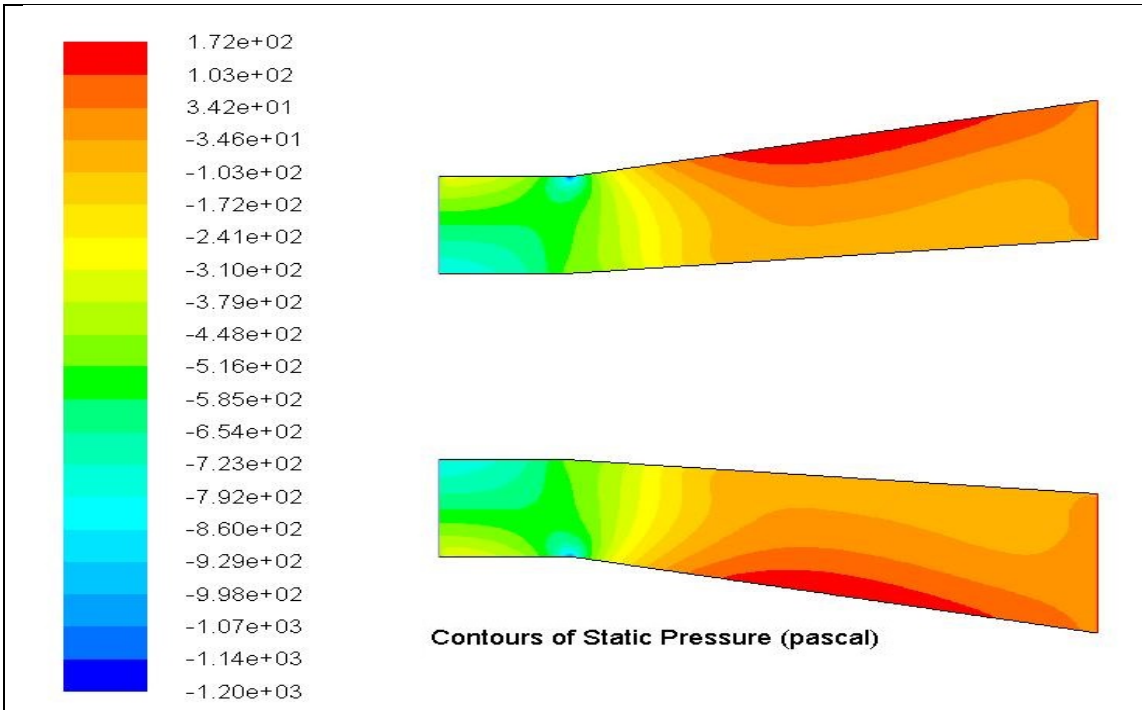

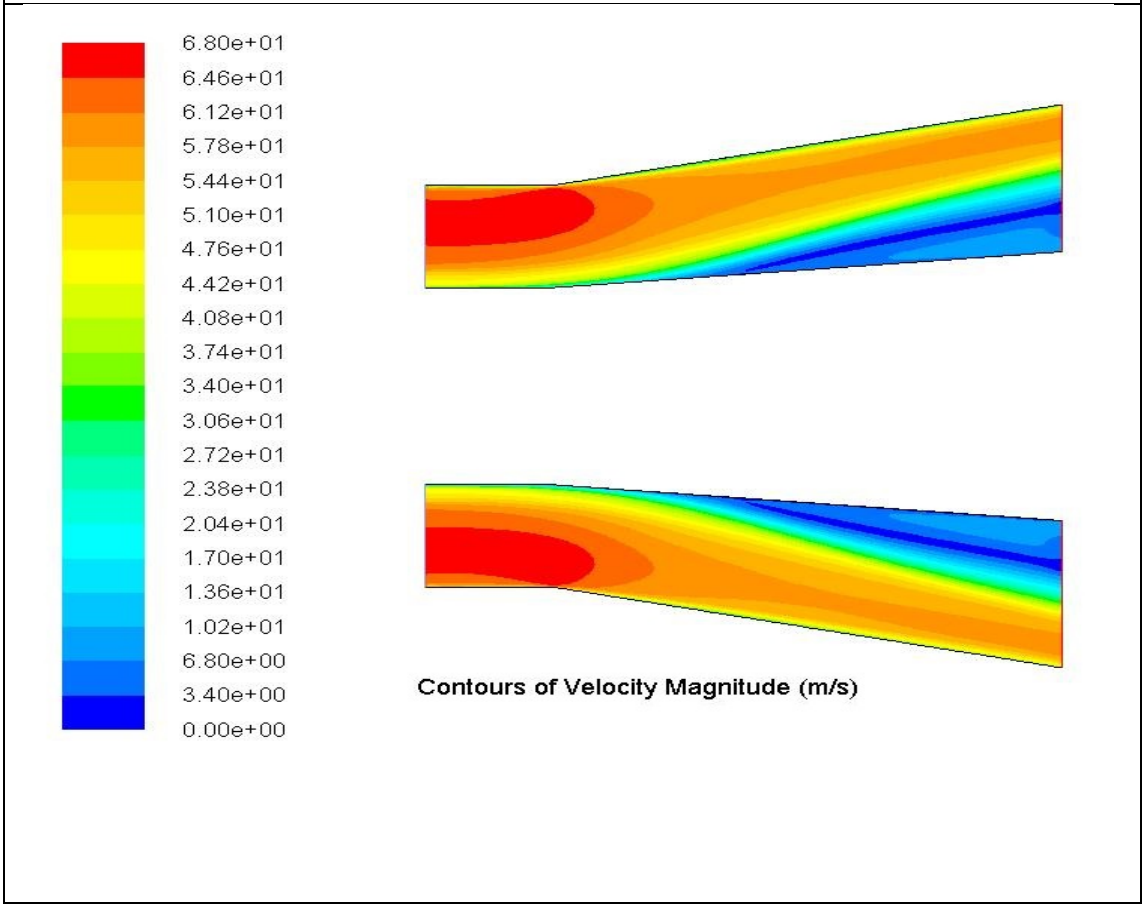

Fig No-5 AR= 2, Swirl Angle = 25^0 , Velocity = 60m/s

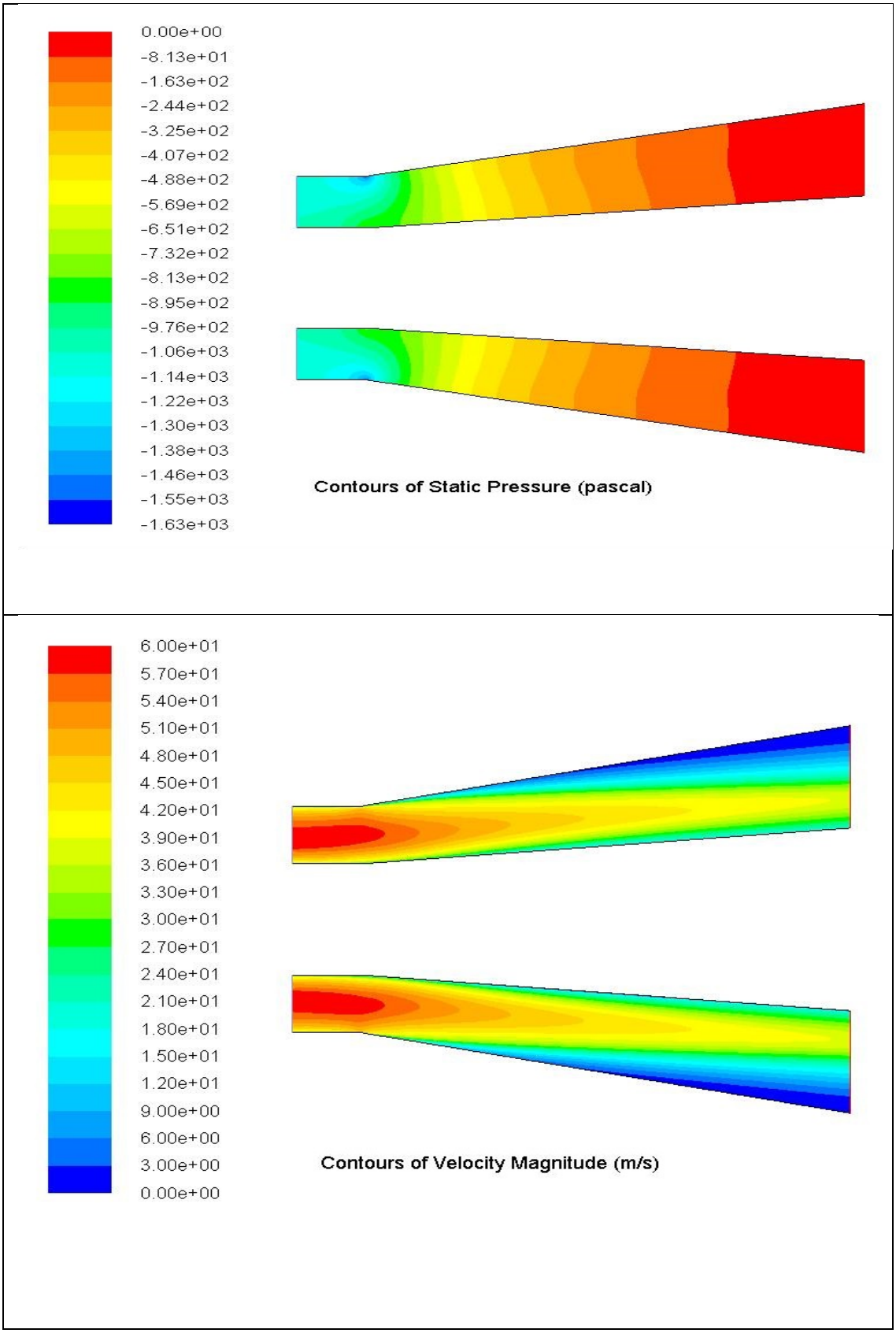

Fig No-6 AR= 3, Swirl Angle = 0^0 , Velocity = 60m/s

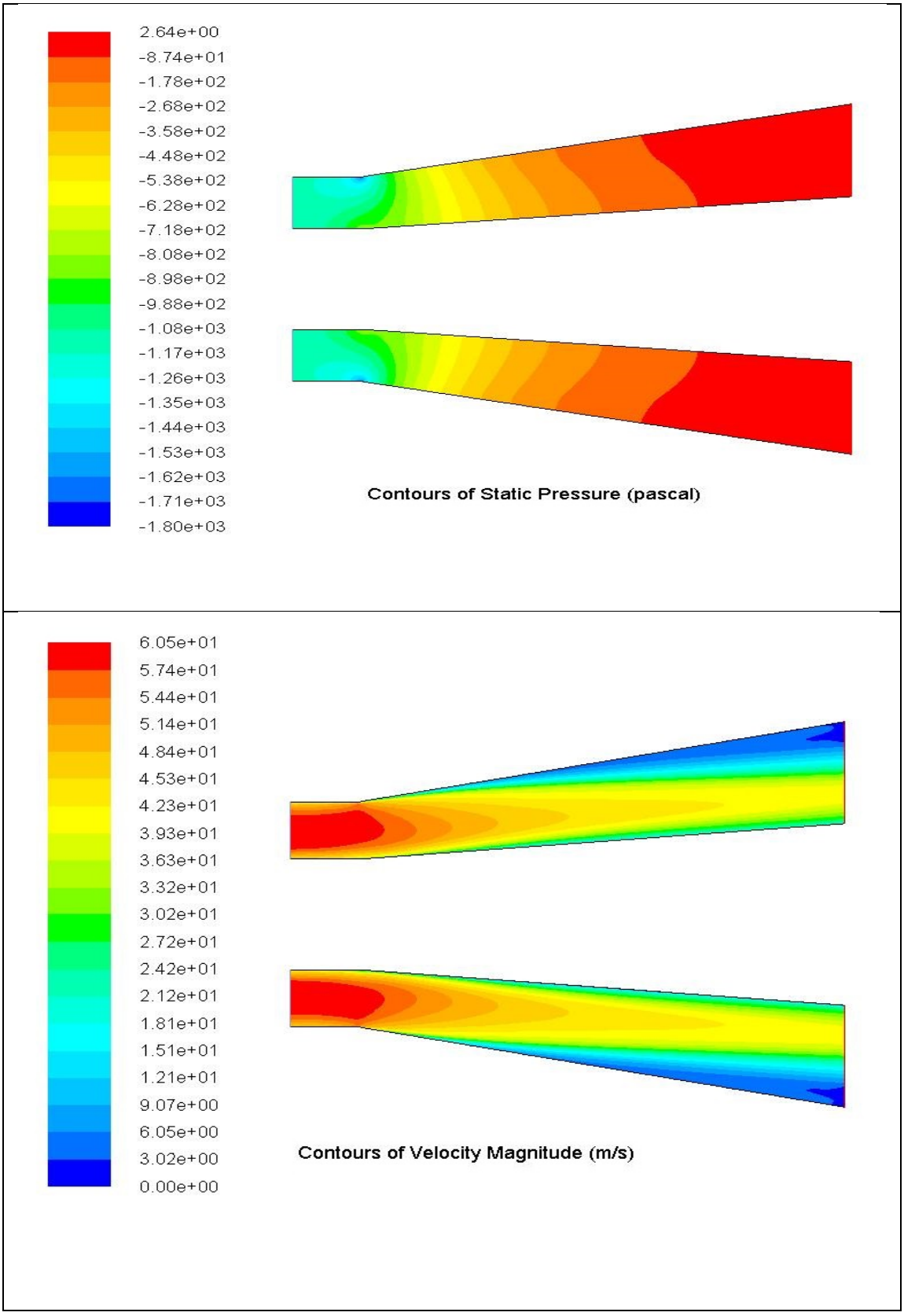

Fig No-7 AR= 3, Swirl Angle = 7.5^0 , Velocity = 60m/s

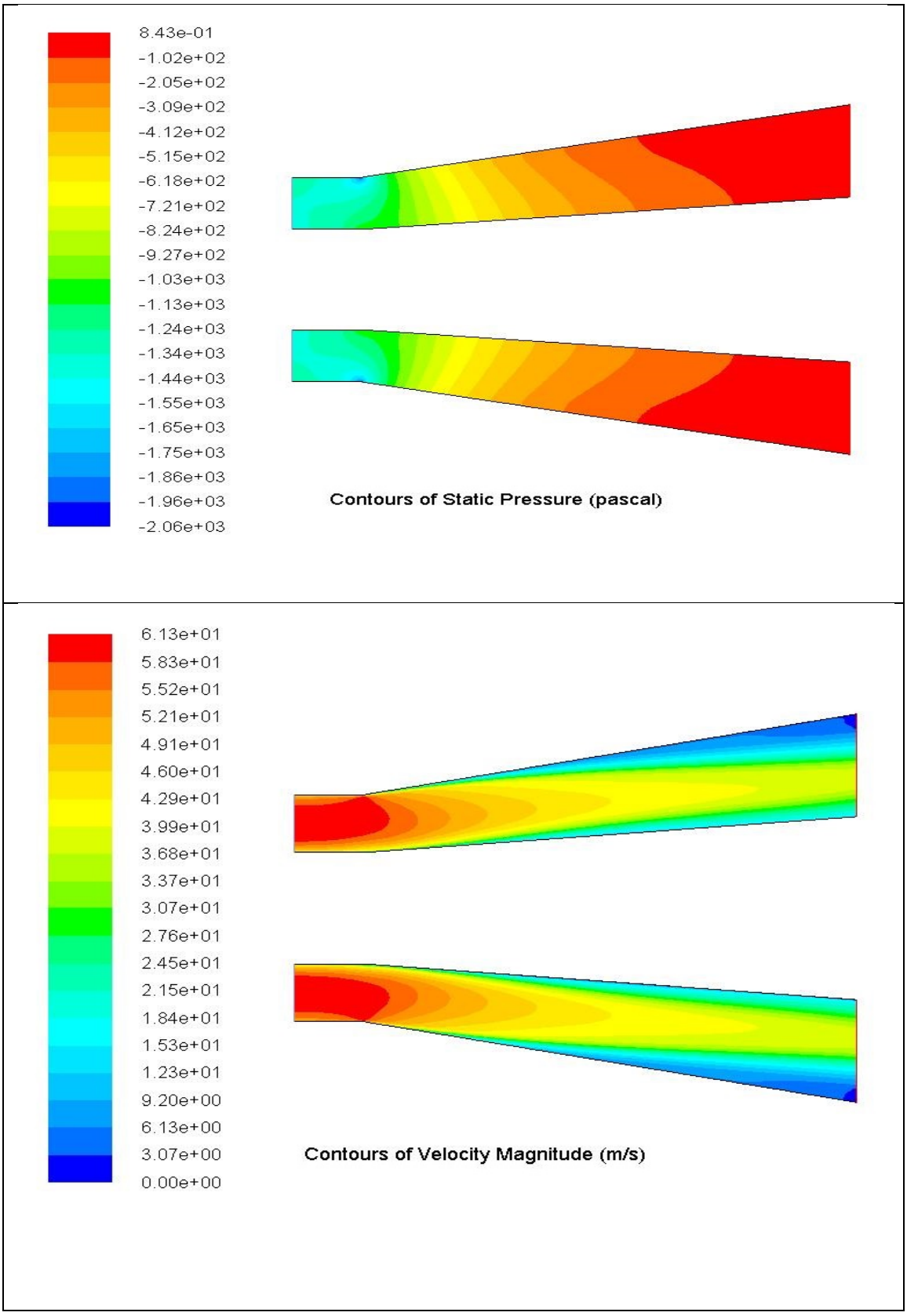

Fig No-8 AR= 3, Swirl Angle = 12.5^0 , Velocity = 60m/s

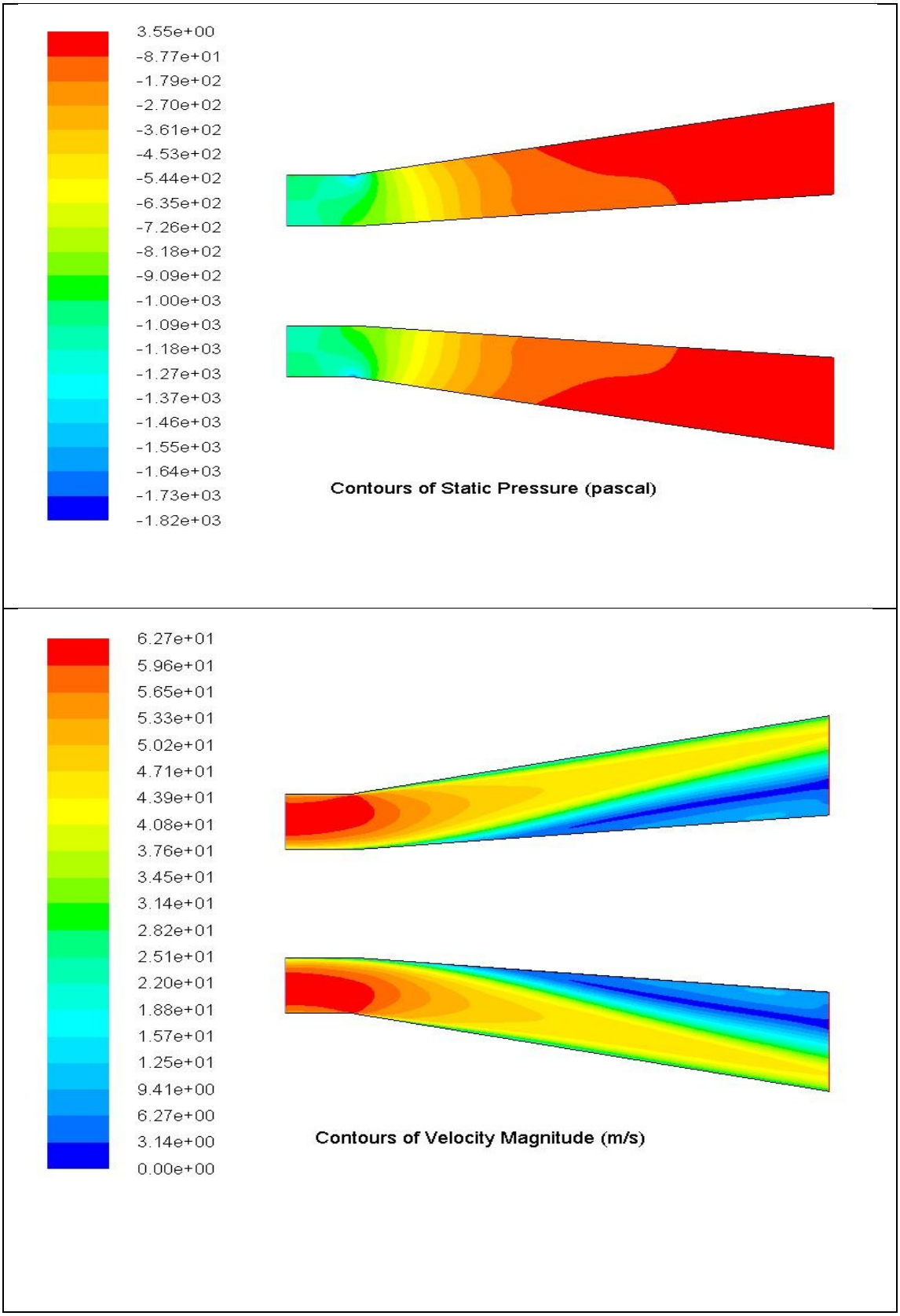

Fig No-9 AR= 3, Swirl Angle = 17.5^0 , Velocity = 60m/s

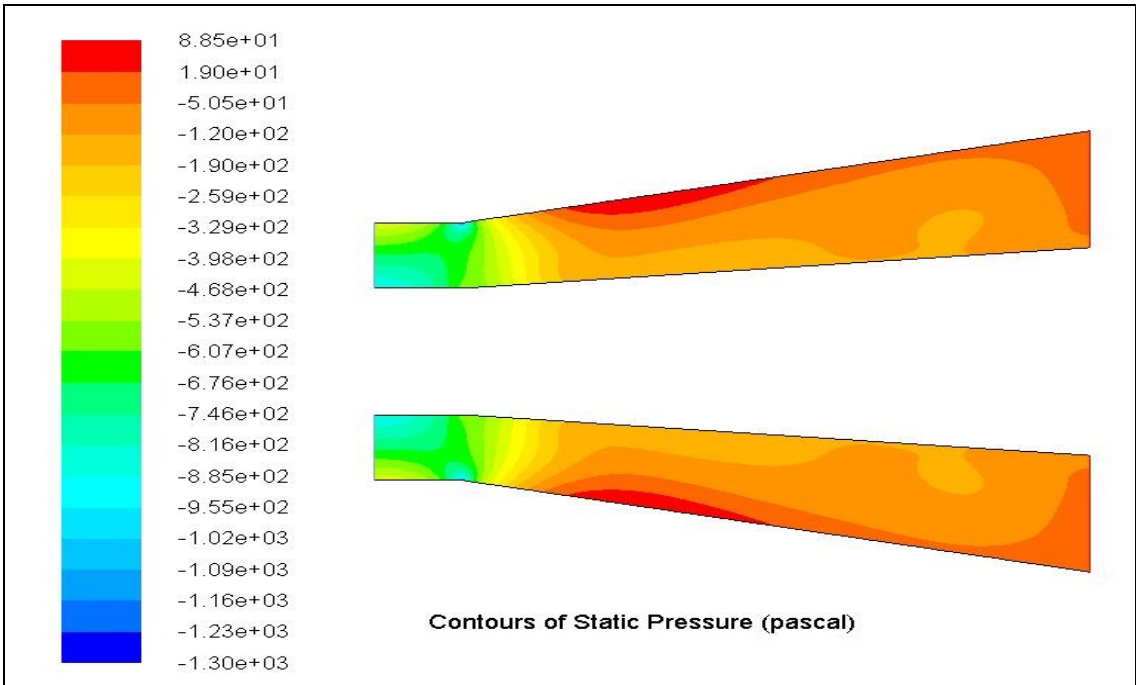

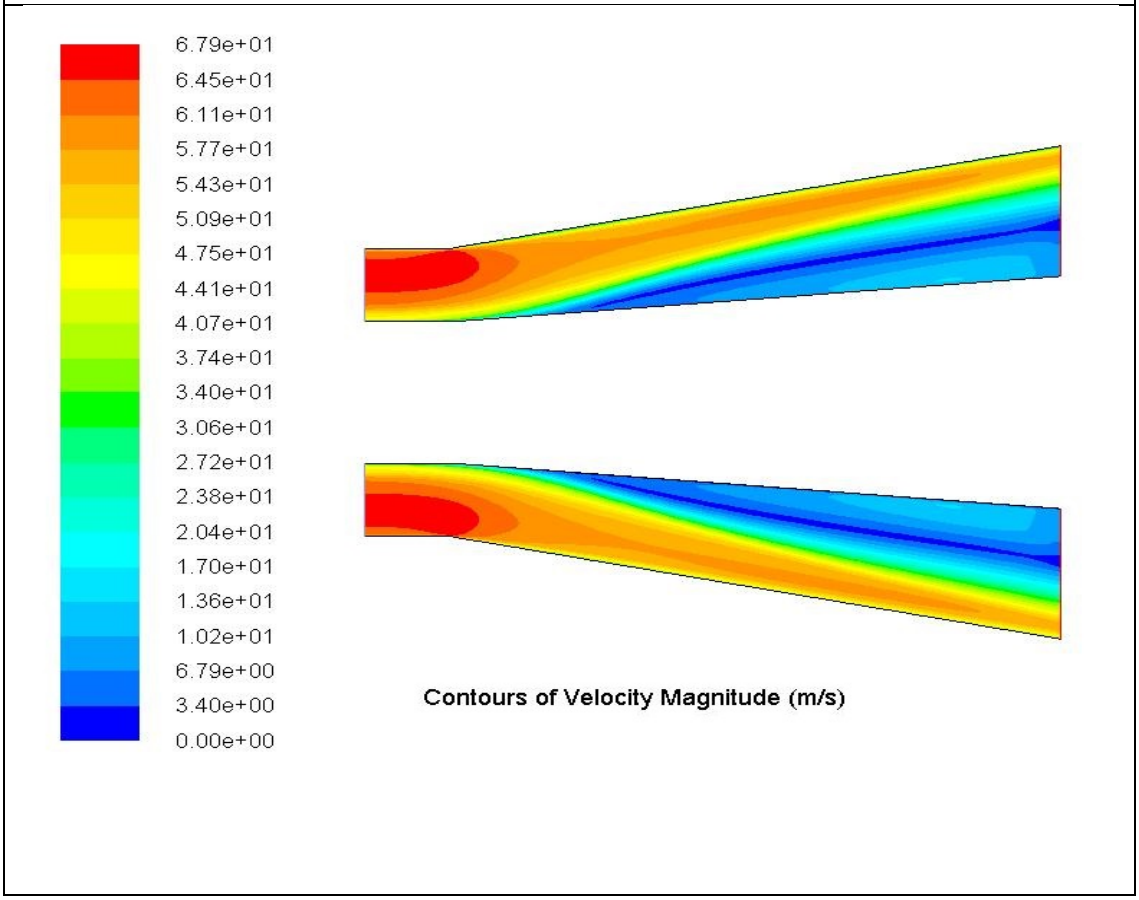

Fig No-10 **AR= 3, Swirl Angle = 25^0, Velocity = 60m/s**

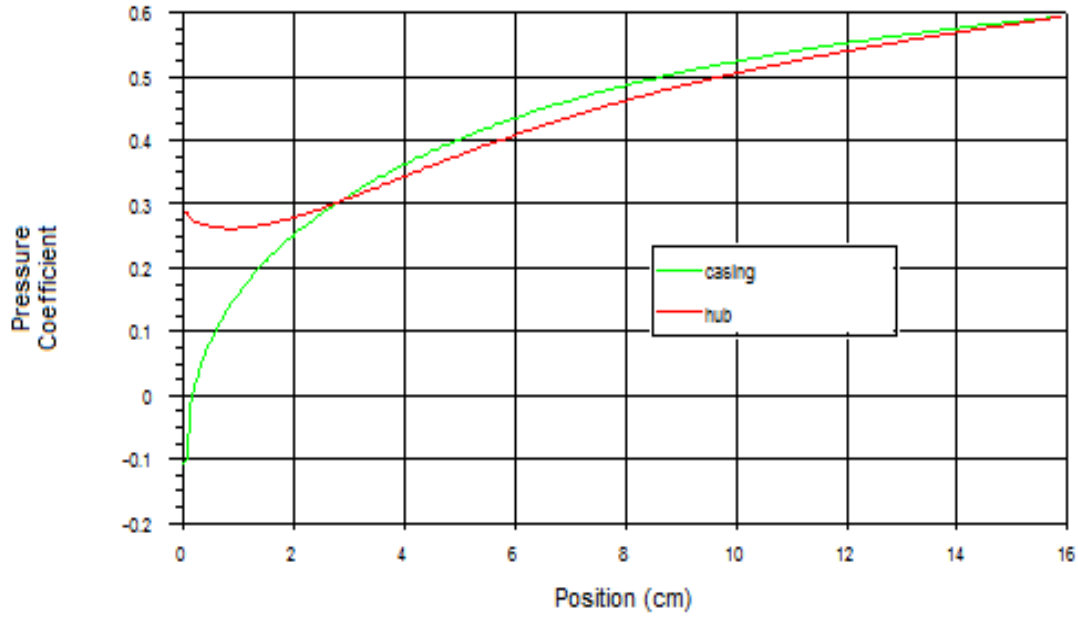

Fig No-11 AR 2, Pressure coefficient for 0^0 swirl, velocity 60m/s

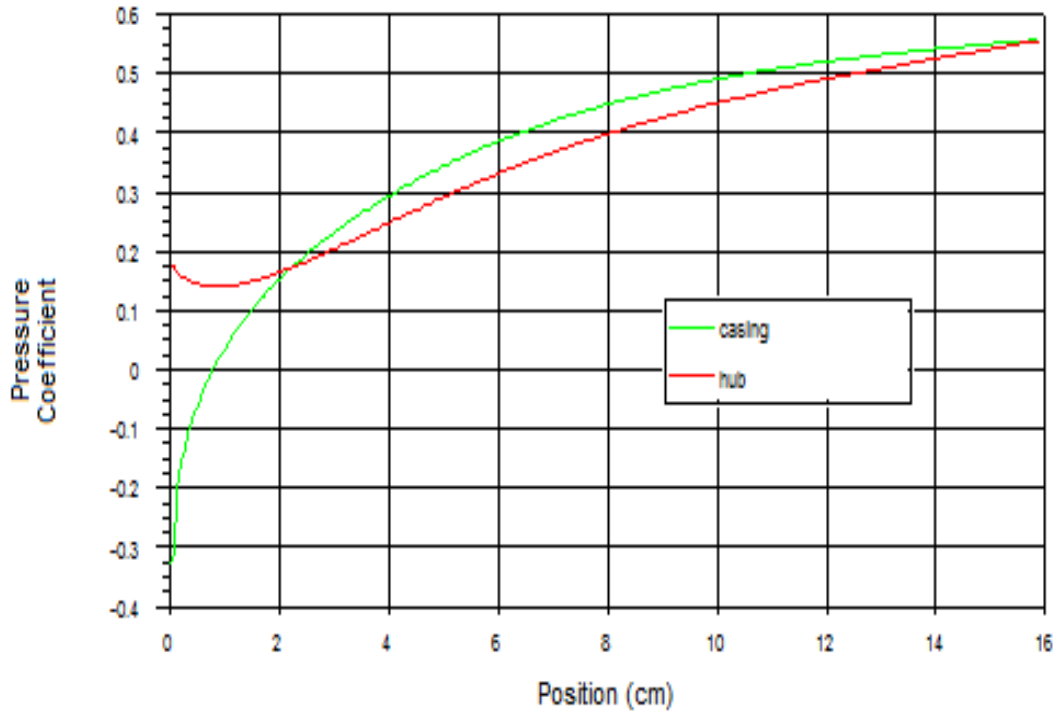

Fig No-12 AR 2, Pressure coefficient for 7.5^0 swirl, velocity 60m/s

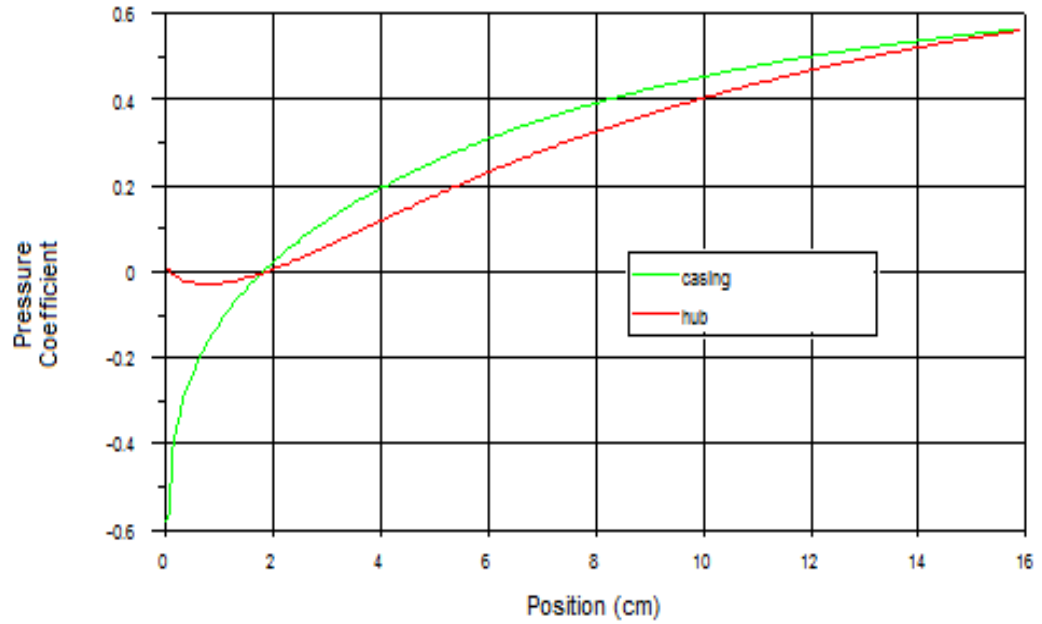

Fig No-13 AR 2, Pressure coefficient for 12.5^0 swirl, velocity 60m/s

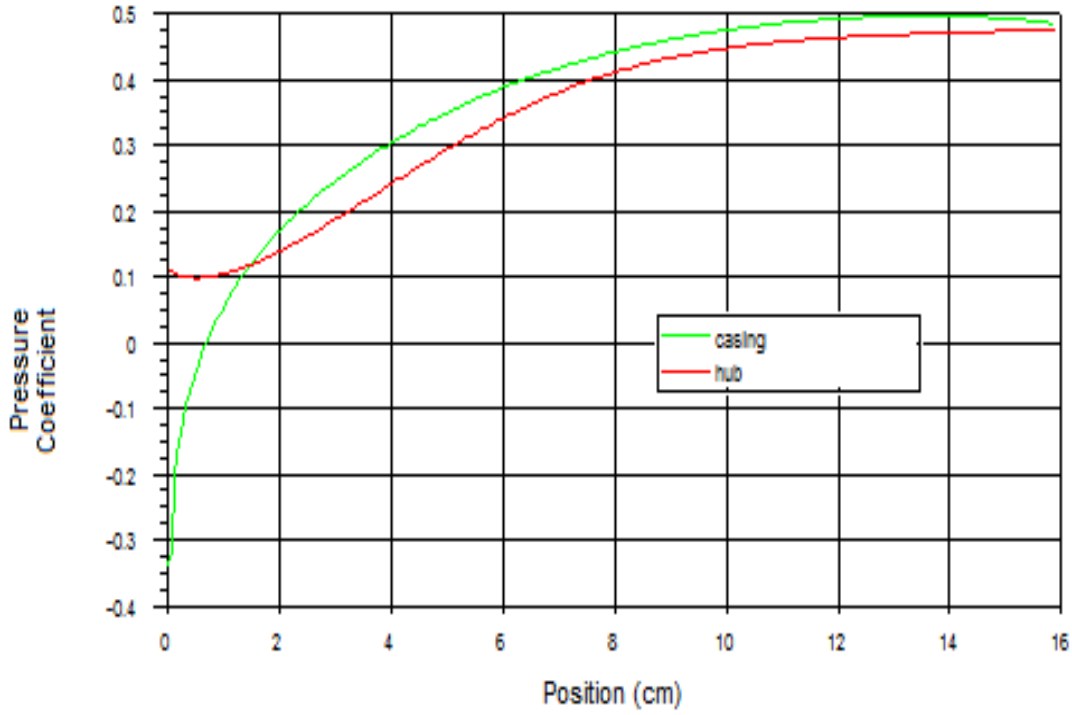

Fig No-14 AR 2, Pressure coefficient for 17.5^0 swirl, velocity 60m/s

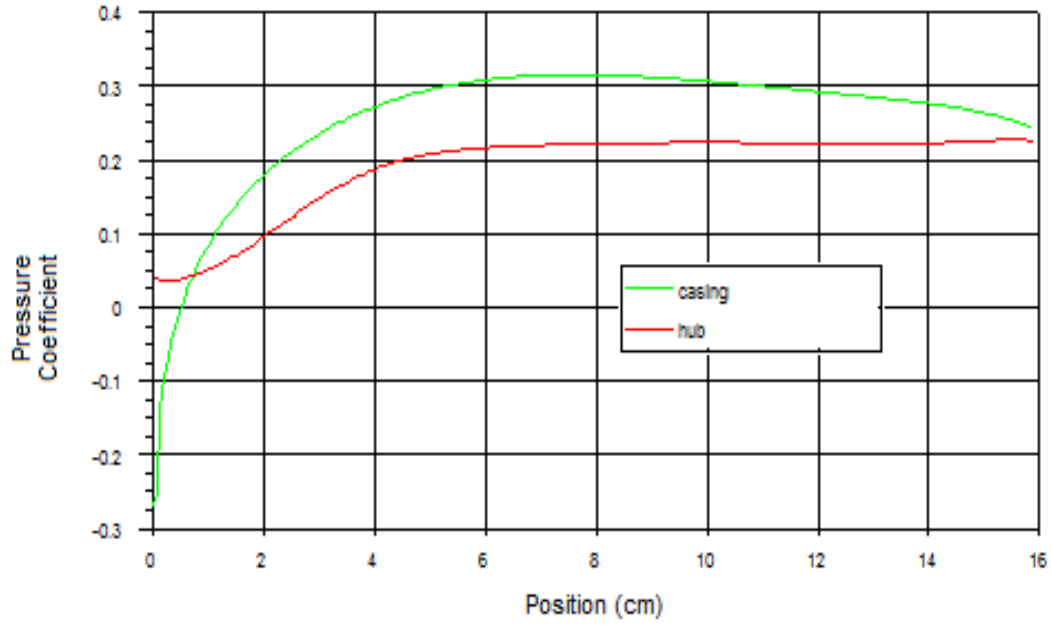

Fig No-15 AR 2, Pressure coefficient for 25^0 swirl, velocity 60m/s

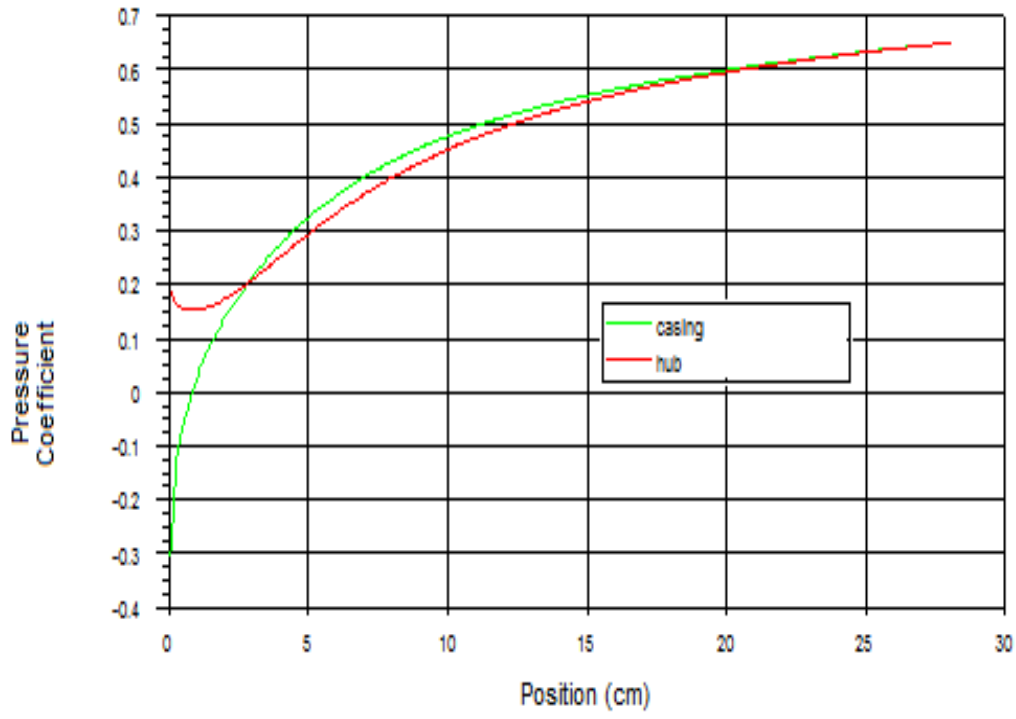

Fig No-16 AR 3, Pressure coefficient for 0^0 swirl, velocity 60m/s

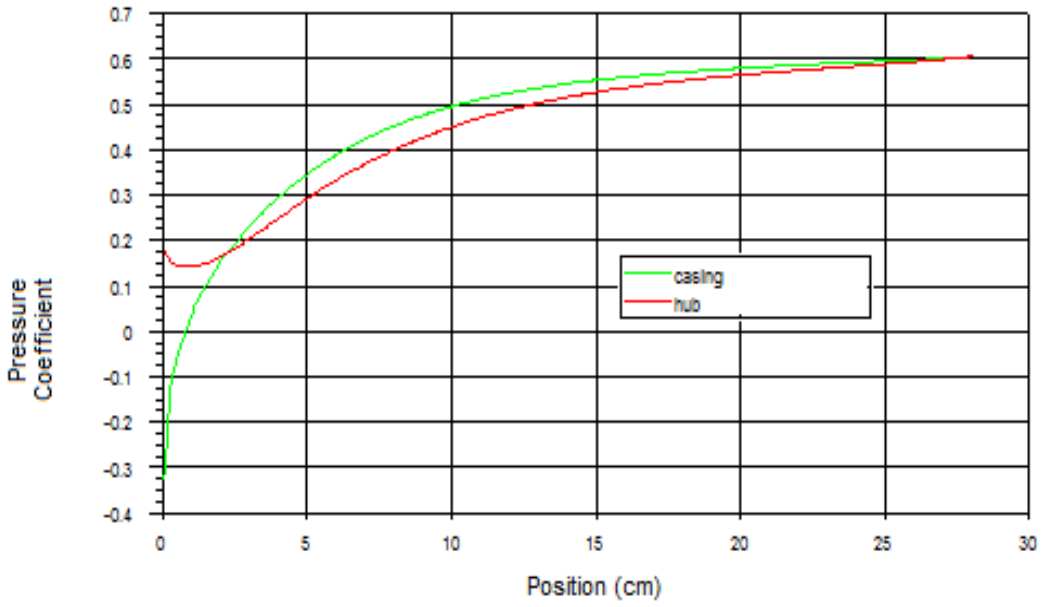

Fig No-17 AR 3, Pressure coefficient for 7.5^0 swirl, velocity 60m/s

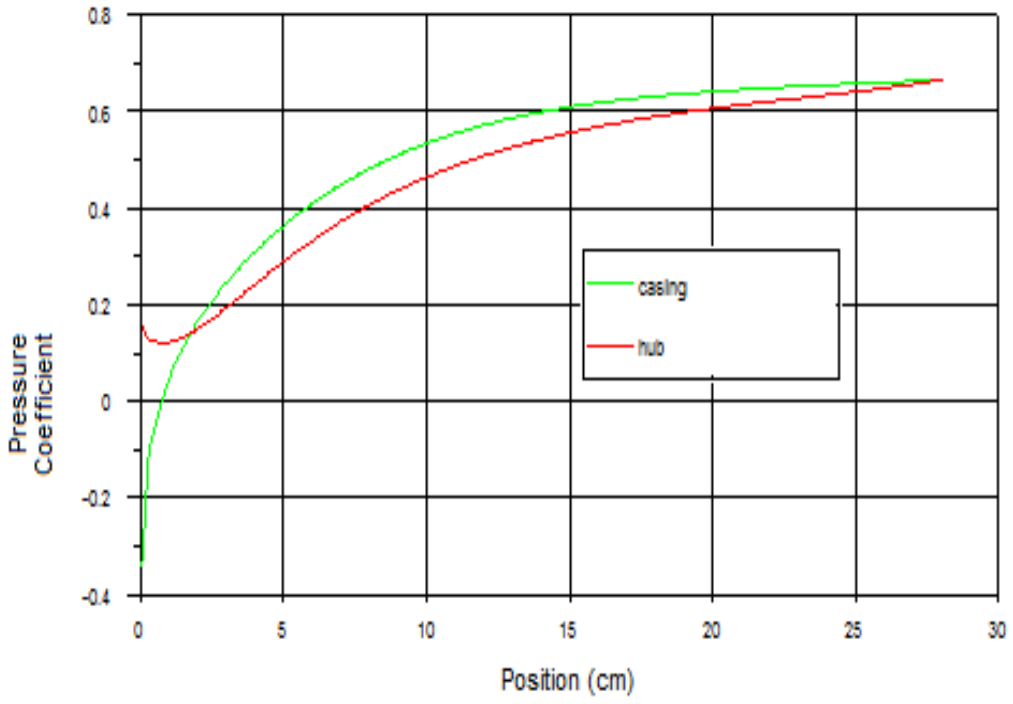

Fig No-18 AR 3, Pressure coefficient for 12.5^0 swirl, velocity 60m/s

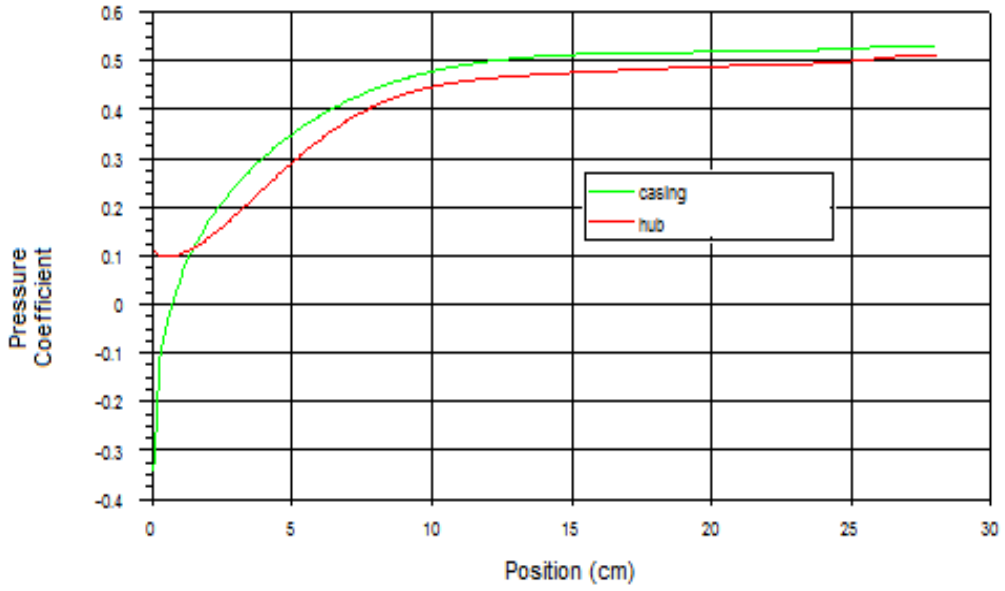

Fig No-19 AR 3, Pressure coefficient for 17.5^0 swirl, velocity 60m/s

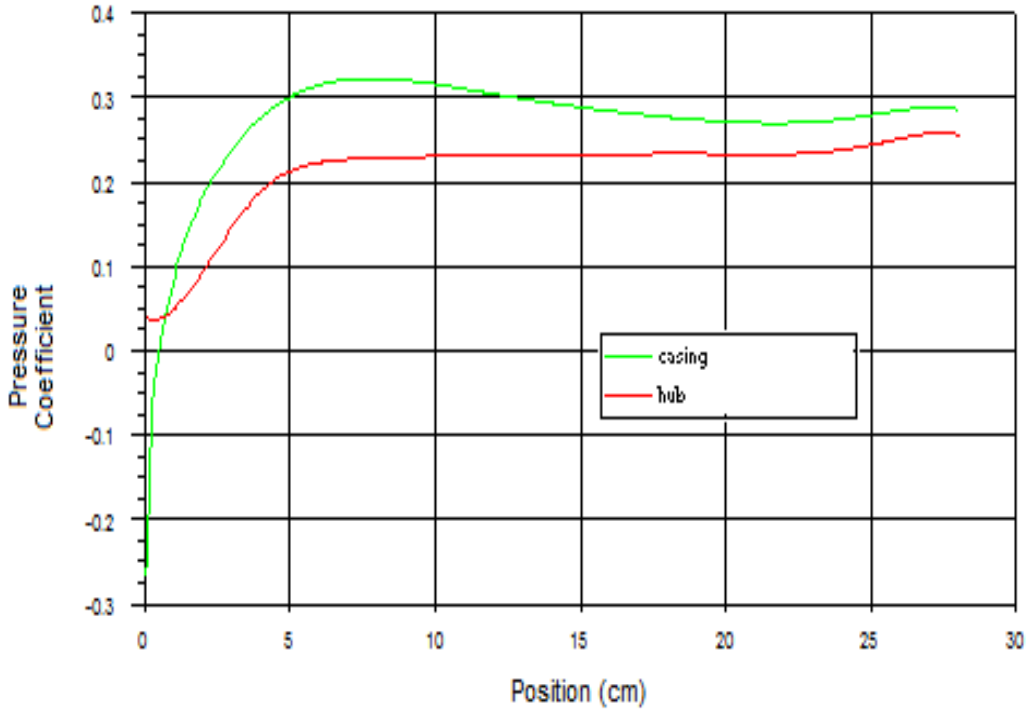

Fig No-20 AR 3, Pressure coefficient for25^0 swirl, velocity 60m/s

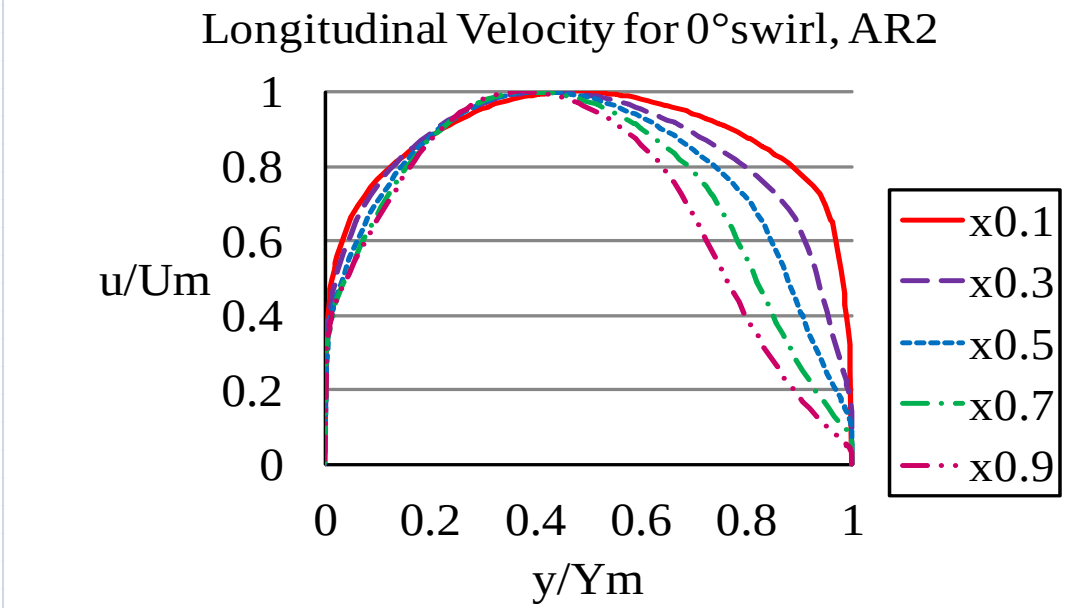

Fig No-21

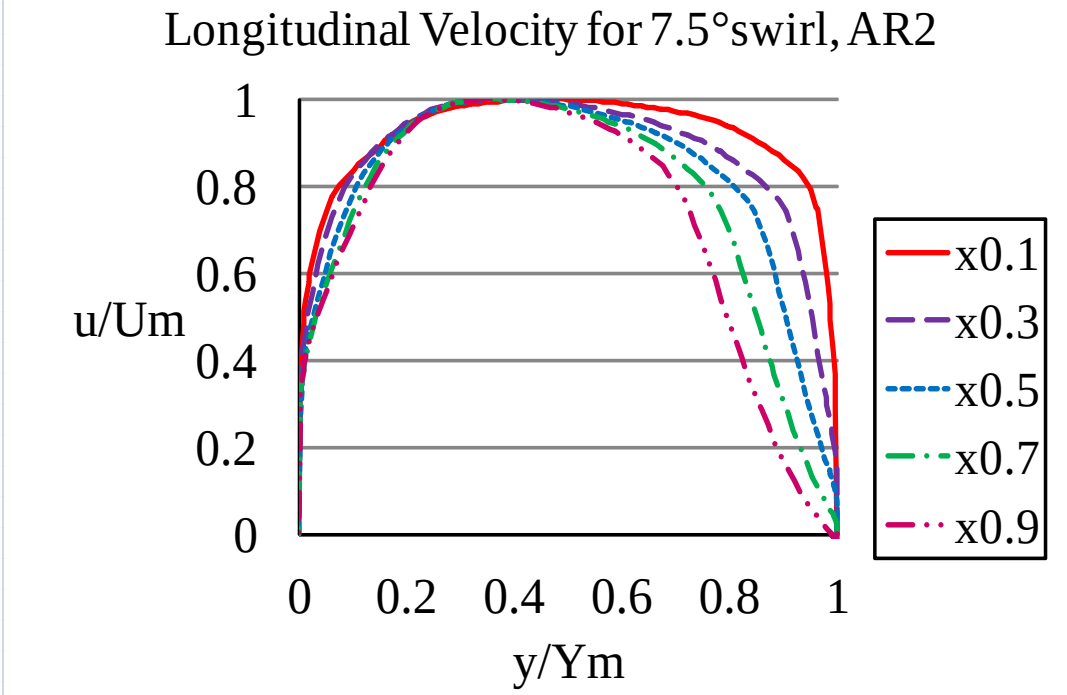

Fig No-22

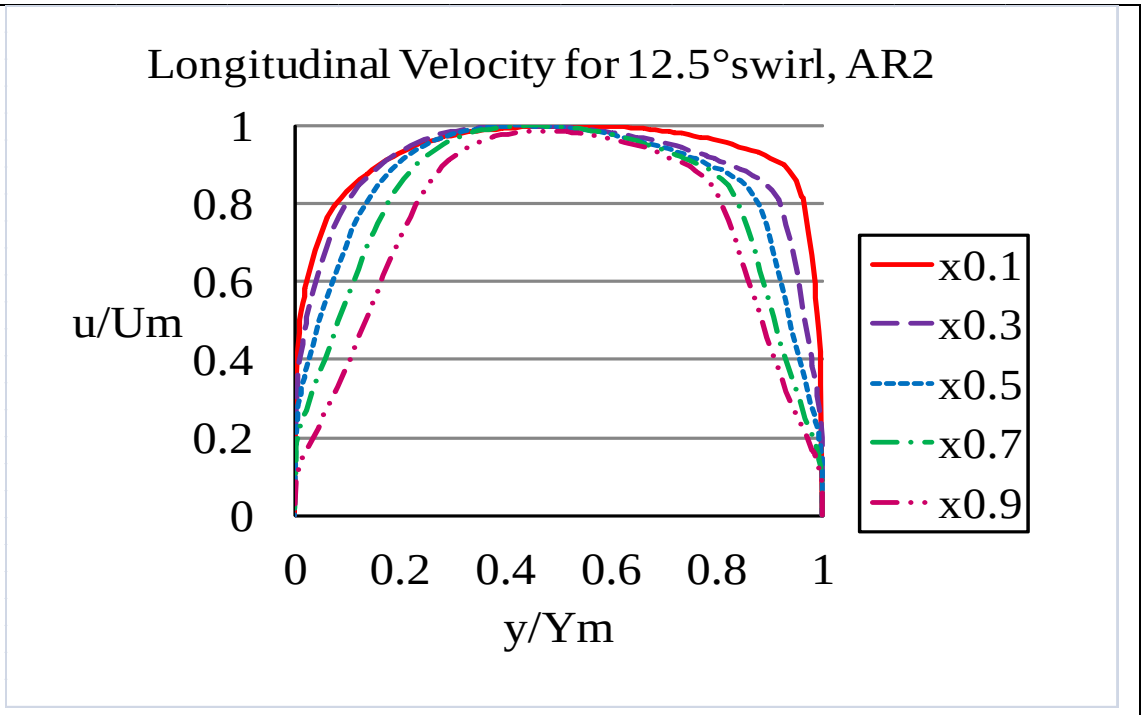

Fig No-23

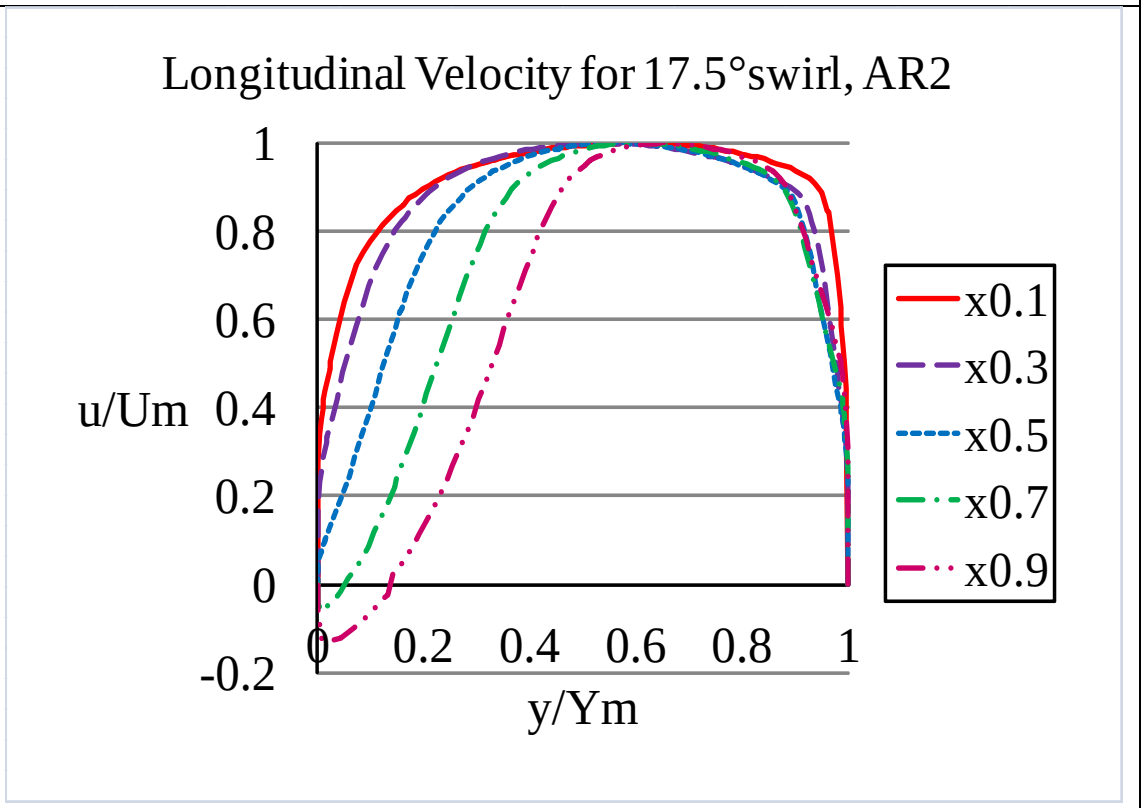

Fig No-24

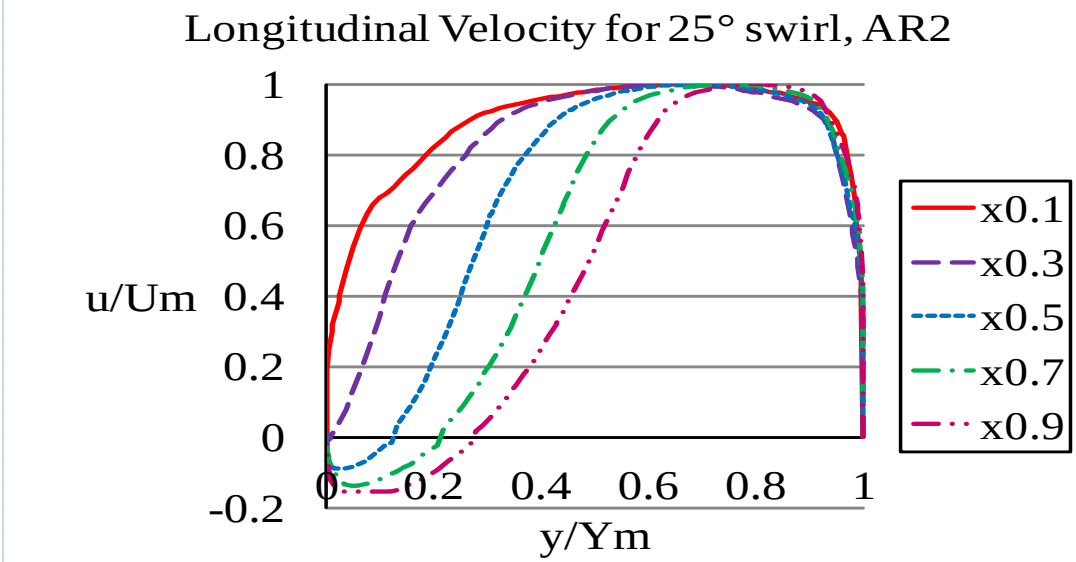

Fig No-25

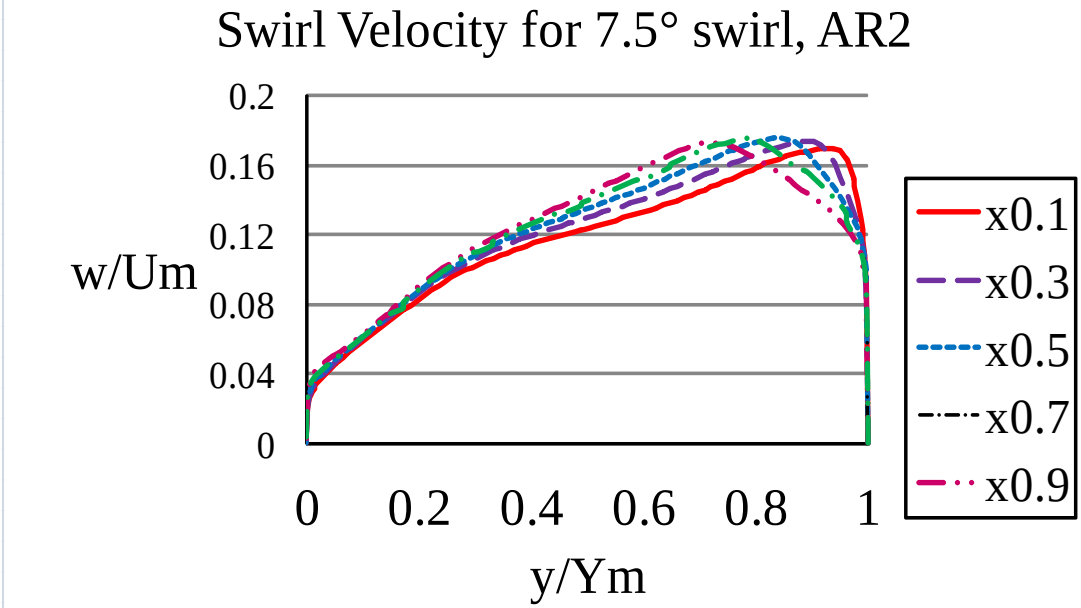

Fig No-26

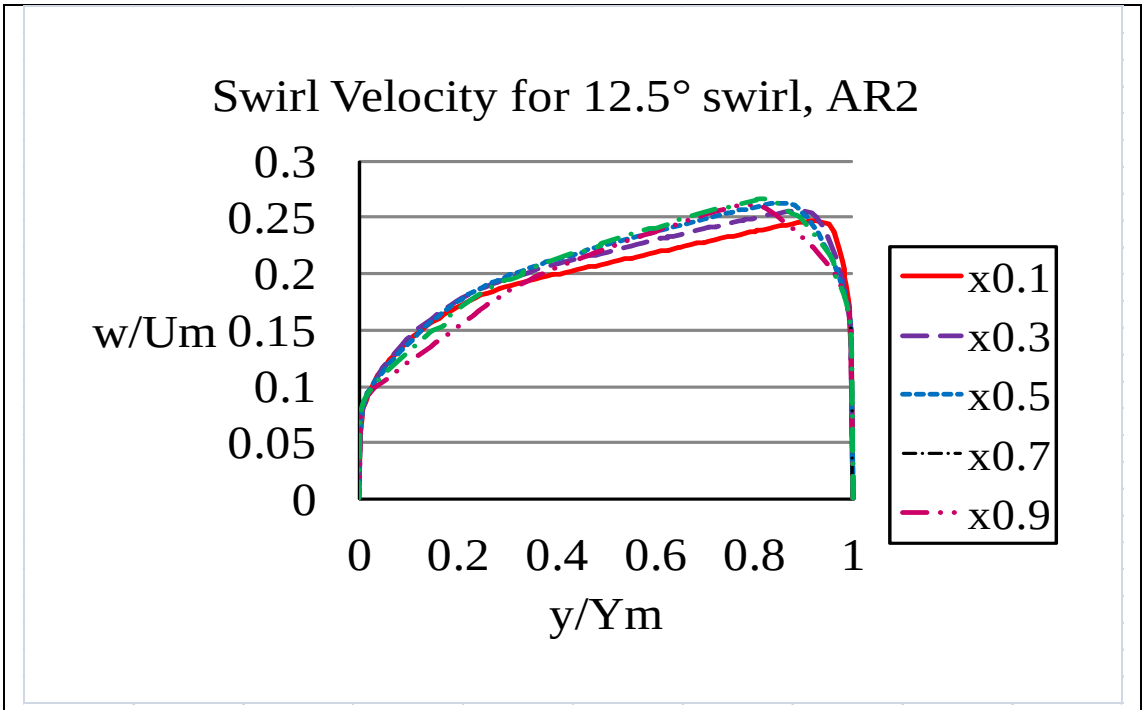

Fig No-27

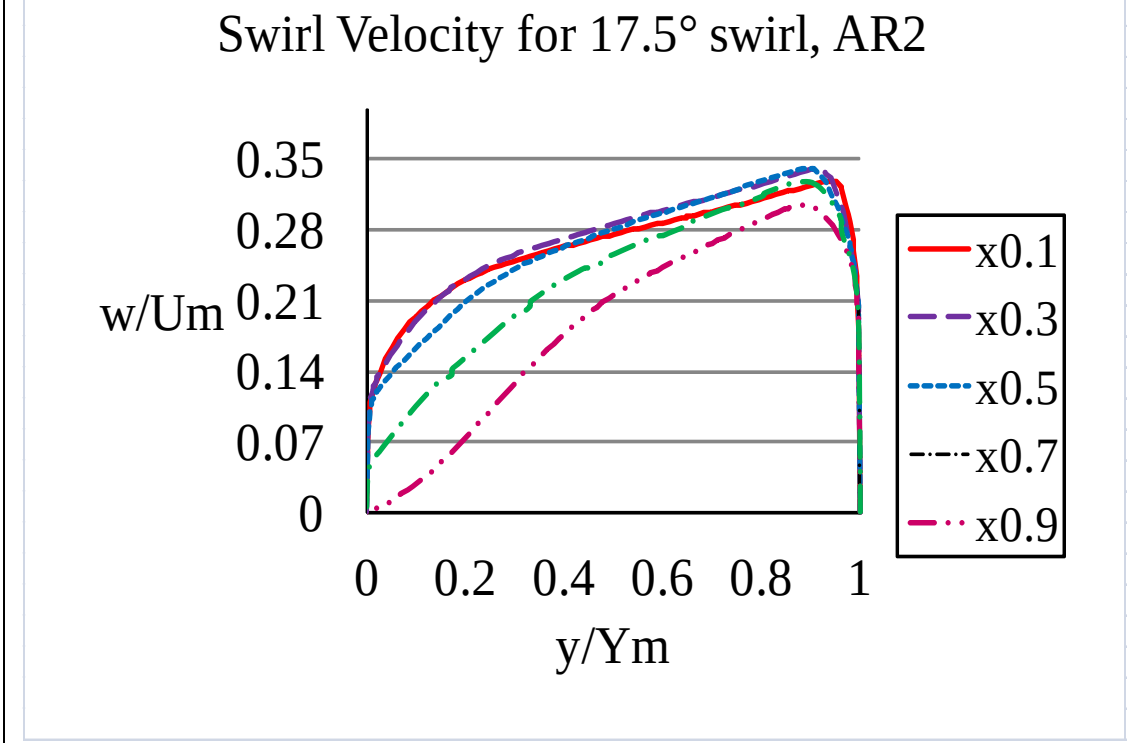

Fig No-28

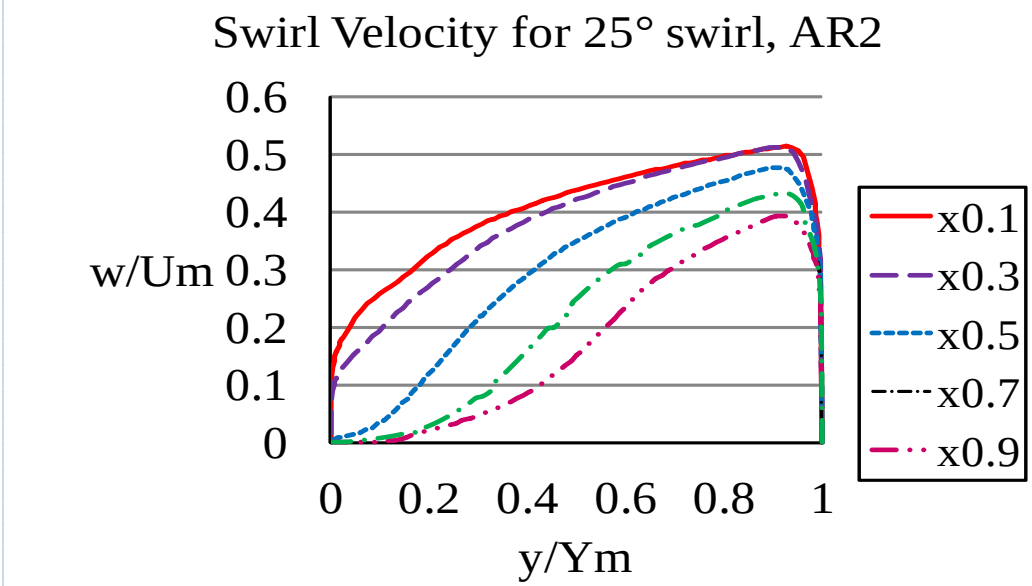

Fig No-29

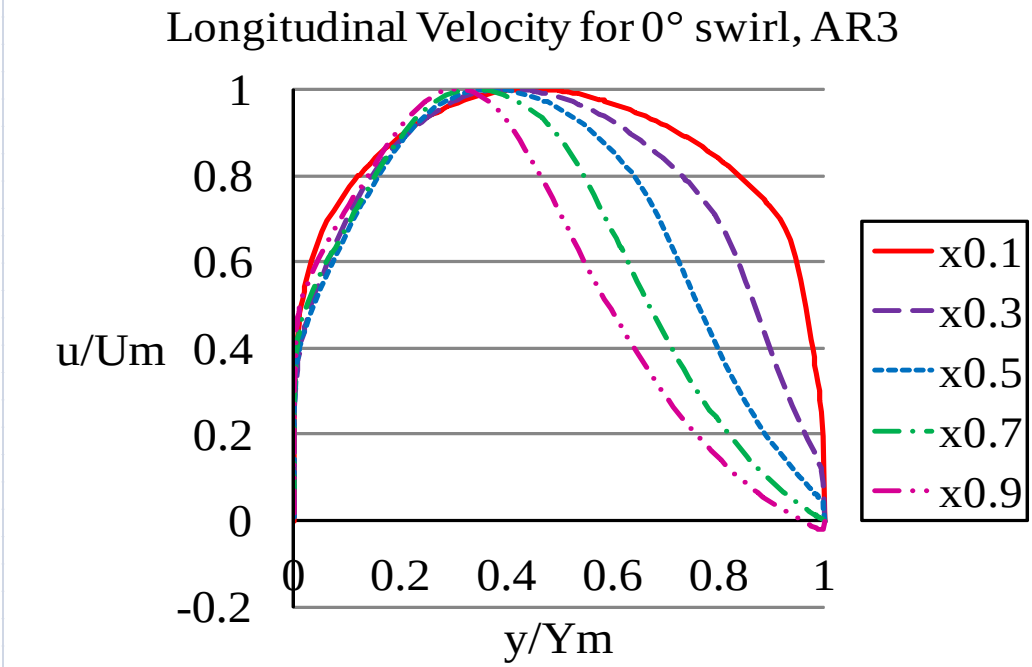

Fig No-30

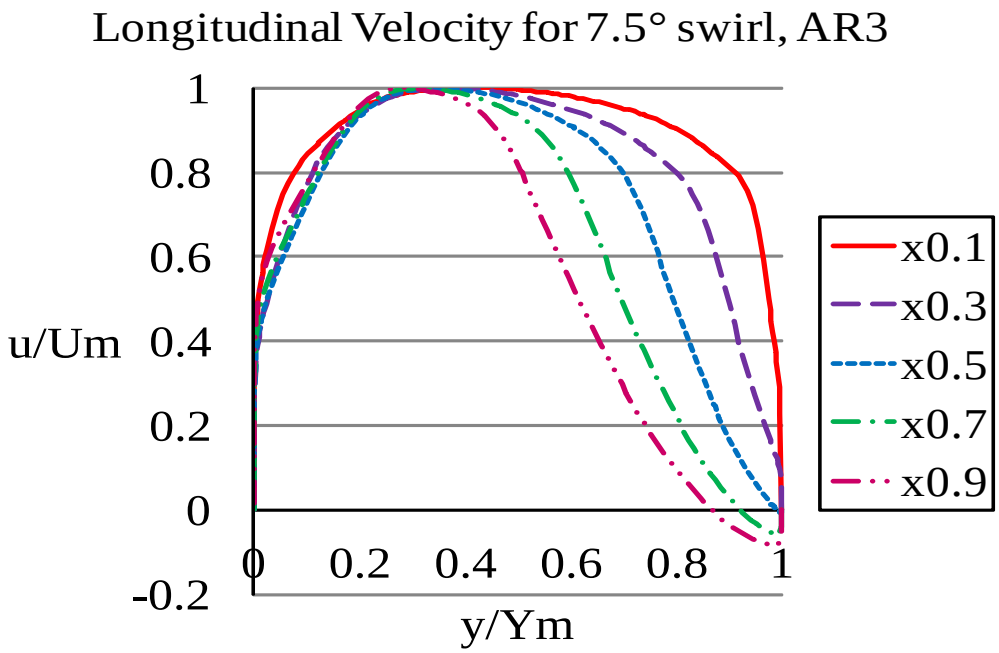

Fig No-31

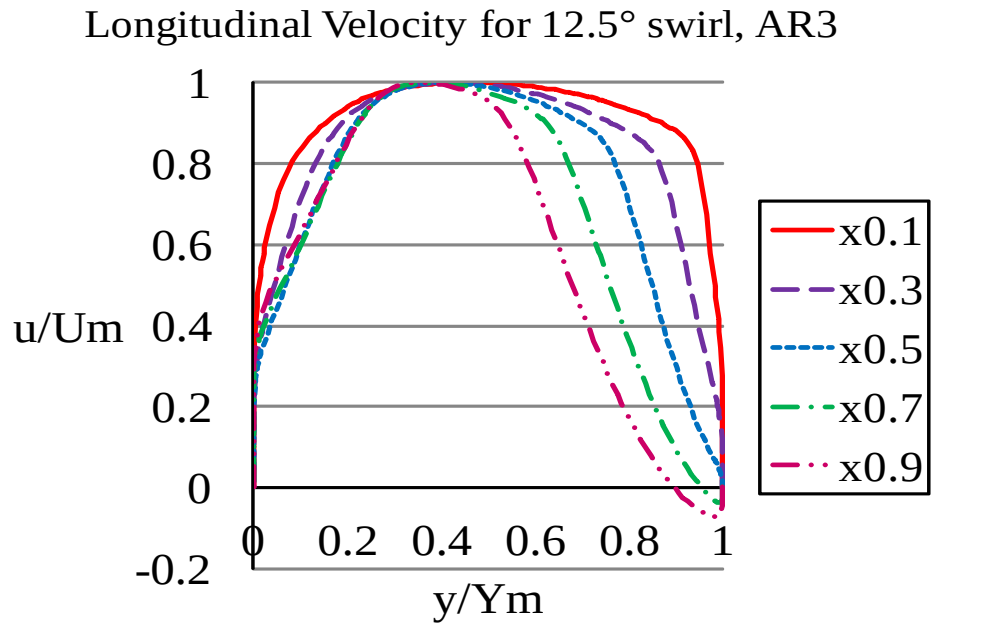

Fig No-32

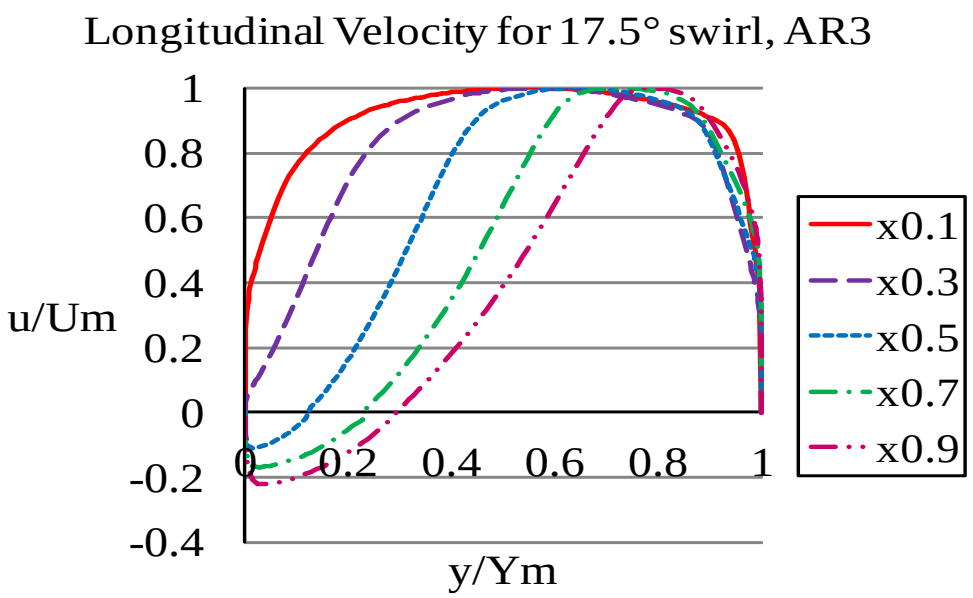

Fig No-33

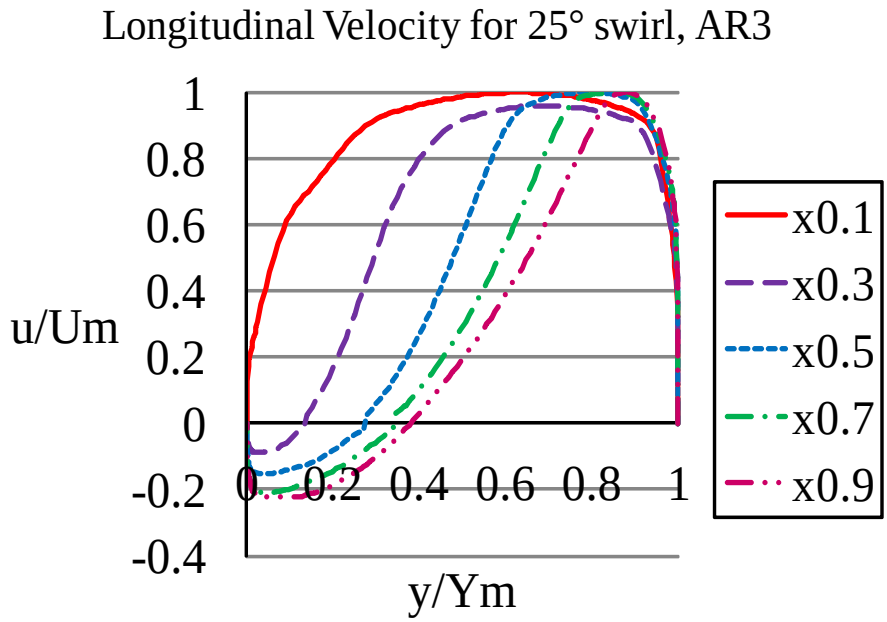

Fig No-34

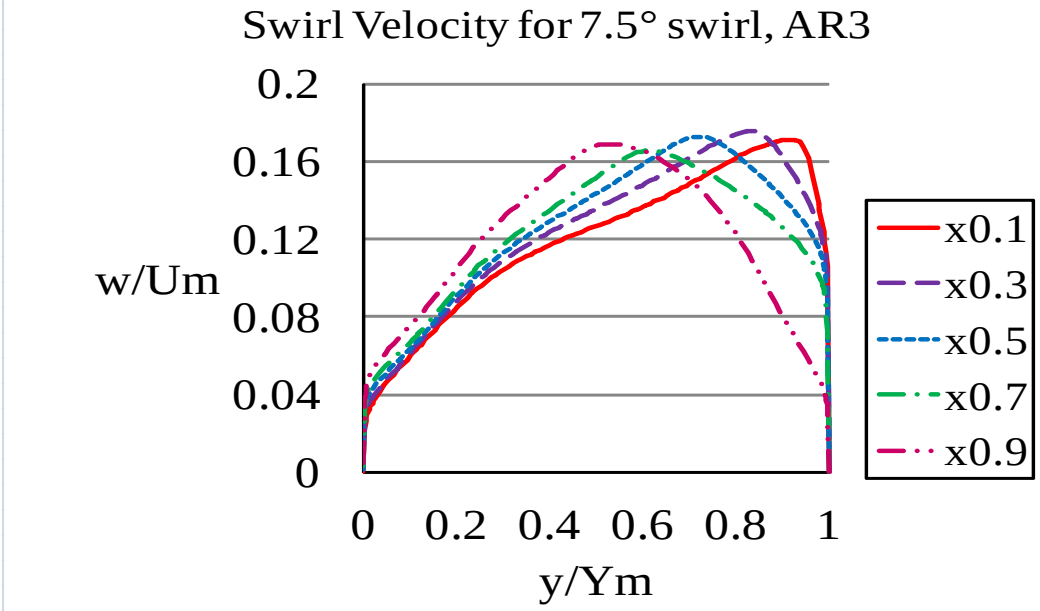

Fig No-35

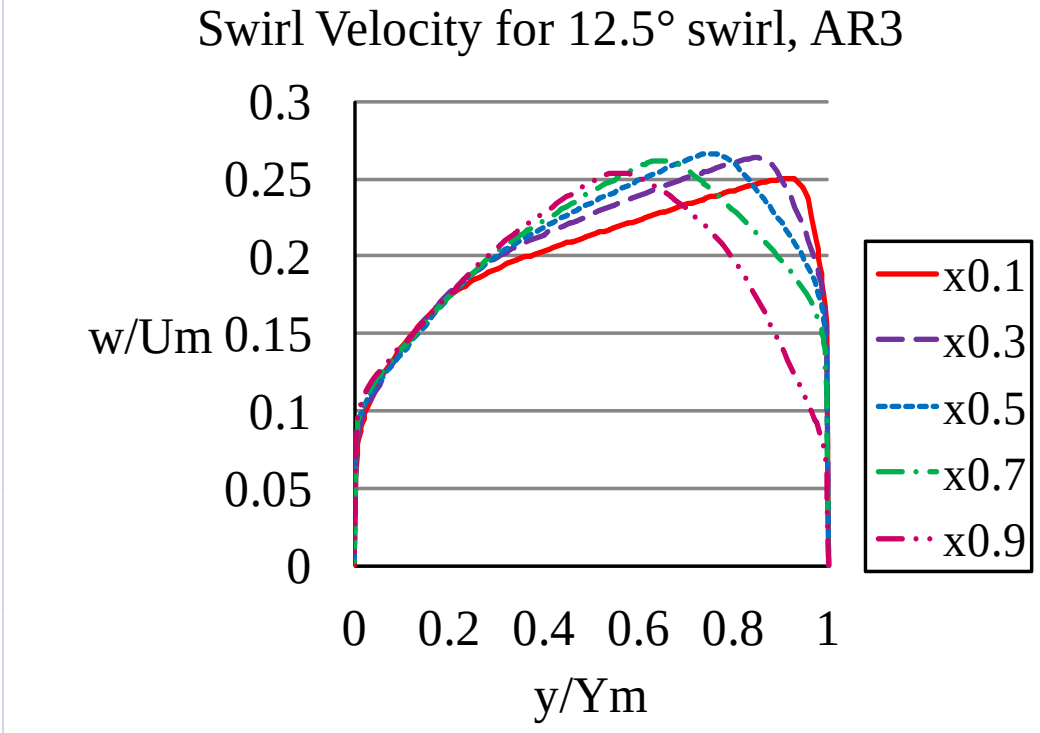

Fig No-36

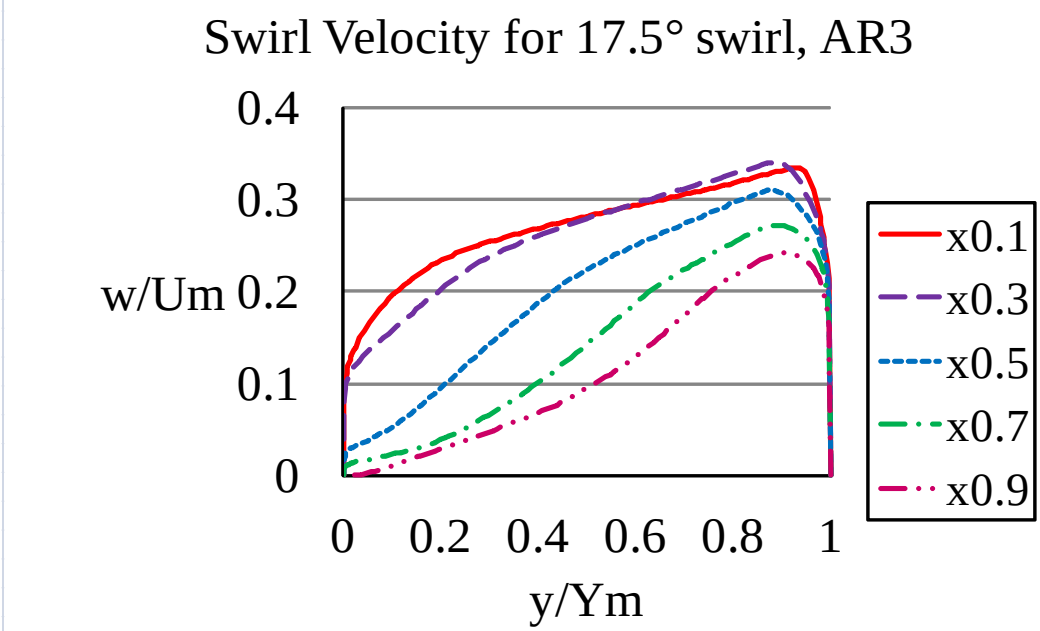

Fig No-37

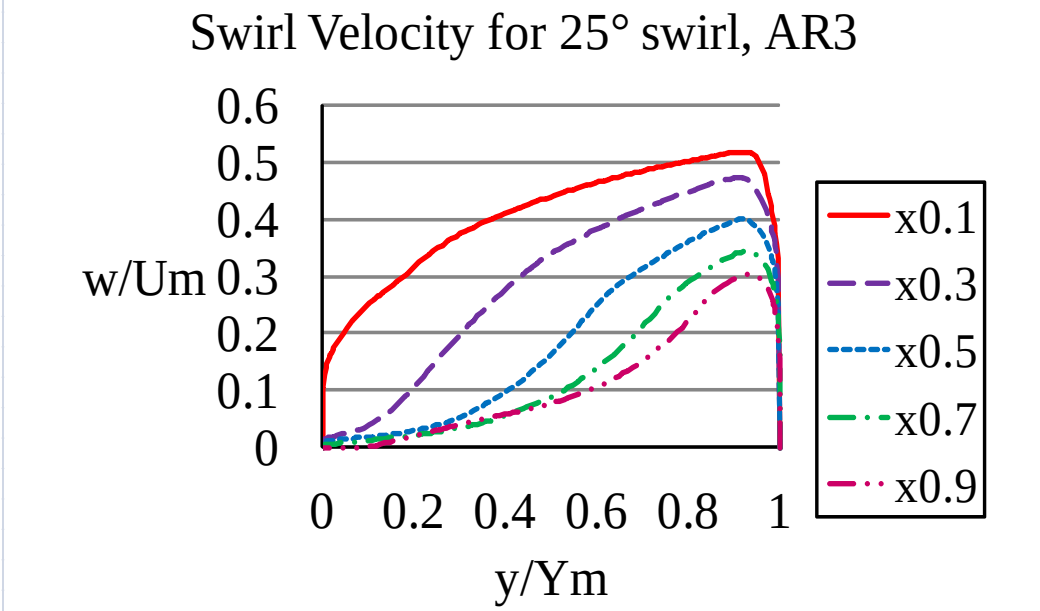

Fig No-38

Flow-Chart for CFD Modeling and Simulation

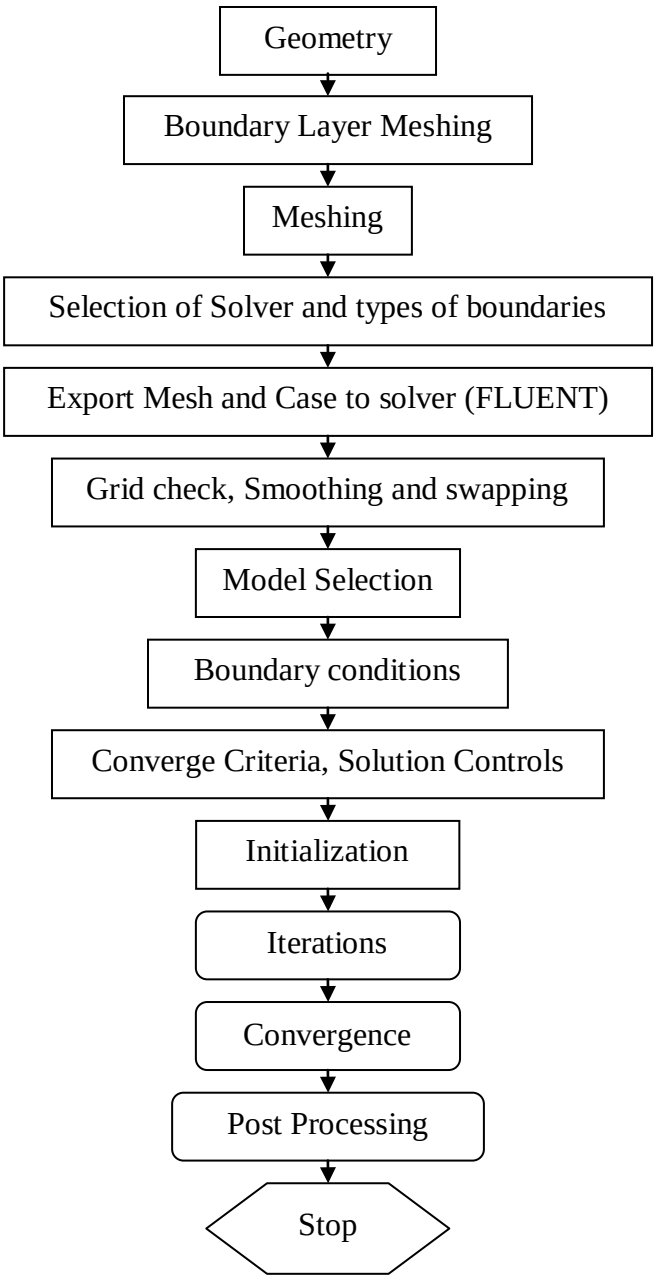

Table: 1 Geometric Parameters of Annular Diffuser

Diffuser Type	AR	Inlet hub Radius=3.8cm		Inlet casing Radius=7.7cm		L
		Wall Angles		Exit Radius (cm)		
		Hub	Casing	Hub	Casing	
Hub and casing diverging with unequal angles	2	5	11	5.18	10.87	15.86
	3	5	11	6.25	13.26	28.04